

Poznan University of Technology  
Faculty of Electronics and Telecommunications  
Chair of Wireless Communications

Doctor of Philosophy Dissertation

# Reliable and Energy-Efficient Spectrum Sensing in Cognitive Radio Systems

Wiarygodne i energooszczędne metody detekcji  
zajętości zasobów widmowych w systemach radia  
kognitywnego

by

**mgr inż. Krzysztof Cichoń**

Supervisor: prof. dr hab. inż. Hanna Bogucka  
Secondary supervisor: dr inż. Adrian Kliks

Poznań, 2016



*To my wife,  
children and parents,  
sisters and brother,  
and Friend*



---

# Table of Contents

---

<b>Table of Contents</b>	<b>i</b>
<b>List of Figures</b>	<b>iv</b>
<b>List of Tables</b>	<b>vii</b>
<b>List of Key Symbols</b>	<b>ix</b>
<b>List of Abbreviations</b>	<b>xi</b>
<b>Introduction</b>	<b>1</b>
<b>1 Spectrum Sensing</b>	<b>7</b>
1.1 Non-Cooperative Spectrum Sensing . . . . .	7
1.1.1 Energy Detector . . . . .	9
1.1.2 Sequential Energy Detector . . . . .	10
1.1.3 Feature-based Cyclostationary Detector . . . . .	12
1.2 Cooperative Spectrum Sensing . . . . .	13
1.2.1 Local Sensing Information Reporting . . . . .	13
1.2.2 Selection of the Sink Node . . . . .	15
1.2.3 Decision Fusion . . . . .	18
1.2.4 Global Decision Reporting . . . . .	20
1.3 Time Domain Relations between Sensing and Access . . . . .	20
<b>2 Autonomous Spectrum Sensing</b>	<b>23</b>
2.1 Practical Implementations of Selected Spectrum Sensing Methods . . . . .	23
2.1.1 Sequential Energy Detection in practical context of real-acquired signal samples . . . . .	23
2.1.2 Experimental Sensing Measurements of Energy Detection and cyclostationary-based algorithms . . . . .	27
2.1.3 Hybrid Approach for Spectrum Sensing Using USRP and GNU Radio . . . . .	32
2.2 The Impact of Hardware Implementation on the Performance of Energy-based Spectrum Sensing Algorithms . . . . .	36

2.2.1	Hardware Implementation Details . . . . .	37
2.2.2	Measurement Analysis . . . . .	38
2.3	The Problem of Noise Power Estimation in practical Energy-Detector Implementation . . . . .	44
2.3.1	Noise Uncertainty . . . . .	45
2.3.2	Noise Estimation Methods with Elimination of the Narrow-band Signals . . . . .	46
2.3.3	Experiments outcome . . . . .	48
<b>3</b>	<b>Cooperative Spectrum Sensing</b>	<b>51</b>
3.1	Considerations about the Cooperative Spectrum Sensing regarding the Implementation Issues . . . . .	51
3.1.1	Practical Implementation of the Cooperative Spectrum Sensing . . . . .	51
3.1.2	Signal Analysis in Cooperative Spectrum Sensing . . . . .	56
3.2	Mobility-Aware, Correlation-Based Node Grouping and Selection for Cooperative Spectrum Sensing . . . . .	61
3.2.1	Correlation-Based Node Selection . . . . .	62
3.2.2	System Model . . . . .	63
3.2.3	Mobility-Aware Correlation-Based Spectrum Sensing . . . . .	64
3.2.4	Simulation Results . . . . .	66
3.2.5	Conclusion . . . . .	72
<b>4</b>	<b>Energy-Efficient Cooperative Spectrum Sensing</b>	<b>75</b>
4.1	Considerations on Energy Efficiency for Spectrum Sensing Algorithms . . . . .	75
4.1.1	Identification of the Figure of Merits . . . . .	75
4.1.2	Single Sensing-Node Power Optimisation . . . . .	76
4.1.3	Energy Efficient Optimisation From the Network Perspective . . . . .	77
4.2	Energy Efficiency in Cooperative Spectrum Sensing: Classification . . . . .	78
4.3	Energy Savings in Local Spectrum Sensing . . . . .	81
4.4	Number of Cooperating Nodes . . . . .	83
4.4.1	Node Selection . . . . .	83
4.4.2	Censoring . . . . .	85
4.4.3	Voting Schemes . . . . .	86
4.5	Fusion Rule . . . . .	87
4.6	Energy-Efficient Network Organisation . . . . .	88
4.7	Final Classification of Energy-Efficiency Options . . . . .	91
4.8	Fuzzy Logic in the Optimisation Process of the Energy-Efficient Cooperative Spectrum Sensing . . . . .	94
4.8.1	Dependency Matrix . . . . .	94
4.8.2	Rose Chart . . . . .	96
4.8.3	Exemplary Use Cases . . . . .	98
4.9	Energy-Efficient Cooperative Spectrum Sensing with Node Sleeping and Relaying	101
4.9.1	System Model and Problem Formulation . . . . .	101
4.9.2	Simulation Scenario . . . . .	104
4.9.3	Simulation Results . . . . .	105

4.10 Energy-Efficient Cooperative Spectrum Sensing with a Merged Clustering Measure	108
4.10.1 System Model . . . . .	109
4.10.2 Simulation Results . . . . .	111
<b>5 Conclusions</b>	<b>115</b>
<b>Bibliography</b>	<b>117</b>

---

# List of Figures

---

1.1	Illustration of the primary and secondary user coexistence in the cognitive radio network . . . . .	8
1.2	Receiver Operating Curves for detection of the frequency modulated signal . . . . .	9
1.3	Energy-Efficiency trade-off observed in a single node sensing phase . . . . .	9
1.4	Decision regions in the energy detector . . . . .	10
1.5	Decibel value of the ratio between energy detector's thresholds and noise power estimate for various values of the number of samples $M_s$ and probability of false alarm $P_f$ . . . . .	11
1.6	Decision regions in the sequential energy-based detector . . . . .	12
1.7	Cooperative spectrum sensing procedure . . . . .	14
1.8	Spectrum sensing possible types of reported decisions: hard-decision, soft-decision and double-bit hard decision . . . . .	14
1.9	Trade-off observed in local sensing information reporting . . . . .	15
1.10	Classification of cooperative sensing: centralised, cluster-based, decentralised and relayed . . . . .	16
1.11	Illustration of the sensing and data transmission period . . . . .	21
1.12	Sensing period-data transmission period trade-off observed in spectrum sensing . . . . .	22
2.1	Block diagram of a SED model . . . . .	24
2.2	Results for Sequential Energy Detector proceeded in $K$ phases: probability of proper decision, medium sensing time . . . . .	25
2.3	Sequential Energy Detector results in terms of SNR for <i>symmetric</i> cases: probability of proper decision, medium sensing time . . . . .	26
2.4	Sequential Energy Detector results in terms of SNR for <i>non-symmetric</i> cases: probability of proper decision, medium sensing time . . . . .	26
2.5	Experimental setup diagram . . . . .	28
2.6	Scheme of the Primary User OFDM transmitter realised in the GNU Radio . . . . .	29
2.7	Scheme of the Secondary User receiver realised in the GNU radio . . . . .	30
2.8	Probability of detection $P_d$ vs SNR for Primary User FM signal . . . . .	31
2.9	Probability of detection $P_d$ vs SNR for Primary User OFDM signal . . . . .	31
2.10	Scheme of the hybrid spectrum sensing detector . . . . .	33

2.11	Experimental setup diagram . . . . .	33
2.12	Probability of detection $P_d$ vs SNR for various PU signals: FM signal, GMSK signal and 8PSK signal . . . . .	35
2.13	Probability of ‘no decision’ state in Sequential Energy Detection scheme after collection of $M_s/K$ samples . . . . .	35
2.14	Hardware employed in the practical implementation experiment: a) PMSE equipment (PU signal) stored in anechoic chamber, b) USRP N210 device, c) WBX daughter-board, d) Personal Computer where sample processing has been conducted . . . . .	38
2.15	Noise power for different frequency of tuning $f_w$ . . . . .	39
2.16	Spectrum mask of noise for exploited hardware as a function of the DC offset shift . . . . .	40
2.17	Influence of temperature on the noise power . . . . .	40
2.18	Noise floor for measurements conducted in three various scenarios . . . . .	41
2.19	Non-linear effects that appear over time . . . . .	42
2.20	Comparison of traditional and pragmatic approaches for high-power incoming signal . . . . .	42
2.21	a) Probability of detection and b) probability of false alarm for traditional and pragmatic approaches . . . . .	43
2.22	Measurements of internal noise with the use of a dedicated switch . . . . .	45
2.23	SNR wall vs noise uncertainty . . . . .	46
2.24	Noise power estimation for a) estimation ranges and median value, and b) Least Median of Squares methods . . . . .	49
2.25	Noise power estimates for selected spectrum portion for all analysed methods . . . . .	49
2.26	Mean estimation error vs frequency for analysed noise estimation methods . . . . .	50
3.1	Illustration of all three sensing devices equipped with the same set, containing USRP with WBX daughter-board and transferring complex base-band signal samples to the computers via Gigabit Ethernet . . . . .	52
3.2	Position of receiving and transmitting entities in the premises of the Faculty of Electronics and Telecommunications in scenario I and scenario II . . . . .	53
3.3	Results of noise power measurements and noise estimations for three receiving entities in scenario I and scenario II . . . . .	53
3.4	Probability of detection $P_d$ vs frequency for each receiving entity separately in scenario I and scenario II . . . . .	54
3.5	Global probability of detection $Q_d$ vs frequency for cooperative spectrum sensing while three fusion rules are adopted in scenario I and scenario II . . . . .	55
3.6	Medium number of samples (medium sensing time) vs frequency for three receiving entities in scenario I and scenario II . . . . .	56
3.7	Location of receiving entities and PMSE during measurements in Scenario III (PU transmission disabled) and Scenario IV (two PU devices active) . . . . .	57
3.8	Measured noise power for each receiving entity with corresponding noise estimation results conducted with <i>estimation ranges</i> method in Scenario III and Scenario IV . . . . .	57
3.9	Detection rate for theory-based thresholds . . . . .	57
3.10	Measurements sensing results in Scenario III and Scenario IV . . . . .	59
3.11	Probability of detection vs frequency while three decision rules are adopted in Scenario III and Scenario IV . . . . .	59

3.12	Signal analysis in scenario III and scenario IV . . . . .	60
3.13	Behaviour of the term related to node velocity used in the Leader Suitability formula	66
3.14	Exemplary state of the system after node selection procedure . . . . .	68
3.15	Global probability of false alarm $Q_f$ in the function of the number of selected nodes .	68
3.16	Global probability of detection $Q_d$ vs time for a) <i>maxPd</i> strategy, $n = 13$ s, b) <i>maxST</i> strategy, $n = 13$ s, c) <i>mixed</i> strategy, $n = 18$ s . . . . .	70
3.17	Global probability of detection $Q_d$ for <i>starting selection</i> for terminal velocities in the range of: a) 1 – 5 m/s, b) 1 – 20 m/s . . . . .	71
3.18	Floor value of the global probability of detection $Q_d$ vs maximum node velocity for three leader selection strategies . . . . .	71
3.19	Number of selected nodes and percentage of sleeping nodes versus maximum node velocity . . . . .	72
4.1	Classification of energy-efficient cooperative spectrum sensing . . . . .	79
4.2	Energy saving areas in a single node . . . . .	81
4.3	Model of centralised CSS system where node selection or censoring is applied . . . . .	84
4.4	Rose-chart for energy consumption comparison . . . . .	97
4.5	Rose-chart for presented use cases . . . . .	100
4.6	Exemplary topology of the network of three sensing nodes and one Fusion Centre . .	104
4.7	Exemplary channel attenuation map for the simulated area $100 \times 100$ m . . . . .	105
4.8	Simulation results for different distances to Primary User . . . . .	105
4.9	Simulation results for various distances of Fusion Centre from central area point . . .	106
4.10	Simulation results vs various spread of nodes . . . . .	106
4.11	Simulation results for various numbers of nodes . . . . .	106
4.12	Performance of the clustering scheme with a merged clustering measure for various weighing coefficient $\lambda$ . . . . .	112

---

# List of Tables

---

1.1	Binary detector decisions . . . . .	8
1.2	Pros and cons for selected topology . . . . .	17
3.1	Key parameters of simulation . . . . .	67
3.2	Global probability of detection $Q_d$ values for <i>ideal selection</i> . . . . .	69
4.1	Classification of energy saving approaches . . . . .	92
4.2	Dependencies between the key CSS parameters . . . . .	95
4.3	Dependencies between the key CSS parameters in mobile dense network use case . . . . .	99
4.4	Dependencies between the key CSS parameters in machine-to-machine use case . . . . .	99



---

# List of Key Symbols

---

$\alpha$	Correlation threshold
$\beta$	Minimum correlation threshold in grouping/clustering procedure
$\epsilon$	Threshold in energy detector
$\epsilon_{\text{HI}}$	Higher threshold in double-threshold energy detector
$\epsilon_{\text{LO}}$	Lower threshold in double-threshold energy detector
$\eta^{(i)}$	Signal-to-noise ratio at the primary to secondary link acquired by the $i$ -th node
$\Gamma$	Matrix of size $N \times N$ containing pair correlation metrics of network members
$\gamma_{\text{merged}}^{(i,k)}$	Merged clustering measure between node $i$ and $k$
$\gamma_{i,k}$	Correlation metric between node $i$ and $k$
$\hat{\sigma}_n^2$	Power of AWGN
$\hat{\tau}_s$	Medium sensing time
$\lambda$	Weighing coefficient of distance and SNR
$\lfloor \cdot \rfloor$	<i>Floor</i> function of the argument
$P_d$	Probability of detection
$P_f$	Probability of false alarm
$\omega$	Correlation coefficient specific for the transmission environment
$\text{erfc}(\cdot)$	Complementary error function
$\psi$	Lag parameter associated to the autocorrelation function
$\rho$	Noise uncertainty in linear scale
$\ \mathbf{x}\ _2$	2-norm of vector $\mathbf{x}$

$\xi$	Cyclic frequency
$d_{\text{corr}}$	Decorrelation distance
$EE_{Q_d}$	Energy Efficiency metric related to the global probability of detection
$F$	FFT size
$f_w$	Frequency of tuning
$K$	Number of phases in sequential detector
$M_n$	Number of samples acquired for noise power estimation
$M_s$	Number of collected samples by detector
$N$	Number of cooperating nodes
$P_{\text{tot}}$	Total power consumed by the network in one sensing and data-transmission period
$Q(\cdot)$	Q-function which is the tail probability of standard normal distribution
$Q_d$	Global probability of detection
$Q_f$	Global probability of false alarm
$S_i(k)$	$k$ -th sensing decision of $i$ -th node
$T_{\text{dt}}$	Total duration of data transmission period
$T_{\text{se}}$	Total duration of sensing period
$T_{\text{tot}}$	Total frame duration
$x^*$	Complex conjugate of $x$
$\mathcal{H}_0$	Hypothesis that the received signal is just noise, i.e., the frequency band is vacant and no Primary User transmission is active
$\mathcal{H}_1$	Hypothesis that the received signal is the sum of noise and Primary User signal, i.e., the frequency band is busy

---

# List of Abbreviations

---

Abbreviation	Description
<b>5G</b>	Fifth Generation
<b>ADC</b>	Analog-to-Digital Converter
<b>BPSK</b>	Binary Phase Shift Keying
<b>CAF</b>	Cyclic Autocorrelation Function
<b>CDR</b>	Constant Detection Rate
<b>CFAR</b>	Constant False Alarm Rate
<b>CH</b>	Cluster Head
<b>CLT</b>	Central Limit Theorem
<b>CPE</b>	Consumer Premise Equipment
<b>CR</b>	Cognitive Radio
<b>CRT</b>	Cognitive Radio Terminal
<b>CS</b>	Compressed Sensing
<b>CSD</b>	Cyclic Spectrum Density
<b>CSS</b>	Cooperative Spectrum Sensing
<b>CR</b>	Cognitive Radio
<b>DAC</b>	Digital-to-Analog Converter
<b>DAF</b>	Decode and Forward
<b>DSP</b>	Digital Signal Processor
<b>DVB-T</b>	Digital Video Broadcasting–Terrestrial
<b>DVB-H</b>	Digital Video Broadcasting–Handheld
<b>ED</b>	Energy Detection

<b>EE</b>	Energy Efficiency
<b>EESM</b>	Exponential Effective SINR Mapping
<b>FC</b>	Fusion Centre
<b>FFT</b>	Fast Fourier Transform
<b>FLOPS</b>	Floating Point Operations Per Second
<b>FM</b>	Frequency Modulation
<b>FPGA</b>	Field Programmable Gate Array
<b>GMSK</b>	Gaussian Minimum Shift Keying
<b>GPS</b>	Global Positioning System
<b>GRC</b>	GNU Radio Companion
<b>GSM</b>	Global System for Mobile Communications
<b>IF</b>	Intermediate Frequency
<b>LAA</b>	Licensed Assisted Access
<b>LMS</b>	Least Median of Squares
<b>LNA</b>	Low Noise Amplifier
<b>LO</b>	Local Oscillator
<b>MAC</b>	Media Access Control
<b>OFDM</b>	Orthogonal Frequency-Division Multiplexing
<b>OMP</b>	Orthogonal Matching Pursuit
<b>PMSE</b>	Programme Making and Special Events
<b>PSD</b>	Power Spectral Density
<b>PU</b>	Primary User
<b>REM</b>	Radio Environment Map
<b>RF</b>	Radio Frequency
<b>RFID</b>	Radio Frequency Identification
<b>ROC</b>	Receiver Operating Curve
<b>SDR</b>	Software Defined Radio
<b>SED</b>	Sequential Energy Detection
<b>SNR</b>	Signal-to-Noise Ratio
<b>SPCAF</b>	Symmetry Property of Cyclic Autocorrelation Function
<b>SPEED</b>	Sequential Pragmatic EnErgy Detection
<b>SU</b>	Secondary User
<b>UHD</b>	USRP Hardware Driver
<b>USRP</b>	Universal Software Radio Peripheral
<b>WRAN</b>	Wireless Regional Area Network

---

# Introduction

---

In recent years, an exponential growth of the mobile data-traffic volume has been observed in radio communication systems [47]. The ever-increasing demand for higher data rates in these systems calls for new methods of handling and managing radio frequency resources. These resources are scarce. On the one hand, there are few available frequency bands that could be assigned to new radio communication systems, while on the other, a number of measurement campaigns conducted in many places world-wide have shown that numerous frequency bands licensed to such systems are significantly underutilised [148, 23, 79, 127, 30, 90, 91]. This observation has inspired researchers to come up with the idea of Cognitive Radio (CR), introduced in fundamental works by J. Mitola III [116, 114, 115]. These publications have also stimulated investigation in the field of efficient spectrum sharing and dynamic spectrum access; new visions on the CR systems have been also proposed, e.g., in [72, 161].

Consequently, CR technology has been proposed as a potential solution to increase the efficiency of spectrum utilisation, as it enables opportunistic access of temporarily unused frequency bands once the presence of so-called Primary Users (PUs), i.e., the users of licensed systems, is excluded. The main point of this idea is to determine, with possibly the highest probability, whether the considered frequency band is available, i.e., not occupied by a PU. This may essentially be achieved in two ways: *i*) based on the knowledge about scheduled primary activities (e.g., stored in a database), or *ii*) based on the real-time measurement of the PU's activity, known as spectrum sensing. The latter solution was initially considered as the main one for future CR systems, but due to long-standing open research issues in the implementation of reliable sensing methods, the interest in databases grew significantly [61, 126]. However, investigation on spectrum sensing is still highly encouraged as sensing can complement and extend the information provided by databases.

This may be observed in recent standardisation activities. For example, the IEEE 1900.6 working group has started a new standardisation project on the topic of the usage of sensing information to support spectrum databases assigned as IEEE 1900.6b [8]. This is the third part of standardisation efforts started by publishing the baseline standard IEEE 1900.6 in 2011 [6] related to spectrum sensing interfaces, continued by the release of the first amendment (assigned as 1900.6a) in June 2014, entitled: "Procedures, Protocols and Data Archive Enhanced Interfaces" [7]. Moreover, spectrum sensing is a function of the *cognitive plane* in the IEEE 802.22 standard of Wireless Regional Area Network (WRAN) in TV bands [9, 152]. In order to protect Primary Users (e.g., television receivers and Programme Making and Special Events (PMSE) equipment),

apart from using the spectrum databases, spectrum sensing is compulsory for base stations and Consumer Premise Equipment (CPE) using this standard. However, IEEE 802.22 does not recommend a specific sensing method, since it only defines the detection level, SNR, time and detection quality requirements.

The next motivation for a continued research on spectrum sensing is the creation of the so-called Radio Environment Maps (REMs), or other databases designed for storing and processing of the reach available context information. The justification for practical deployment of such databases relies on the assumption that the more (true and verified) information available in the system, the better its efficiency. The problem of accurate channel state information at the transmitter and receiver in a classical example proves this somehow trivial observation. However, the concept of utilising of the so-called context information can be easily extended to other aspects of wireless communications. *Information crumbles* collected by the system at a certain time and location can be smartly utilised in the future. In the context of Fifth Generation (5G), or in the future, next-generation systems, the information about spectrum utilisation (including some historical knowledge and past experience, etc.) will be the basis of flexible spectrum management foreseen as one of the key technological enablers, even if the ideal cognitive radio concept is not applied in practise. The deployment of REMs and their advanced management is a practical tool for achieving this goal. Cooperative spectrum sensing, decision making and reporting will then be used as an efficient way of permanent spectrum monitoring and delivering periodic updates of database entries. Thus, it is necessary to define solutions for non-cooperative and cooperative spectrum sensing.

### **Dissertation thesis and major aims**

The thesis of the dissertation is the following:

*There exist new methods for spectrum sensing, both autonomous and cooperative, with enhanced reliability and/or energy efficiency compared to the existing solutions.*

The main goal of the thesis is to propose such enhanced techniques and in particular:

- To implement selected spectrum sensing techniques and assess the impact of hardware and noise estimation in these implementations (This goal is addressed in Chapter 2).
- To assess the gains which support the cooperation scheme in cooperative spectrum sensing including correlation-based scheme and taking mobility of the sensing nodes into account (This goal is addressed in Chapter 3).
- To identify possible directions in energy-efficient cooperative spectrum sensing schemes and to classify the main directions of optimisation. Then, to draw the dependencies between these areas (This goal is addressed in Chapter 4).
- To develop the energy-efficient techniques for cooperative spectrum sensing with the use of node selection, node relaying and clustering (This goal is addressed in Chapter 4).

## Overview of the dissertation contributions

The first Chapter presents the essence of the spectrum sensing prepared by the author of the thesis.

Chapter 2 is devoted to non-cooperative spectrum sensing. The main contributions are the implementations of the spectrum sensing techniques in various configurations in USRP platform and proceeded in GNU Radio environment. The sequential energy detector implementation has shown that it is possible to shorten the mean sensing time, but the process is burdened with limited reliability. This is overcome by the cyclostationary-based technique which guarantees substantially higher reliability at the cost of complexity. The gains from these two techniques are connected in the hybrid approach. The next contribution is the checking how the sensing methods are impacted by the hardware. The measurements have shown that the energy detector is highly sensitive to phenomena such as DC offset, temperature and ambient noise. The author of the thesis proposes then the pragmatic approach which is robust against close-high power signals and minimise the negative influence of existing hardware. The influence of proper noise estimation has been also analysed: three methods known from literature were compared for signal samples taken from different receiving entities.

In Chapter 3 the implementation considerations are broadened to cooperative approaches. The author of the thesis has conducted the experiment with three sensing entities with identical hardware and software configuration and conducted simultaneous measurements. It has been shown that the results should be verified using, e.g., temporal analysis in order to limit the insistent false alarm rate. The correlation-based cooperative solution taken from the literature has been substantially improved. The mobility of nodes has been taken into account, the analysed model has been changed into a more realistic and strict one. The new metric for election of the leader from the selected groups has been proposed which allows to perform grouping procedures more seldom.

In Chapter 4, the problem of energy-efficient cooperative spectrum sensing is addressed. First, energy efficiency in Cooperative Spectrum Sensing (CSS) is described and a new metric for energy efficiency in CSS is proposed. Then, the author of this thesis has proposed a classification of main directions in energy-efficient CSS solutions, i.e.: *i*) energy-efficient local spectrum sensing, *ii*) number of cooperating nodes, *iii*) fusion rule, *iv*) energy-efficient network organisation. The analysis of various solutions has shown that the existing works focus on one or at most two aforementioned directions in energy efficiency. However, the solution merging more directions is not only complex, but also not so efficient. The optimisation of one area of CSS may, however, influence the other direction and as a result the energy efficiency gain may be limited. Thus, the dependencies between CSS directions have been drawn with the methods known from fuzzy logic such as dependency matrix and rose chart. It has been shown that some optimisation solutions highly impact the others while there exists a group of solutions independent from the energy efficiency point of view. Then, an analysis of promising energy-efficient directions has been done, for instance, by taking into account node relaying and node selection. The conducted simulations have highlighted that node relaying is not always beneficial from Energy Efficiency (EE) point of view, while the node selection is more promising. Moreover, it is possible to improve energy efficiency of clustering by taking into account the distances between nodes with their experienced SNRs.

Finally, the conclusions of the considerations and results presented in this dissertation are drawn in Chapter 5.

### Author's published contributions

The above-described major contributions of this dissertation have been published in a number of papers listed below.

Papers in international and national journals:

1. K. Cichoń, A. Kliks, H. Bogucka, "Energy-Efficient Cooperative Spectrum Sensing: A Survey", *IEEE Communications Surveys & Tutorials*, vol. 18, no. 3, pp. 1861-1886, third-quarter 2016.
2. K. Cichoń, L. De Nardis, H. Bogucka, M. G. Di Benedetto, "Mobility-aware, correlation-based node grouping and selection for cooperative spectrum sensing", *Journal of Telecommunications and Information Technology*, vol. 2014, no. 2, pp. 90-102, 2014.
3. A. Kliks, P. Kryszkiewicz, K. Cichoń, A. Umberto, J. Perez-Romero, F. Casadevall, "DVB-T Channels Measurements for the Deployment of Outdoor REM Database", *Journal of Telecommunications and Information Technology*, vol. 2014, no. 3, pp. 42-52, 2014.
4. K. Cichoń, A. Kliks, H. Bogucka, "Optymalizacja oszczędności energetycznej kooperacyjnej detekcji sygnałów w ujęciu logiki rozmytej", *Przegląd Telekomunikacyjny i Wiadomości Telekomunikacyjne*, vol. 2016, no. 6, pp. 385-388, 2016.
5. K. Cichoń, H. Bogucka, "Udział węzłów przekaźnikowych w oszczędności energetycznej kooperacyjnej detekcji sygnałów", *Przegląd Telekomunikacyjny i Wiadomości Telekomunikacyjne*, vol. 2015, no. 8-9, pp. 830-835, 2015.
6. K. Cichoń, H. Bogucka, "Oszczędność energetyczna kooperacyjnej detekcji sygnałów w radiu kognitywnym", *Przegląd Telekomunikacyjny i Wiadomości Telekomunikacyjne*, vol. 2015, no. 4, pp. 229-232, 2015.
7. K. Cichoń, H. Bogucka, "Estymacja mocy szumu w praktycznej implementacji detektora energii", *Przegląd Telekomunikacyjny i Wiadomości Telekomunikacyjne*, vol. 2014, no. 8-9, pp. 889-894, 2014.
8. K. Cichoń, A. Kliks, H. Bogucka, "Praktyczna implementacja kooperacyjnego algorytmu wykrywania sygnału użytkownika licencjonowanego", *Przegląd Telekomunikacyjny i Wiadomości Telekomunikacyjne*, vol. 2014, no. 6, pp. 341-344, 2014.
9. K. Cichoń, A. Kliks, "SEKWENS - algorytm sekwencyjnego wykrywania sygnałów", *Przegląd Telekomunikacyjny i Wiadomości Telekomunikacyjne*, vol. 2013, no. 8-9, pp. 1283-1289, 2014.
10. K. Cichoń, H. Bogucka, "Wybór węzłów mobilnych w algorytmie korelacji decyzji w radiu kognitywnym", *Przegląd Telekomunikacyjny i Wiadomości Telekomunikacyjne*, vol. 2013, no. 6, pp. 314-317, 2013.

11. K. Cichoń, A. Kliks, "Sekwencyjny algorytm wykrywania transmisji użytkownika pierwotnego", *Przegląd Telekomunikacyjny i Wiadomości Telekomunikacyjne*, vol. 2012, no. 8-9, pp. 640-645, 2012.
12. K. Cichoń, "MAC algorithms in V2V transmission systems", *Przegląd Telekomunikacyjny i Wiadomości Telekomunikacyjne*, vol. 2012, no. 4, pp. 157-160, 2012.

Papers published in the proceedings of international conferences:

1. A. Nafkha, M. Naoues, K. Cichoń, A. Kliks, B. Aziz, "Hybrid Spectrum Sensing Experimental Analysis Using GNU radio and USRP for Cognitive Radio", 12th International Symposium on Wireless Communication Systems, ISWCS 2015, Brussels, Belgium, 25-28 August 2015.
2. K. Cichoń, H. Bogucka, "An Energy-Efficient Cooperative Spectrum Sensing", IEEE International Black Sea Conference on Communications and Networking, BlackSeaCom 2015, Constanta, Romania, 18-21 May, 2015.
3. K. Cichoń, A. Kliks, "The Impact of Hardware Implementation on the Performance of Spectrum Sensing Algorithms", 11th International Symposium on Wireless Communication Systems, ISWCS 2014, Barcelona, Spain, 26-29 August 2014.
4. K. Cichoń, A. Kliks, H. Bogucka, "Performance aspects of cooperative spectrum sensing in hardware implementation", URSI General Assembly and Scientific Conference, Beijing, China, 16-23 August 2014.
5. A. Nafkha, M. Naoues, K. Cichoń, A. Kliks, "Experimental Spectrum Sensing Measurements using USRP Software Radio Platform and GNU-Radio", 9th International Conference on Cognitive Radio Oriented Wireless Networks, CROWNCOM 2014, Oulu, Finland, 2-4 June 2014.
6. A. Kliks, P. Kryszkiewicz, K. Cichoń, A. Umbert, J. Pérez-Romero, F. Casadevall, "DVB-T channels power measurements in indoor/outdoor cases", IEICE Information and Communication Technology Forum 2014, Poznań, 28-30 May 2014.
7. K. Cichoń, A. Kliks, H. Bogucka, "Signal analysis in cooperative spectrum sensing hardware implementation", NATO IST-123/RSY-029 Symposium on "Cognitive Radio & Future Networks", Hague, The Netherlands, 12-13 May 2014.
8. I. Dagres, A. Polydoros, D. Denkovski, V. Rakovic, V. Atanasovski, L. Gavrilovska, K. Cichoń, A. Kliks, S. Baban, O. Holland, "An Integrated Platform for Source Detection, Identification and Localization with Applications to Cognitive-Radio", European Wireless, Guildford, United Kingdom, 16-18 April 2013.



## Chapter 1

---

# Spectrum Sensing

---

### 1.1 Non-Cooperative Spectrum Sensing

The main goal of spectrum sensing is to identify the presence or absence of a Primary User (PU) at a certain location, at a given moment, and in a specified frequency band (1.1). Spectrum sensing in its simplest non-cooperative form is considered as single-device (or single-node) sensing (Fig. 1.1), where each node makes an independent decision on the availability of a frequency band, and acts accordingly (transmits in this band or not). From this perspective, numerous spectrum sensing algorithms have been proposed, such as the ones described in [13, 19, 55, 133, 173].

The goal of spectrum sensing is for the cognitive-radio entities (Secondary Users (SU)) to decide on the presence of a licensed-system signal (a PU signal). If a SU detects signal  $r(x)$ , the spectrum sensing decision  $D(x)$  can be treated as a double-hypothesis statistic test:

$$D(x) = \begin{cases} \mathcal{H}_0 & \text{if } r(x) = n(x) \\ \mathcal{H}_1 & \text{if } r(x) = s(x) + n(x), \end{cases} \quad (1.1)$$

where  $\mathcal{H}_0$  is the hypothesis that the received signal is just noise  $n(x)$ , i.e., the frequency band is vacant, and  $\mathcal{H}_1$  is the hypothesis that the  $r(x)$  is the sum of noise and PU signal  $s(x)$ , i.e., spectrum is occupied. The sensing quality is described by the probability of detection  $P_d$ , i.e., the probability that  $D(x) = \mathcal{H}_1$  in the case when the PU is, in fact, active, and by the probability of miss-detection  $P_{md}$ , i.e., the probability that  $D(x) = \mathcal{H}_0$  in the same case, when the PU is active. Moreover, an important sensing-quality metric is the probability of false alarm  $P_f$ , i.e., the probability that  $D(x) = \mathcal{H}_1$  in the case when the PU is actually not active. These metrics are typical for binary detector which, in fact, is proper for spectrum sensing. In Table 1.1 the set of decisions for binary detector with regarding probabilities is illustrated [80].

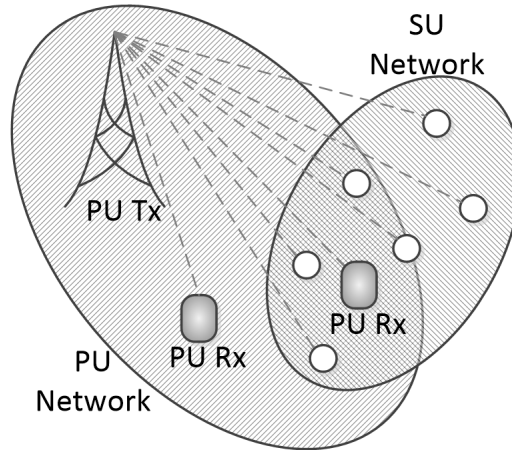


**Figure 1.1:** Illustration of the primary and secondary user coexistence in the cognitive radio network

**Table 1.1:** Binary detector decisions

Detector decision \ Reality	PU absent	PU present
Hypothesis $\mathcal{H}_0$	Probability of acquisition $P_a$	Probability of miss-detection $P_{md}$
Hypothesis $\mathcal{H}_1$	Probability of false alarm $P_f$	Probability of detection $P_d$

In general, it is beneficial to maximise the detection probability and minimise the false alarm probability. However, the optimisations of these two metrics are contradictory goals, i.e., an increase of the detection probability (by lowering the requirements for the decision threshold) leads to a higher number of false alarms and consequently to an increase of the probability of false alarm. Similarly, raising the detection threshold lowers both the detection probability and the probability of false alarm. Thus, for every sensing method, a trade-off has to be found that aims at keeping a possibly low number false alarms while guaranteeing a high detection rate. This constituted trade-off is shown in Fig. 1.2, where a few so-called Receiver Operating Curves (ROCs), presenting  $P_d$  vs  $P_f$ , have been illustrated for various signal-to-noise ratios. One can observe that the higher the Signal-to-Noise Ratio (SNR), the better the receiver characteristic, understood as a lower false alarm rate for a given detection rate or a higher detection rate for the stated false alarm rate.

**Identified energy versus quality trade-off in single-node sensing.** It is easy to indicate the following trade-off between sensing accuracy and certainty on the one hand, and processing time on the other. In a nutshell, the longer the sensing time or the more complex the sensing procedure, the more accurate the decision made by a single node (the lower the probability of interference that could be generated by a SU to a PU system and the better the frequency band utilisation). However, a more accurate sensing procedure requires the shortening of the

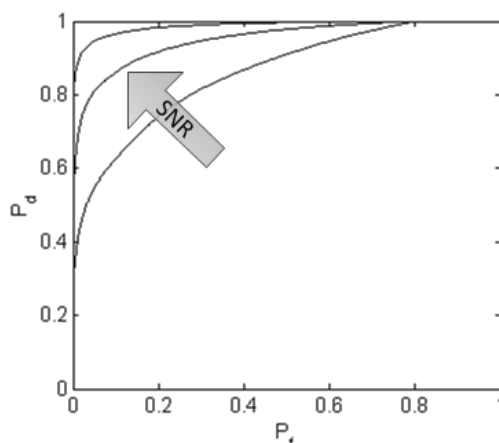


**Figure 1.2:** Receiver Operating Curves for detection of the frequency modulated signal

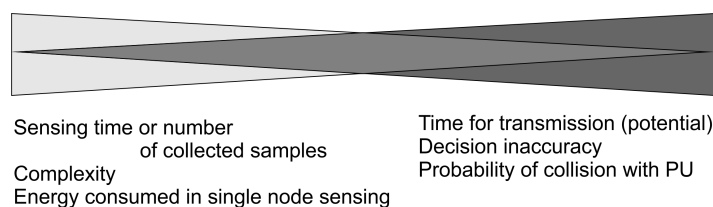


**Figure 1.3:** Energy-Efficiency trade-off observed in a single node sensing phase

transmission phase and an increase of energy consumption in the sensing phase. This trade-off is graphically illustrated in Fig. 1.3.

Note that there exist a number of single-node sensing methods which may be blind or make use of some a priori knowledge of the noise- and detected signal characteristic. Surveys of these sensing techniques can be found in [73, 104, 123, 135, 173]. These methods may be classified into three categories [118]: *a*) techniques requiring both PU signal and noise variance information, *b*) techniques requiring only noise variance information (known as *semi-blind* methods), *c*) techniques not requiring any information about PU signal or noise variance (*blind* methods). Examples of blind sensing methods would be eigenvalue based detection [174], wavelet based detection [160], second order statistical based detection [31], and symmetry property of cyclic autocorrelation function based detection [86]. In the three following subsections a selected set of sensing methods is presented in more detail.

### 1.1.1 Energy Detector

One of the simplest way for Primary User detection is to calculate the amount of received power in the considered frequency subband and compare this value with the noise variance. If the received power is higher than the previously approximated power of noise, the energy detector will make a decision on the spectrum occupancy by the PU signal. In turn, the channel will be assumed to be vacant if the computed noise power will be close to the noise variance at the certain level of certainty. There are several parameters that influence the reliability of any spectrum sensing algorithm. In the case of traditional energy detection, the crucial role is played

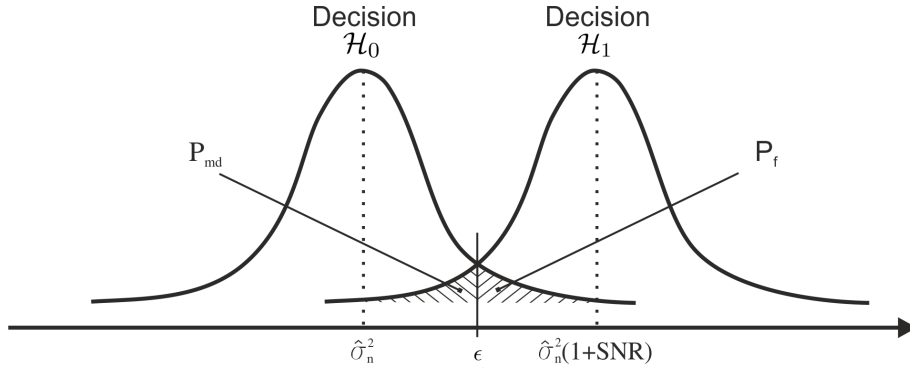


**Figure 1.4:** Decision regions in the energy detector

by properly defined decision threshold, and in consequence, by the accuracy of noise variance approximation, and the duration of sensing time (expressed in seconds or—for discrete signals—in terms of number of gathered samples). For the given values of probability of false alarm,  $P_f$ , number of collected samples  $M_s$ , and the (equivalent-)noise variance  $\hat{\sigma}_n^2$ , the decision threshold can be defined as following:

$$\epsilon = \hat{\sigma}_n^2 \left( Q^{-1}(P_f) \cdot \sqrt{2M_s} + M_s \right), \quad (1.2)$$

where  $Q(\cdot)$  represents the Q-function which is defined as  $Q(x) = \frac{1}{\sqrt{2\pi}} \int_x^{+\infty} e^{-\frac{u^2}{2}} du$ . Having in mind that the total power of  $M_s$  collected samples in the given frequency band can be represented as the random variable  $P_{M_s} = \sum_{k=0}^{M_s-1} r[k]$ , then based on (1.1) the generic decision rule  $D_{M_s}$  can be then modified to the considered case:

$$D_{M_s} = \begin{cases} P_{M_s} \leq \epsilon & \longrightarrow \mathcal{H}_0 \\ P_{M_s} > \epsilon & \longrightarrow \mathcal{H}_1 \end{cases} \quad (1.3)$$

It is worth noting that the reliability of energy-detectors strongly depends on the received power and on the accuracy of approximated variance noise  $\hat{\sigma}_n^2$ . The latter can be improved by increasing the number of collected samples  $M_s$ . In practice, however, even if the number of collected samples is infinitive, the performance upgrade is limited due to inaccurate noise power estimation. This phenomenon is known as  $\text{SNR}_{\text{wall}}$  and is described in Section 2.3 [159].

In Fig 1.5, one may observe the relation between the decision threshold  $\epsilon$  and the number of collected samples, probability of false alarm and noise power approximate. First, the higher the number of collected samples, the lower the decision threshold due to noise averaging. Besides, it should be noted that the decision threshold and noise power estimate have relatively low difference (for  $P_f = 0.02$  and  $M_s = 500$  it is about 0.4 dB, while for  $M_s = 100$  it is about 0.8 dB).

### 1.1.2 Sequential Energy Detector

The behaviour of the traditional energy detector can be improved in various ways, e.g., by application of the adaptively modified threshold. The other possibility is to adopt the double-threshold energy detection and sequential energy detector which possesses the same reliability as the traditional one but its application could reduce the sensing time. The main concept is based on

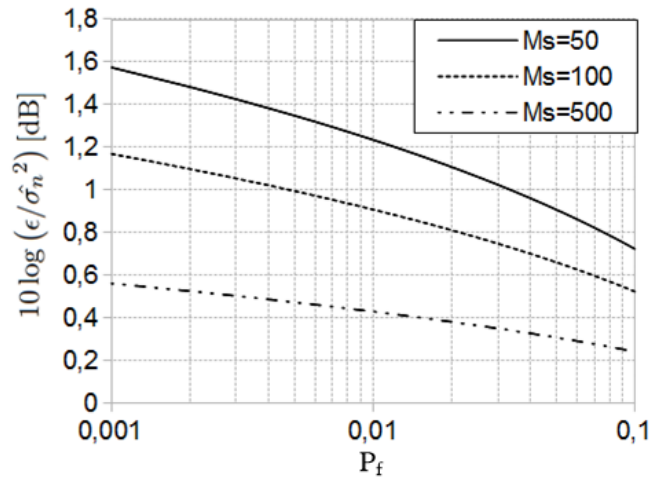


**Figure 1.5:** Decibel value of the ratio between energy detector's thresholds and noise power estimate for various values of the number of samples  $M_s$  and probability of false alarm  $P_f$

the assumption that for very strong PU signal, or—contrarily—in the presence of noise only, the number of samples that should be collected for reliable decision can be reduced. If this is the case, the sensing time is minimised increasing the time devoted to data transmission and reducing the energy consumption devoted for observation phase. In order to achieve this goal, two decision thresholds have been applied,  $\epsilon_{HI}$  and  $\epsilon_{LO}$ . In brief, the procedure can be realised in the following iterative way for  $K$  sequential phases. The Energy Detector collects the signal samples in period  $M_s/K$ , which is  $K$ -times shorter than sensing period in traditional Energy Detection (ED), and tries to make the decision. If the amount of power is greater than  $\epsilon_{HI}$ , the decision of the PU signal presence is made; if the received power is lower than  $\epsilon_{LO}$  the considered channel is decided as vacant. If the calculated value falls between these thresholds, the sequential energy detector collects next block of  $M_s/K$  samples and repeats the procedure (Fig. 1.6). When the total number of sequential phases  $K$  is reached (i.e., the maximum sensing time is reached), and the sensing decision has not been reached in final phase, then the decision is made as for traditional algorithms. The decision rule for the  $i$ -th iteration can be defined as follows:

$$D_{M_s^{(i)}} = \begin{cases} P_{M_s^{(i)}} \leq \epsilon_{LO}^{(i)} & \rightarrow \mathcal{H}_0 \\ P_{M_s^{(i)}} \in (\epsilon_{LO}^{(i)}, \epsilon_{HI}^{(i)}) & \text{continue} \\ P_{M_s^{(i)}} \geq \epsilon_{HI}^{(i)} & \rightarrow \mathcal{H}_1, \end{cases} \quad (1.4)$$

where  $P_{M_s^{(i)}}$  denotes the average power after collecting  $M_s^{(i)} = i \times M_s/K$  samples,  $i \in \{1 \dots K\}$ . The  $\epsilon_{HI}^{(i)}$  and  $\epsilon_{LO}^{(i)}$  are defined in 1.5, where  $P_{f,LO,i}$  and  $P_{f,HI,i}$  denote the probability of a false alarm assumed for low and high thresholds in the  $i$ -th iteration.

$$\begin{cases} \epsilon_{LO}^{(i)} = \hat{\sigma}_n^2 \cdot \left( Q^{-1}(P_{f,HI,i}) \cdot \sqrt{2M_s^{(i)}} + M_s^{(i)} \right) \\ \epsilon_{HI}^{(i)} = \hat{\sigma}_n^2 \cdot \left( Q^{-1}(P_{f,LO,i}) \cdot \sqrt{2M_s^{(i)}} + M_s^{(i)} \right). \end{cases} \quad (1.5)$$

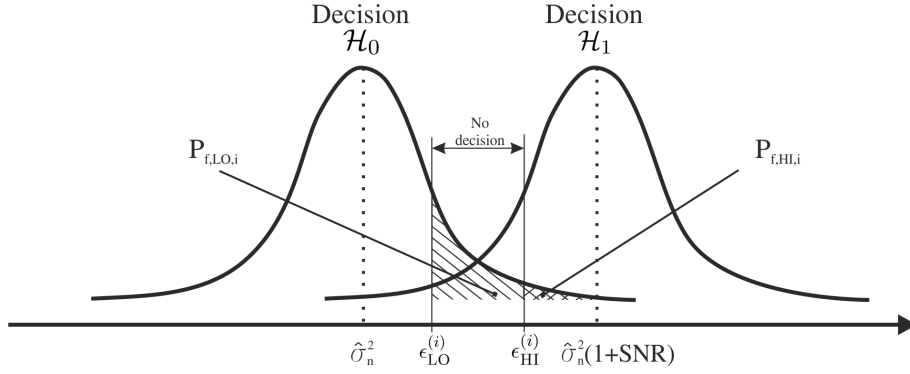


**Figure 1.6:** Decision regions in the sequential energy-based detector

Using the fact that the noise uncertainty has a bounded model which can be included in the *no decision* region, it is possible to evaluate the two thresholds in eq. (1.5) based on the estimated noise variance [119]. The example of the application of the sequential procedure in an integrated statistical-inference platform may be found in [51].

### 1.1.3 Feature-based Cyclostationary Detector

In wireless communications, the transmitted signals show very strong cyclostationary features [62]. Therefore, identifying a unique set of features of a particular radio signal can be used to detect its presence based on its cyclostationary features. In the context of spectrum sensing extensive research has been conducted on using the cyclostationary features to detect the presence of PU in the radio environment [104, 118]. In general, this method can guarantee a higher detection rate than the energy detector. However, its main drawbacks are the complexity associated with the detection technique and the need for some a priori knowledge of the PU signal (e.g., cyclic frequency). The cyclostationary feature detector can be realised by analysing the Cyclic Autocorrelation Function (CAF) of a received signal  $r(x)$ . The CAF of a received signal  $r(x)$  at the SU can be expressed as:

$$R_r(x, \psi) = \sum_{\xi} R_r^{\xi}(\psi) \exp(2\pi j \xi x), \quad (1.6)$$

where  $\psi$  is a lag associated to the autocorrelation function,  $\xi$  the cyclic frequency and  $R_r^{\xi}(\psi)$  is given by (1.7):

$$R_r^{\xi}(\psi) = \lim_{M_s \rightarrow \infty} \frac{1}{M_s} \sum_{x=0}^{M_s-1} R_r(x, \psi) \exp(-2\pi j \xi x). \quad (1.7)$$

#### Classical Cyclostationary feature-based detector

The classical approach to realise the cyclostationary detector is based on the Cyclic Spectrum Density (CSD) or the spectral correlation function of the received signal  $r(x)$ .

$$\Upsilon_r^{\xi}(f) = \frac{1}{M_s} \sum_{x=0}^{M_s-1} R_r^{\xi}(\psi) \exp(-2j\pi f \psi). \quad (1.8)$$

The CSD function presented in (1.8) exhibits peaks when the cyclic frequency  $\xi$  equals the fundamental frequencies of  $s(x)$  the transmitted signal. Under the  $\mathcal{H}_0$  hypothesis, the CSD function does not have peaks since the noise is generally non-cyclostationary. Using this technique, it is possible to distinguish even weak PU signals from the noise at a very low SNR, where the energy detector is not applicable.

### Symmetry Property of Cyclic Autocorrelation Function (SPCAF) detector

The discrete-time consistent and unbiased estimation of the CAF of a random process is given as:

$$\tilde{R}_{rr^*}^{\xi}(\psi) = \frac{1}{F} \sum_{x=0}^{F-1} r(x)r^*(x+\psi) \exp(-2j\pi\xi x). \quad (1.9)$$

For a given lag parameter  $\psi \in \{1, 2, \dots, L\}$ , the cyclic autocorrelation function (CAF) can be seen as a Fourier transform of  $[r(0)r^*(0+\psi), r(1)r^*(1+\psi), \dots, r(F-1)r^*(F-1+\psi)]$ , where  $F$  is Fast Fourier Transform (FFT) size. As shown in the work of Khalaf et al. [86], the CAF is an  $F$ -dimensional sparse vector in cyclic frequency domain for a fixed lag parameter  $\psi$ . Moreover, it presents a symmetry property as illustrated in (1.10).

$$\|\tilde{R}_{rr^*}^{\xi}(\psi)\|_2 = \|\tilde{R}_{rr^*}^{-\xi}(\psi)\|_2. \quad (1.10)$$

Using a Compressed Sensing (CS) recovery technique like the Orthogonal Matching Pursuit (OMP) algorithm, it is possible to accurately estimate the CAF using a limited and small number of received samples  $M_s \ll F$ . If the obtained CAF verifies the property (1.10), then  $\mathcal{H}_1$  is true; otherwise,  $\mathcal{H}_0$  is true. It is important to note that even under  $\mathcal{H}_0$  the obtained CAF verifies the symmetry property. However, when using a small number of samples, the probability to obtain a symmetrical CAF under  $\mathcal{H}_0$  is very small [86]. This SPCAF technique can perform with a limited number of samples and consequently with lower complexity and shorter observation time compared to the classical approach.

## 1.2 Cooperative Spectrum Sensing

Several investigations pointed out that sensing carried out locally by single devices is not accurate enough for the safe coexistence of primary and secondary users [26, 63, 113]. Thus, it is generally agreed that one of the ways to increase the reliability of spectrum sensing is to apply cooperation between nodes. In cooperative spectrum sensing every node in a cognitive network senses the spectrum, and reports local sensing results which are then used for acquiring a global decision characterised by the global probability of detection (see Fig. 1.7). These phases will be discussed in detail in the following subsections. In the end of each subsection one may find the identified trade-offs highlighting the most relevant relations in cooperative spectrum sensing, e.g., the quality versus energy-efficiency trade-off.

### 1.2.1 Local Sensing Information Reporting

One of the simplest techniques for sharing the sensing information is based on the nodes' local decisions on the PU presence in a given band and on delivering local binary decisions to selec-

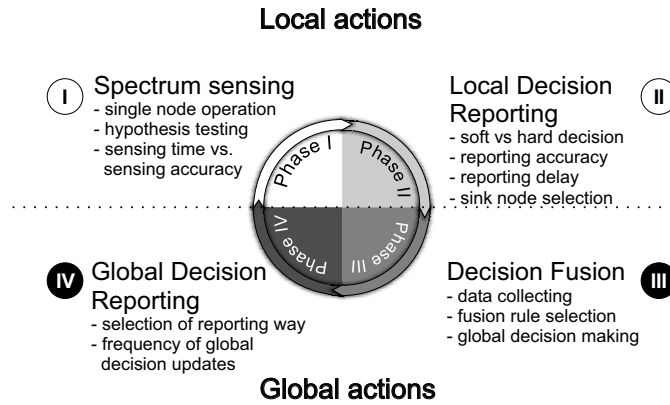


**Figure 1.7:** Cooperative spectrum sensing procedure

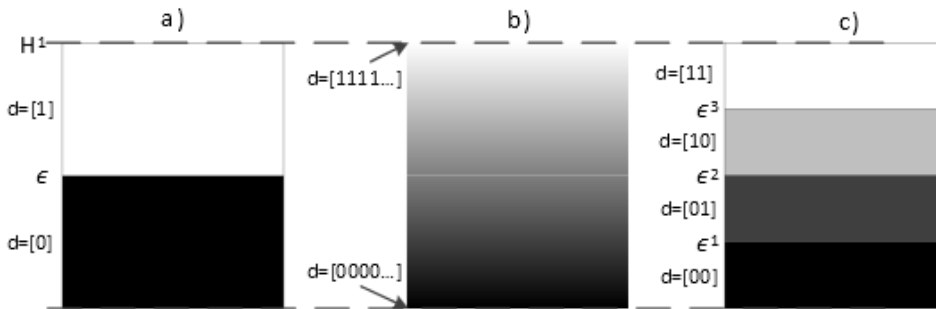


**Figure 1.8:** Spectrum sensing possible types of reported decisions: a) hard-decision, b) soft-decision, c) double-bit hard decision

ted node(s) determined by a Media Access Control (MAC) layer. This procedure is known as hard-decision combining and requires just one bit for the local decision representation (e.g., 1 can represent spectrum occupancy, whereas 0—vacancy). It is very concise and easy-to-decode, therefore, decision fusion may be easily adopted here (see Section 1.2.3). However, such a concise quantisation of sensing information may be imprecise, and the quality of the decision made by the node is not reflected in its binary representation. In Fig. 1.8a, one may observe that sensing information is binarized, i.e., only presence/absence messages are generated. If the value of the decision variable (such as the received power, the presence of periodicity in the received signal, etc.) is above a specified threshold (denoted here arbitrarily as  $\epsilon$ ), the node will decide on the hypothesis  $\mathcal{H}_1$  and the message will be  $d = [1]$ , otherwise it will be  $\mathcal{H}_0$  with  $d = [0]$ .

In the soft-decision reporting scheme, soft sensing-information with an assumed level of accuracy is encoded and shared. In this scheme, the reported message may be extended by additional useful information, such as sensing-channel quality information, sensing decision quality, a dedicated metric characterising the node's previous decisions etc. Thus, soft-decision reporting may be very precise and neatly used in order to increase global detection quality; for example, one may find an optimum soft-decision scheme based on the Neyman-Pearson criterion in [105]. However, soft-metric reporting is burdened with large data overhead and computational complexity due to the large size of reporting messages. Additionally, large reporting messages introduce additional delay in transmission. From the perspective of energy efficiency, the size of reported

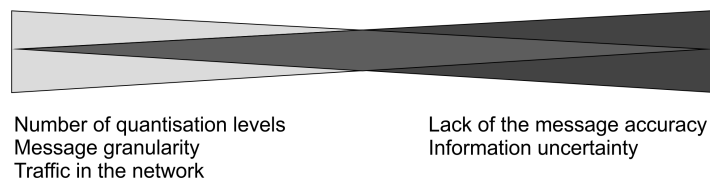


**Figure 1.9:** Trade-off observed in local sensing information reporting

messages should be limited: on the one hand precise soft reporting information leads to a high detection quality but also a large size of messages; on the other hand, limited precision provides a lower detection rate but also reduces the overhead significantly. Such a situation is illustrated in Fig. 1.8b, where no decision threshold  $\epsilon$  is identified. Message  $d$  shared by the node can be used to somehow reflect the degree of uncertainty of the node's decision, e.g., the vector of ones  $d = [111 \dots 1]$  will correspond to the certainty of the correctness of hypothesis  $\mathcal{H}_1$ . The higher the number of bits in vector  $d$ , the higher the accuracy of the decision. A comparison between hard-decision and soft-decision reporting is provided, e.g., in [156], where in the latter scheme, all nodes transmit information on the observed signal energy to the fusion centre.

However, in practical applications, the soft decisions have to be quantised with an assumed and rather low number of bits. This leads to solutions known as *quantised-soft reporting* which merge soft and hard reporting. As an example, the so-called quantised soft-bit schemes were proposed and discussed in [21, 22]. In particular, in double-bit reporting, two bits are used in reporting messages, which gives four cases in reporting [105], as shown in Fig. 1.8c. A detailed analysis of the aforementioned schemes is presented in [164, 117, 28], whereas in [134], various quantisation schemes applied to reported message are analysed. Moreover, some discussion on the energy efficiency of various reporting and fusion rules is presented in [15].

**Identified trade-off in sensing information reporting.** Again, it is easy to indicate the following trade-off between the accuracy and granularity of transmitted information and the energy and time needed for this action. The higher the granularity of the transferred information, the higher the generated traffic in the network and energy consumption in that particular phase, but at the same time, the more detailed and accurate the message delivered to the fusion centre. This trade-off is graphically illustrated in Fig. 1.9.

### 1.2.2 Selection of the Sink Node

The preparation of sensing information that will be put into the reporting message is followed by the process of sharing (spreading to selected nodes) the local observations. There are several possible configurations for spreading these local observations to other nodes. This essentially relies on local conditions such as: the presence of a Fusion Centre (FC), the qualities of sensing channels or the availability of a reporting channel [28].

One of the simplest possibilities is to select the central entity, namely the FC, and send (report) the local sensing information to this entity. The FC collects sensing-decisions from the nodes, generates a global decision, and broadcasts it back to nodes. In Fig. 1.10a, such a centralised topology is presented. The black node which is the fusion centre is surrounded by several cognitive nodes reporting the sensing observations.

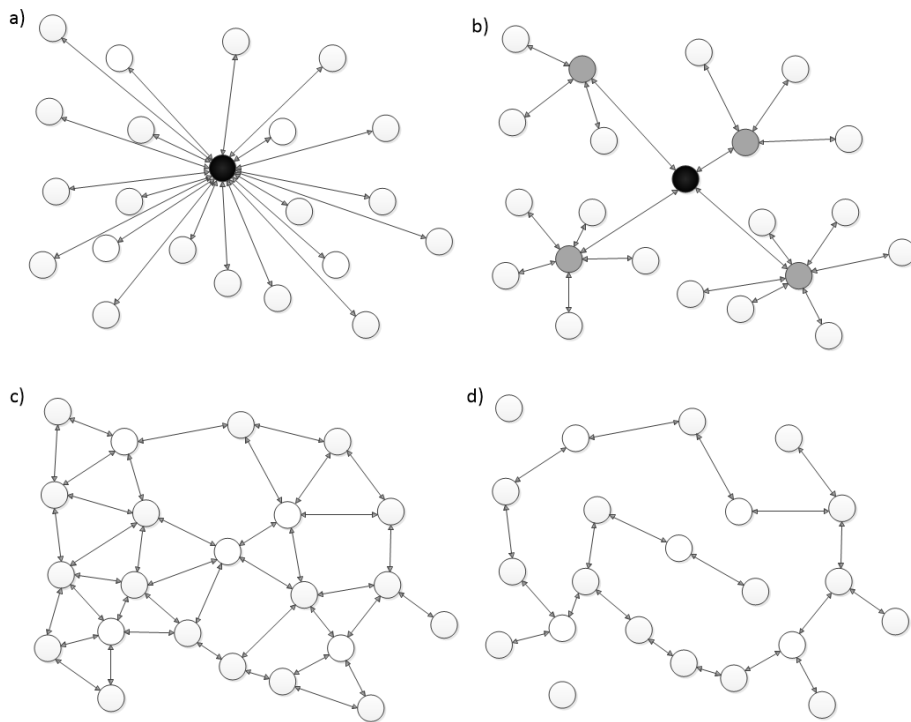


**Figure 1.10:** Classification of cooperative sensing: a) centralised, b) cluster-based, c) decentralised and d) relayed

The centralised topology is highly dependent on the proper FC selection: if the FC location is shadowed (in the sense of radio signal shadowing) the gain of such a centralised cooperative scheme is limited. Moreover, if the security aspects are crucial, the network sensing-performance should not be solely dependent on one node (the FC). Finally, the centralised scheme may have to deal with relatively large distances of some of the reporting channels, which may be inefficient energy-wise.

In the cluster-based scheme, the reporting channels distances are smaller. Geographically neighbouring nodes cooperate with each other, forming a closed group (called a cluster) with a selected cluster-head. All nodes report their local decisions to the local cluster head (instead of reporting them to the global FC), and it is the role of these cluster heads to either forward the collected decisions to the FC, or to make a decision at the cluster level, and report it to the FC. Such a case is illustrated in Fig. 1.10b, where the black node is the FC and the grey nodes are the cluster heads. The cluster-based scheme introduces a delay in sensing message sharing, and involves a specific procedure for organising nodes into clusters and the selection of cluster heads.

Unlike the centralised and cluster-based schemes, in the distributed topology, there is no selected single node that manages the sensing process in the network. Nodes interchange their observations in a somehow determined order, and make global decisions by combining their own observations with the ones acquired from messages sent by other nodes. The adopted distributed algorithm is determined by the applied distributed-network protocol. Distributed cooperative sensing is illustrated in Fig. 1.10c. There, every node takes a global decision on its own after

collecting the sensing information from sensing entities. Note that the distributed sensing scheme may be slowed down by a large number of signalling messages exchanged in the network.

Cooperation in a network may be implemented not only in the centralised, cluster-based or distributed manner. Relaying topology may also be adopted. Here, local sensing information is directed according to channel qualities experienced by a node. If its sensing or reporting channel is weak, the node may decide to cooperate with its neighbours in order to increase the detection probability. This cooperation may include relaying the reported sensing messages by another node to the FC or a selected node (if the direct reporting channel has poor quality). This is illustrated in Fig. 1.10d, where some channels between nodes are active, while others are not used. Note that the relaying procedure introduces the problem of delays in the network where the message is relayed by a number of nodes. Moreover, a high complexity of network management may be observed here.

Detailed discussions on sensing network topologies, efficient data exchange, clusters and cluster head management can be found in the rich literature on wireless sensor networks, such as [14, 84, 93, 96].

**Identified trade-off in the sink node selection.** The trade-off that exists in the FC (also called sink-node) selection phase can be characterised as follows. The more links between the nodes involved in exchanging of sensing information, the longer the duration of this phase and the more energy is consumed for this purpose. However, each topology should be analysed separately, since the topology selection highly affects this trade-off. A simple comparison of pros and cons for each proposed topology is presented in Table 1.2 below.

**Table 1.2:** Pros and cons for selected topology

Topology	Pros	Cons	Reference
Centralised	<ul style="list-style-type: none"> <li>• Detailed information acquired by the sink node, thus a more reliable decision made.</li> <li>• For <math>N</math> nodes, <math>N - 1</math> messages have to be transmitted (fewer than in the decentralised case).</li> </ul>	<ul style="list-style-type: none"> <li>• Assuming that sensing messages are transmitted via a dedicated control channel, the need for delivery of <math>N - 1</math> messages results in high quality-requirements for this channel.</li> <li>• The higher the number of nodes, the longer the phase of single-node decision collection.</li> <li>• The more nodes, the longer the average distance between the sink node and the <math>i</math>-th node, thus, the more energy used for the transmission of sensing information.</li> </ul>	[63, 108, 129]
Continued on next page			

Table 1.2 – continued from previous page

Topology	Pros	Cons	Reference
<b>Cluster-based</b>	<ul style="list-style-type: none"> <li>• The number of links is the same as for the centralised topology.</li> <li>• The time required for message delivery can be reduced by a factor close to the number of cluster heads, i.e., message delivery from individual nodes to cluster heads can be realised in parallel.</li> <li>• The average distance over which the message has to be sent is smaller compared to the centralised topology, thus lower transmit power can be used.</li> </ul>	<ul style="list-style-type: none"> <li>• Data processing in each cluster head may consume a considerable amount of energy.</li> <li>• In mobile networks, the frequency of invoking the cluster-head selection procedure may increase compared to the centralised-topology case, where the procedure of centralised node selection may be less frequent.</li> </ul>	[54, 98, 156, 178]
<b>Decentralised</b>	<ul style="list-style-type: none"> <li>• The number of links can be highly reduced, as each node makes a decision on its own.</li> <li>• If relaying is not allowed, each node collects sensing messages only from the surrounding nodes.</li> </ul>	<ul style="list-style-type: none"> <li>• If each node gathers information from all other nodes, the number of sensing-messages transmissions grows significantly.</li> <li>• The energy required for data processing in each node may be high (the scheme may be inefficient in terms of energy consumption).</li> </ul>	[27, 57]
<b>With relays</b>	<ul style="list-style-type: none"> <li>• The number of links is similar as in the centralised-topology case.</li> <li>• Distances between neighbouring nodes are shorter than the average distance in the centralised scheme.</li> <li>• The time required for message exchange depends on the longest route in the sensing network, but is shorter than in the centralised-topology case.</li> </ul>	<ul style="list-style-type: none"> <li>• As in the cluster-based scheme, the energy required for data processing in each relay increases the energy consumption in a network.</li> <li>• There is a need for fast and accurate route selection, which also consumes energy and time.</li> </ul>	[94, 169, 180]

### 1.2.3 Decision Fusion

After collecting the local sensing results, an effective fusion has to be performed by a selected sink-node (e.g., fusion centre). This is actually done by adopting the fusion rule [69, 105, 137, 142] and making the final decision [74, 107, 162, 176]. Various rules are possible, and their comparison is possible after the adoption of relevant global metrics. These are associated with cooperative decisions based on local decisions acquired from  $N$  secondary (sensing) nodes. Assuming the general  $k$ -out-of- $N$  rule (where a positive decision is made only if the number of positive answers is not lower than  $k$ ), the global probability of false alarm  $Q_f$  and the global probability of detection  $Q_d$  can be obtained as follows [177]:

$$Q_f = \sum_{i=k}^N \binom{N}{i} P_f^i (1 - P_f)^{N-i}, \quad (1.11)$$

$$Q_d = \sum_{i=k}^N \binom{N}{i} P_d^i (1 - P_d)^{N-i}, \quad (1.12)$$

where  $P_f$  and  $P_d$  are averaged over the statistics of  $N$  nodes, so for instance,  $P_f$  is equal to:

$$P_f = \frac{1}{N} \sum_{i=1}^N P_{f,i}, \quad (1.13)$$

and  $P_{f,i}$  represents the probability of a false alarm of the  $i$ -th node. General formulas (1.11) and (1.12) may be modified in order to express three widely used fusion rules: the *OR*, the *AND* and the *majority* rule. Moreover, for any specific rule, the global probabilities of false alarm and detection are obtained in an analogous way, therefore only formulas related to detection quality are presented. In the case of the AND-rule ( $N$ -out-of- $N$  rule) and the OR-rule (known as 1-out-of- $N$  rule) the above formula for  $Q_d$  is simplified to:

$$Q_d^{\text{AND}} = \prod_{i=1}^N P_d = P_d^N, \quad (1.14)$$

$$Q_d^{\text{OR}} = 1 - \prod_{i=1}^N (1 - P_d) = 1 - (1 - P_d)^N, \quad (1.15)$$

respectively. Furthermore,  $Q_d$  for the majority-rule, when at least half of the nodes have to detect the PU activity, is given by:

$$Q_d^{\text{MAJ}} = \sum_{i=\lceil N/2 \rceil}^N \binom{N}{i} P_d^i (1 - P_d)^{N-i}. \quad (1.16)$$

The Constant False Alarm Rate (CFAR) scheme assumes that in the network the global probability of false alarm  $Q_f$  remains constant, i.e., is set for the whole secondary network. Thus, the corresponding value of  $P_{f,i}$  is assumed to be identical for every node and can be obtained for the OR rule as:

$$P_{f,i} = 1 - \sqrt[N]{1 - Q_f} \quad \text{for } i = 1, \dots, N. \quad (1.17)$$

Thus, the aim of the CFAR scheme is to maximise the received probability of detection. On the other hand, under the Constant Detection Rate (CDR) requirement, the value of  $Q_d$  is set for the network, while the false alarm probability is minimised. The network starts in this case with assumed local probabilities of detection for each node (which are stated in an analogous way as for CFAR).

**Identified quality versus energy-efficiency trade-off in the decision fusion.** The analysis of the quality versus energy-efficiency trade-off, in the case of decision fusion, is not straight-forward. The application of OR rule approach results in a high probability of detection and a high probability of a false alarm, thus also in a low probability of a potential collision with a PU. However, this also means that the probability of data transmission by a SU is reduced as well. Moreover, including the influence of the transmission channel, one can observe that the OR rule can result in the lack of identification of transmission opportunities. In such a case, the spectral efficiency (and thus also the energy efficiency) is very poor. On the other hand, the AND

rule can be described in a *reversed* way. Thus, one can generally say that there is a trade-off between the certainty of the decision made by a fusion centre and the energy efficiency. However, this observation is not valid in all cases. If the probability of detection is low, the number of potential collisions with a PU increases leading to an increase of retransmissions for both the PU and the SU, and in consequence, to a lower energy efficiency. Finally, as mentioned above, typically, the assumed level of uncertainty (either in terms of  $Q_d$  or  $Q_f$ ) must be assumed as constant in the network. Thus, the selection of the rule will depend highly on the topology.

#### 1.2.4 Global Decision Reporting

The last step in the CSS scheme is sharing (spreading) the global information and the global decision on the spectrum vacancy. In the centralised topology, until this step, every node is aware of the local decision. However, it is the awareness of the global decision that can create the expected gain in the cooperative network. To this end, the central entity spreads the global decision usually by sending a broadcast message. Then, based on this received information, the nodes plan future actions.

Unlike in the centralised scheme, in the distributed scheme, there is actually no need for sending the global decision. Here, the nodes acquire the information about their neighbours' observations during the local-decision reporting stage. Although this involves additional reporting messages, the decision fusion is performed by each node separately, and no broadcast message with a global decision is needed.

Finally, in the clustered scheme, the global decisions are sent back to the cluster-heads, and these nodes are in charge of the further distribution of this message within the controlled group of nodes.

**Identified quality versus energy-efficiency trade-off in the global decision reporting.** Global decision reporting phase of CSS is rather short and requires the delivery of the final decision to all nodes. However, one of the questions that can be posed here is the following: is it more energy-efficient to broadcast the information to all nodes or to reduce the transmit power and deliver this decision to the cluster heads, and allow them to further redistribute this message to more distant nodes?

**Trade-offs' impact on energy efficiency.** The identification of the existing trade-offs in each phase of CSS shows that there is a high number of degrees of freedom in the optimisation of the energy efficiency of cooperative sensing networks. Moreover, some of these trade-offs are mutually dependent, and overlap, making this problem even more challenging. This issue is further analysed in Chapter 4, where one may find how selected key aspects of CSS are structured.

### 1.3 Time Domain Relations between Spectrum Sensing and Spectrum Access

In general, SU needs to periodically sense the availability of the considered frequency band (either in a cooperative or non-cooperative manner), and if the band is vacant, it can start or continue its transmission in this band (can access the spectrum). Such an exemplary situation is illustrated in Fig. 1.11, where one sensing and data-transmission period is shown. One can

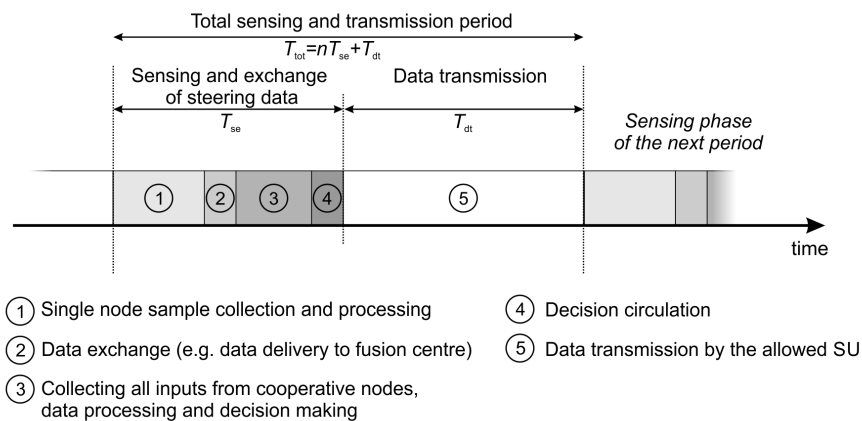


**Figure 1.11:** Illustration of the sensing and data transmission period

observe that the sensing phase consists of four sub-phases, i.e., the time needed for single-node spectrum sensing (including the collection of samples and their processing), the time required for decision delivery to the so-called fusion centre (in the centralised case) or its exchange among neighbouring nodes (in the distributed case), and finally, the time needed for data processing in the fusion centre and decision circulation among interested nodes. The total duration of this phase can be denoted as  $T_{\text{se}}$ . If the decision for a given SU is not positive, i.e., the considered frequency band is occupied, the spectrum sensing phase has to be repeated until the spectrum is free. Once it is available, the SU can transmit its data over period  $T_{\text{dt}}$ . Assuming the total number of spectrum sensing phases equals  $n$ , the duration of the sensing and data transmission period can be calculated as  $T_{\text{tot}} = n \cdot T_{\text{se}} + T_{\text{dt}}$ . This observation is true if the sensing node performs the sensing procedure asynchronously until it determines that the frequency band is vacant, i.e., the next portion of samples is collected either continuously or after a short period. The formula is different if the synchronous approach is applied, in which each sensing period  $T_{\text{se}}$  is succeeded by a transmission period  $T_{\text{dt}}$ , i.e., when the sensing node detects that the wanted spectrum is occupied, it waits over time  $T_{\text{dt}}$  until the next sensing period begins. Thus, for  $n$  tries, the total time equals  $T_{\text{tot}} = n \cdot T_{\text{se}} + n \cdot T_{\text{dt}}$ .

The above considerations lead to the conclusion that in order to maximise the spectral and energy efficiency of the sensing-based opportunistic spectrum access, the sensing period should be optimised to allow for reliable detection of spectrum opportunities, and at the same time, leave enough time for actual information-data transmission. This sensing-throughput trade-off has gained significant attention recently that resulted in a number of works treating the subject of sensing time optimisation (the most relevant ideas are described in Section 4.3), as well as regarding the spectrum access. The exemplary paper may be [76], where SU access is maximised through the penalties policy regarding interference with a PU, and [29], where an adaptive random access protocol is described.

One of the key trade-offs in spectrum sensing is to adjust the sensing time and the spectrum-access time. The first one impacts sensing reliability (and thus, the PU protection and their throughput), the latter—the SU spectral efficiency. Both impact the energy efficiency of a system: the longer the sensing time, the more energy is spent on sensing, the less time is left for

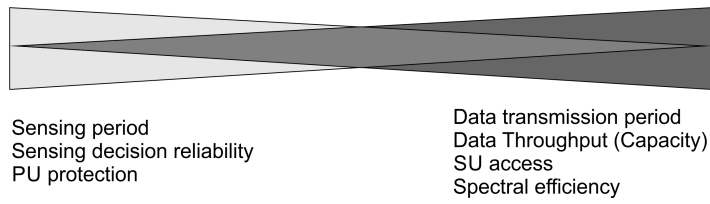


**Figure 1.12:** Sensing period-data transmission period trade-off observed in spectrum sensing

actual SU transmission, the lower the throughput, and the lower the energy efficiency of the SU transmission. On the other hand, a longer sensing time increases the sensing reliability and decreases the interference level experienced by both the PUs and SUs, which results in higher PU links throughput and higher energy efficiency of their transmission. Therefore, the sensing period has to be carefully adjusted in order to guarantee a given level of sensing reliability (and PU protection), which is meant as a sufficiently low false alarm rate and an instantly high detection rate. A shorter sensing time and a longer data transmission period usually result in a higher spectral efficiency, due to higher throughput and increased capacity. This trade-off is illustrated in Fig. 1.12.

As discussed above, optimisation of the sensing- and access-time alone might be contradictory goals, therefore, it has been proposed to analyse these two jointly. For instance, in [165], the authors suggest a joint optimisation of the spectrum sensing period and the transmission stage (spectrum access). They prove that there exists a suitable proportion between the sensing period and the access period guaranteeing the highest channel efficiency, i.e., a suitably low false alarm rate for a minimised sensing period. Similarly, in [99], under detection and energy-based detector constraints, an optimal sensing period is delivered that maximises the throughput. Secondly, cooperative detection is applied where the optimal sensing period is shortened, when compared to a non-cooperative scheme. This conclusion is reinforced in [147]. The cooperation adopted in [147], by forming coalitions, allows the improvement of sensing times and node link capacities. To this end, each SU may make an independent decision on joining or leaving the coalition based on a calculated utility, which jointly optimises the average sensing time and the average acquired capacity. Another joint optimisation of the sensing-and-throughput period is performed in [81]. There, SUs adopt a distributed learning algorithm in order to converge to an evolutionarily stable strategy, where some nodes sense the spectrum, while others may access it. The work puts emphasis on dealing with selfish users who want to access the spectrum without a contribution to sensing. By embedding rewards to the sensing contributors, in the learning algorithm, every node is inclined to apply the required sensing strategy. Finally, in [122], the authors prove that the maximum throughput is gathered for a low number of reported bits and a moderate number of samples.

## Chapter 2

---

# Autonomous Spectrum Sensing

---

### 2.1 Practical Implementations of Selected Spectrum Sensing Methods

In the following section the author of the thesis presents his work on implementation of some autonomous sensing algorithms. In Section 2.1.1, the outcomes of the practical experiment at Sequential Energy Detection (SED) are presented. The method has been analysed in Matlab environment where real-samples of signal acquired by Universal Software Radio Peripheral (USRP) have been processed. Then, in Section 2.1.2, the implementation of SED and cyclostationary-based algorithms is presented. Both methods are implemented in USRP platforms and GNU Radio environment. The comparison of these techniques puts forward the proposal of the so-called hybrid solution described in Section 2.1.3.

#### 2.1.1 Sequential Energy Detection in practical context of real-acquired signal samples

Sequential Energy Detection has gained considerable attention recently. The rationale behind this algorithm is as follows: it stops working at the latest phase after the collection of  $M_s$  samples as the traditional ED algorithm. However, if the decision on the presence or absence of the signal could be made earlier with accepted certainty, the algorithm will stop before gathering all  $M_s$  samples [43]. The goal is to reduce the sensing time in the case where the signal is strong enough (or there is not signal at all) to be detected before collecting the assumed maximum number of samples  $M_s$ . In other words, by decreasing the observation time, uncertainty about the received power value is increased, thus, proper estimation of noise variance becomes a significant problem. More details about sequential energy detection may be found in Section 1.1.2, where one may find, e.g., the definition of thresholds  $\epsilon$ ,  $\epsilon_{LO}$ ,  $\epsilon_{HI}$ .

The presented implementation has been conducted with a USRP N210 device (one may find more information in Section 2.1.2) which has been used to acquire signal samples. The real-acquired-samples were then analysed and processed in Matlab software environment.

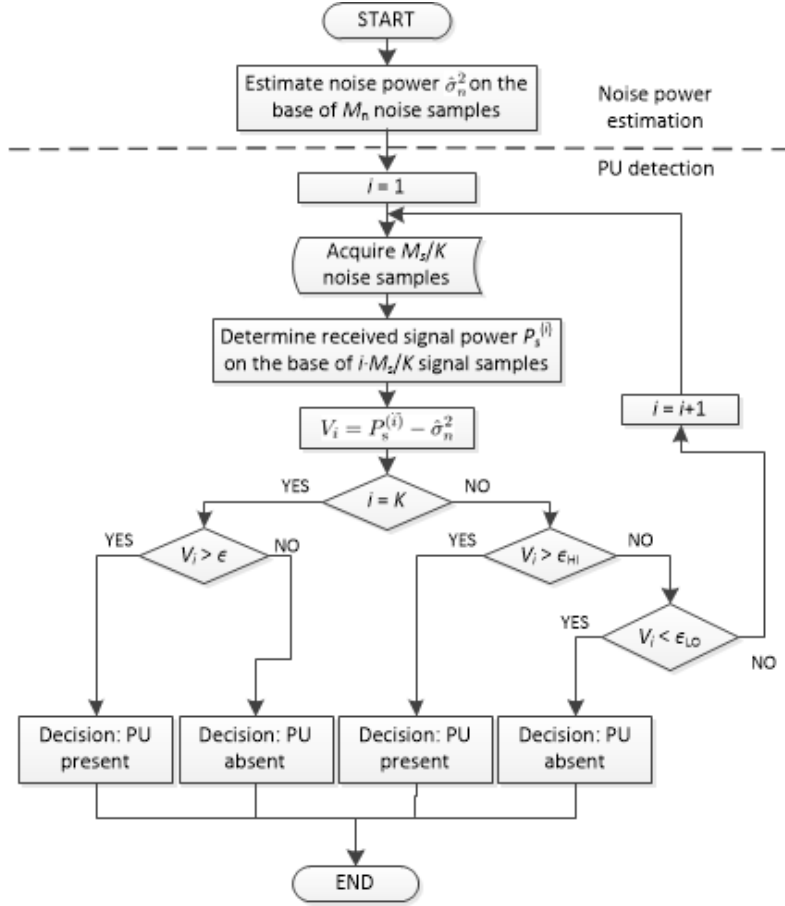


Figure 2.1: Block diagram of a SED model

### Simulation Model

The effectiveness of SED algorithm has been analysed for various number of phases  $K = \{1, 2, \dots, 5\}$ . Detector decision about PU presence/absence is done for the whole observed spectrum portion. The values of thresholds are constantly set as:  $\epsilon_{LO}$  and  $\epsilon_{HI}$  equal to 0.05 and 0.75, respectively,  $\epsilon = 0.4$ . The number of repetitions for one set of parameters is equal to 250 thousands.

In the first preliminary stage a reliable noise estimation is conducted (Fig. 2.1). By taking  $M_n$  noise samples, noise power estimate  $\hat{\sigma}_n^2$  is derived. Then, in the main stage,  $M_s/K$  samples from observed spectrum bandwidth is acquired being the base for calculation of received signal power  $P_s^{(i)}$ , where  $i$  is the index of current phase. Then, the  $V_i$  metric is found:

$$V_i = P_s^{(i)} - \hat{\sigma}_n^2. \quad (2.1)$$

Then, the calculated value is compared with detection thresholds (see eq. 1.5). If the calculated  $V_i$  goes in the  $(\epsilon_{LO}, \epsilon_{HI})$  range, the reliable decision cannot be taken and another portion of  $M_s/K$  samples has to be acquired. Thus, in the second phase of the algorithm, the decision is taken on the basis of samples from the two phases, i.e., on the basis of  $i \cdot M_s/K$  samples.

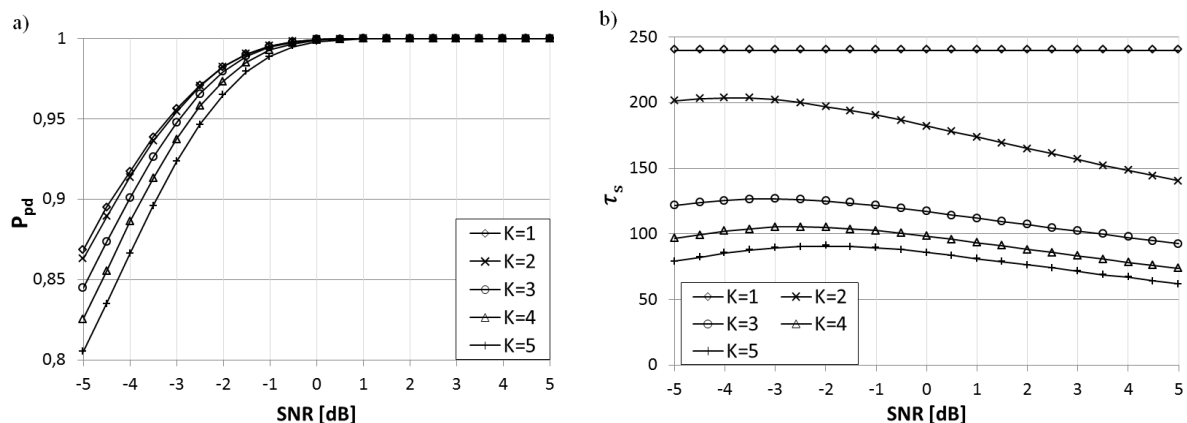


**Figure 2.2:** Results for Sequential Energy Detector proceeded in  $K$  phases: a) probability of proper decision, b) medium sensing time

As it is stated in classical detection theory, the detection quality may be improved by increasing detection time [159], equivalent to the increased number of samples. However, it has been also proved that sensing time increased to infinity does not provide the infinite sensing performance improvement (for clarification see Section 2.3). Thus, the total number of sequential phases is finite. If, after reaching the maximum number of phases and acquiring the maximum number of samples, value  $V_K \in (\epsilon_{LO}, \epsilon_{HI})$ , then as in the classical ED, one-threshold decision is found, i.e., by comparing  $V_i$  with threshold  $\epsilon$ .

### Simulations outcome

The effectiveness of the SED has been assessed in terms of the probability of proper decision for a given SNR:

$$P_{pd} = P_p (1 - P_f) + P_a (1 - P_{md}), \quad (2.2)$$

where  $P_p$  is the probability of PU presence and  $P_a$  is the probability of PU absence, and it is known that:

$$P_p + P_a = 1. \quad (2.3)$$

However, the proper detection has to be undertaken in reasonable time, thus, the second parameter—medium sensing time  $\hat{\tau}_s$ —has been introduced. In order to make the results independent from sampling frequency, this parameter has been expressed as medium number of samples and on the plot axes the unit of  $\hat{\tau}_s$  is the sample. The experiments have been conducted for SNR in the range of  $(-5 \text{ dB}, 5 \text{ dB})$ .

In Fig. 2.2, the comparison of SED performance for various number of phases  $K$  is presented. For each parameter set the number of noise-estimation samples  $M_n$  is 240. One may observe that when  $K$  is increasing, the medium sensing time is lowered but vulnerable to lower sensing performance. Relevant gain in terms of medium sensing time is observed for three-phases case, where 47% time may be saved in comparison to one-phase variant. The greatest time reduction (62%) is possible for the greatest number of phases ( $K = 5$ ), however, this case is burdened with significant reduction of proper decision probability. Thus, the conclusion is that in low-SNR

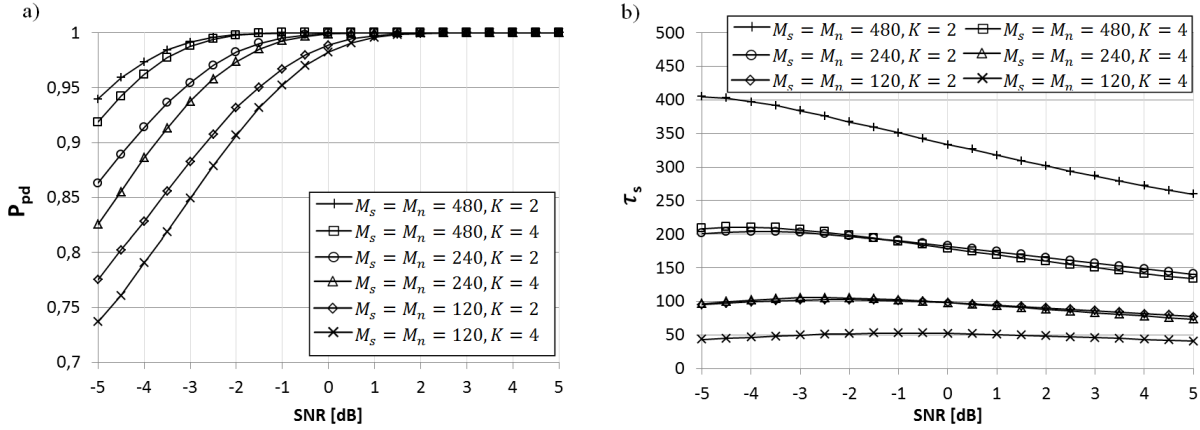


**Figure 2.3:** Sequential Energy Detector results in terms of SNR for *symmetric* cases: a) probability of proper decision, b) medium sensing time

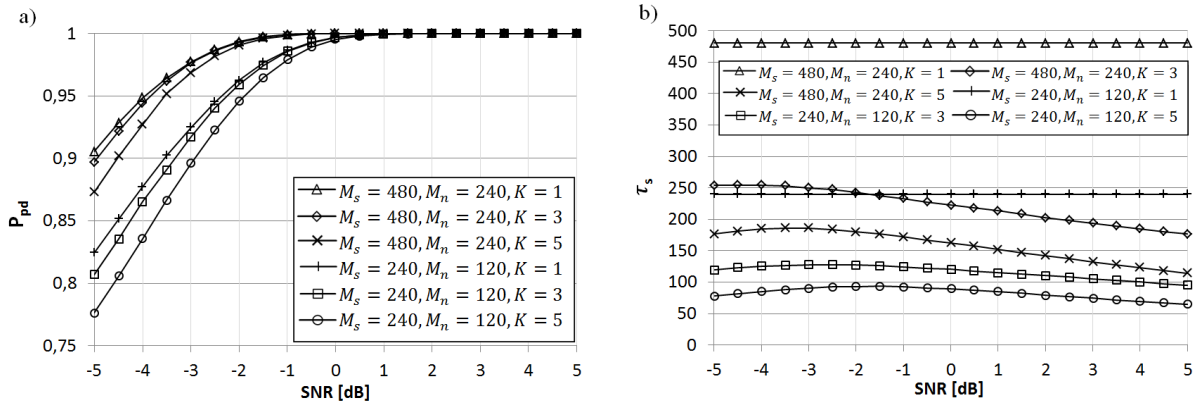


**Figure 2.4:** Sequential Energy Detector results in terms of SNR for *non-symmetric* cases: a) probability of proper decision, b) medium sensing time

region it is possible to lower medium sensing time yet at the cost of performance degradation. However, for SNR higher than 1 dB, when the probability of proper decision is close to 1, the adoption of SED algorithm brings visible and safe gain—it is possible to shorten the sensing time without performance degradation. This conclusion lays the foundation for the so-called hybrid approach, described in detail in Section 2.1.3.

Apart from the different number of phases, the influence of proper noise estimation has been also analysed. In Figs. 2.3 and 2.4, the results for two following cases have been specified: symmetric one (Fig. 2.3), where the number of collected samples during noise estimation phase and detection phase are equal  $M_s = M_n$ , and non-symmetric (Fig. 2.4), where the number of samples collected during noise estimation phase is limited  $M_s > M_n$ .

Detailed analysis of figures may indicate that there exist variants from distinct groups with the similar medium sensing time. For instance, in Fig. 2.3b this phenomenon may be observed twice (1.  $M_s = M_n = 120, K = 2$  and  $M_s = M_n = 240, K = 4$ ; 2.  $M_s = M_n = 240, K = 2$  and  $M_s = M_n = 480, K = 4$ ). Although, the medium time is similar in these cases, the proper decision probability is different: it is higher for cases where more sequential steps are considered

at all. Moreover, one should note that the single portion of acquired samples is equal for both cases. Therefore, the following observation may be posed: the higher number of possible phases does not increase the medium sensing time but it may enhance the so-called quality of sensing. Two reasons for this situation may be stated. First, higher  $K$  value induces greater number of degrees of freedom. If the sensing observations are reliable, then the decision will be taken very soon, however, if it is not possible, then the additional number of samples will be loaded, thus increasing the probability of proper decision. The second reason is the influence of the noise samples number. Precise noise estimation results in higher detection performance. This vulnerability of ED is deeply analysed in Section 2.3.

Regarding the proper noise estimation, one may find the results for non-symmetric cases which are presented in Fig. 2.4 interesting. In these variants the number of noise estimation samples is two times lower than the number of signal-power-estimation samples. In general, the results for non-symmetric cases are significantly worse than for symmetric ones. For instance, in the case described as  $M_s = 480, M_n = 240, K = 5$  similar medium sensing time is observed as in  $M_s = M_n = 480, K = 4$  (Fig. 2.3b), however, it is corrupted by lower probability of proper detection.

## Conclusion

The analysis of the Sequential Energy Detector has shown that it is possible to shorten the time of spectrum sensing for a moderate SNR region without detection performance degradation. Moreover, it is beneficial to increase the number of sequential phases, while keeping the medium detection time unchanged, resulting in increasing the probability of detection. Thus, these observations are the basis for the hybrid approach described in Section 2.1.3. During experiments it has been shown that proper noise estimation plays a key role in the ED-based spectrum sensing. This aspect is analysed further in Sections 2.2 and 2.3.

### 2.1.2 Experimental Sensing Measurements of Energy Detection and cyclostationary-based algorithms

In the practical implementation, the simplest spectrum sensing method capable of detecting the presence of a PU signal is the one based on energy detection which is a semi-blind method [118]. However, as stated in Section 2.1.1, ED is vulnerable from low detection reliability when compared to other sensing techniques. Experimental results shown above and taken from literature of the energy detector outlined impact of noise uncertainty on the performance of detection [17].

In this section, the main aim of the conducted experiment is to sense the spectrum at a given frequency range and makes the decision as reliable as possible on the potential presence of the PU signal in the observed spectrum fragment. Thus, in the following section two sensing methods are implemented and compared: SED, and Symmetry Property of Cyclic Autocorrelation Function (SPCAF) which is a kind of a blind method, described in detail in Section 1.1.3. Both methods were implemented in hardware and software.

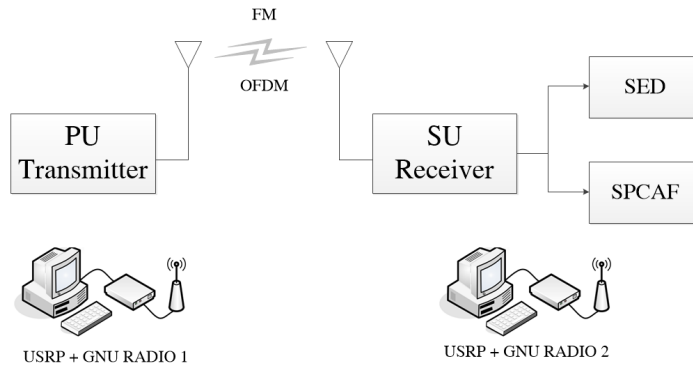


**Figure 2.5:** Experimental setup diagram

### Hardware/Software overview

The performance of the selected spectrum sensing algorithms has been verified in conducted experiments realised by means of USRP boards by Ettus Research being a part of the National Instruments Company. USRP platforms, as the low-cost and high-quality realisation of the Software Defined Radio (SDR) concept, deliver various functionality allowing efficient, real-time realisation of even very complicated wireless systems that operate in the Radio Frequency (RF) band. The main role of the USRP platform is to convert the digital base-band signal delivered from the computer to analogue signal in the RF band and vice versa. This process is carried out in two steps. In the first step, the digital signal is converted to the digital Intermediate Frequency (IF) domain; this phase is realised in the so-called mother-board, being the basis of the USRP platform. After that the signal is converted from digital to analog in the 16-bit Digital-to-Analog Converter (DAC) working with the speed of 400 MS/s. Then, the analogue IF signal is processed in the dedicated daughter-board, where it is transformed to its analogue form in RF band. Finally, the signal is radiated by means of the mounted RF aerial. The variety of available daughter-boards creates imposing opportunities to the user, since these are designed to convert the IF signal to different part of the RF spectrum. Being the realisation of the SDR concept, USRP is steered from the software level, i.e., the whole data processing in the base-band is realised on the computer side. Various software platforms can be applied for that purposes, including commercial and open-source solutions.

In the presented experiments, two USRP boards have been utilised: the PU signal has been generated by means of the first board, whereas the second one has been used for spectrum sensing purposes and acted as the Secondary User. The whole software processing has been realised in the open-source GNU Radio environment [138]. It is based on combination of C++ and Python programming languages; the former possesses the functionalities of given blocks (e.g., responsible for samples reception or FFT), the latter—is used for blocks connection (e.g., classifying interfaces and input/output types).

In the experiment, two sensing scenarios were considered: first, with the PU narrow-band Frequency Modulation (FM) signal, and second, where the PU transmits Orthogonal Frequency-Division Multiplexing (OFDM) signal. During the measurements, the PU and SU were located in one room and separated by a distance of 2 m.

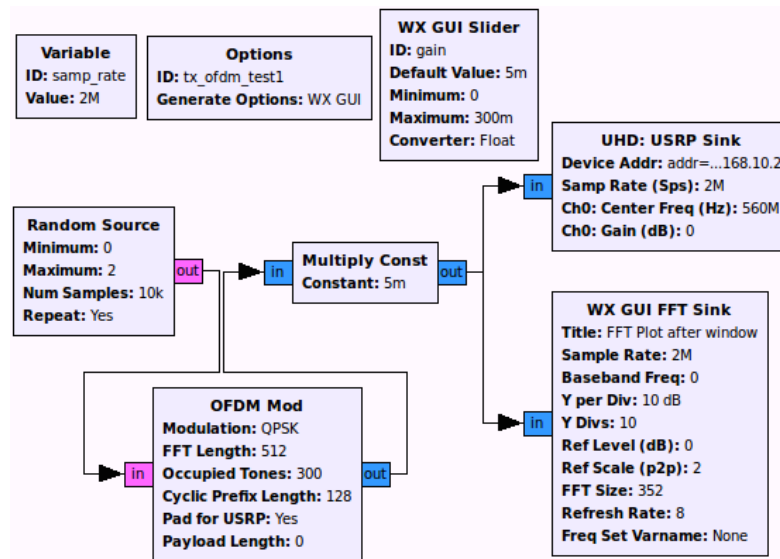


Figure 2.6: Scheme of the Primary User OFDM transmitter realised in the GNU Radio

### Transmitter side

At the transmitter side, two types of signals were generated, the narrowband FM signal, and wideband multicarrier signal based on OFDM. In the former case, the composite radio signal was created and frequency modulated before sending to the USRP board via Ethernet cable. It means that assumed frequency deviation ( $\pm 75$  kHz deviation from the assisted centre frequency) in the bandwidth of the spectrum occupied by the FM signal is narrow (144 kHz). On the contrary, the spectrum of the multicarrier signal is assumed to be wider—the OFDM symbol with 512 subcarriers of the width 1.2 MHz is used.

As it has already been mentioned, the base-band processing was realised on the PC in the GNU Radio environment, and in particular in the graphical tool called GNU Radio Companion (GRC), where the whole system was built from blocks. The example of the program is presented in Fig. 2.6, where the illustration of the OFDM transmitter implementation is shown. The *Random Source* is the signal source block that generates repeatedly random data, which is mapped to Binary Phase Shift Keying (BPSK) symbols and then is the subject of OFDM modulation (realised in an *OFDM Mod* block). 300 subcarriers out of 512 available are occupied, while the applied cyclic prefix is  $1/4$ . The signal samples are then sent to the local spectrum analyser (*FFT plot*) and to the USRP (*USRP Sink*), responsible for sending data to the USRP platform. Note that due to the complex sampling frequency equal to 1 MS/s, the observed bandwidth is 1 MHz while the centre frequency is 560 MHz. This TV band frequency is one of the most ‘pure’ bandwidths, where the level of interference from distant digital-television stations is sufficiently low in the location where the experiment was conducted.

### Receiver side

In the receiver, as indicated in Fig. 2.5, two spectrum sensing algorithms are implemented: the one based on energy detection, and the second—on the cyclostationary features analysis. As in

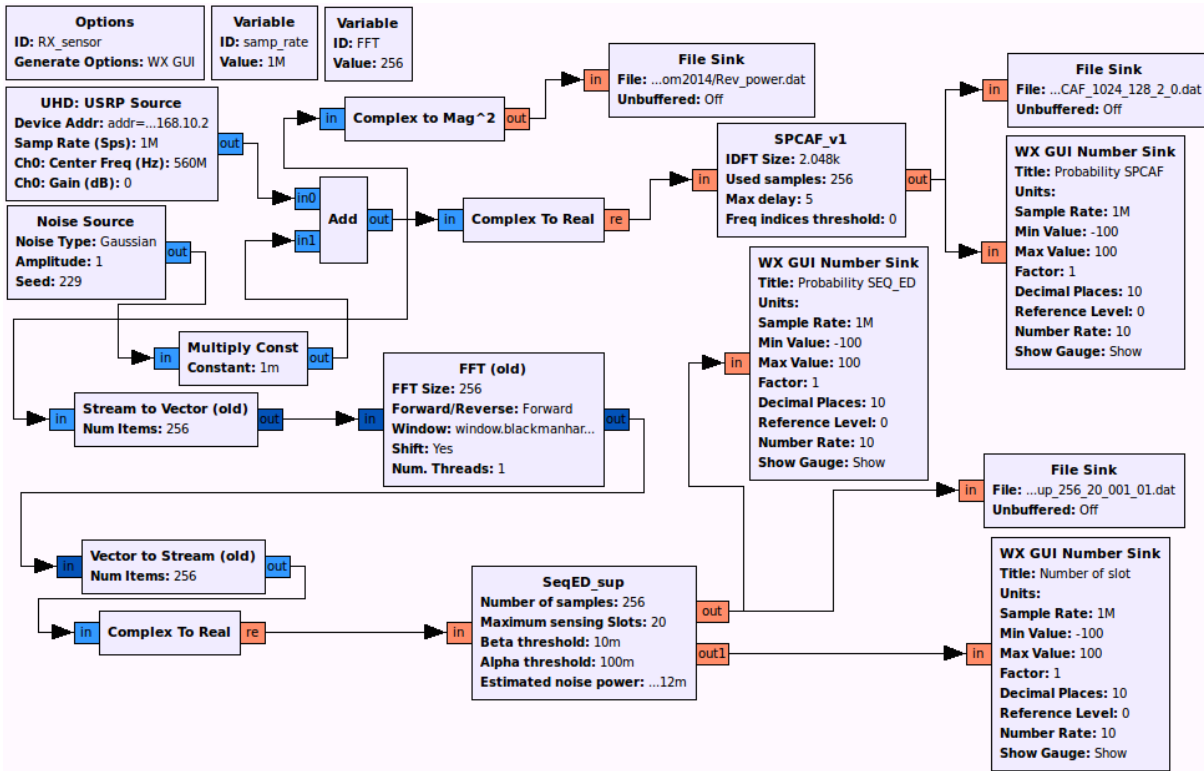


Figure 2.7: Scheme of the Secondary User receiver realised in the GNU radio

the transmitter chain, the whole base-band processing in the receiver that is performed in the SU was realised in the computer side with the GNU Radio environment. The schematic diagram of blocks being the receiver is shown in Fig. 2.7.

The *USRP Source* block realises signal samples delivery from USRP to the computer via USRP Hardware Driver (UHD). The signal is then summed with artificial noise generated in *Noise Source* block. After adder, it is split into two parallel chains: *i*) cyclostationary-based algorithm chain (upper chain), *ii*) Sequential Energy Detection (SED) algorithm chain (lower one). Both sensing techniques operate on the same set of received samples making the comparison fair. In the SED detector chain, the signal is transformed to the frequency domain in *FFT* block. Then, the key functionalities of SED are implemented in *SeqED\_sup* block, where the sensing decision on the occupancy of each frequency bin is done separately. The decisions are finally transferred to the graphical sink. In the upper processing chain, devoted to the SPCAF algorithm, the signal is converted from complex to real type, and such modified signals are subject to processing in the *SPCAF\_v1* block, realising the functionality of the SPCAF algorithm described in Section 1.1.3. Please note that these two key blocks (*SPCAF\_v1* and *SeqED\_sup*) have been written in C++ from scratch and added to the GNU Radio block list.

## Experimental results

During the measurements, the performance of the sensing algorithms was compared in two scenarios: narrow-band and wide-band PU signal.

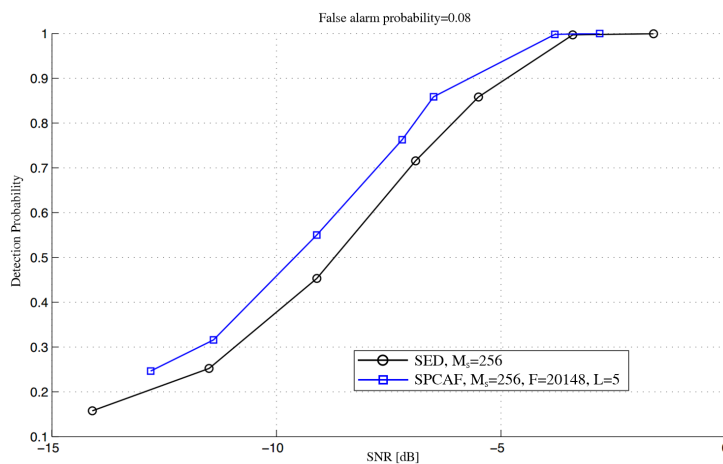


**Figure 2.8:** Probability of detection  $P_d$  vs SNR for Primary User FM signal ( $P_f = 0.08$ )

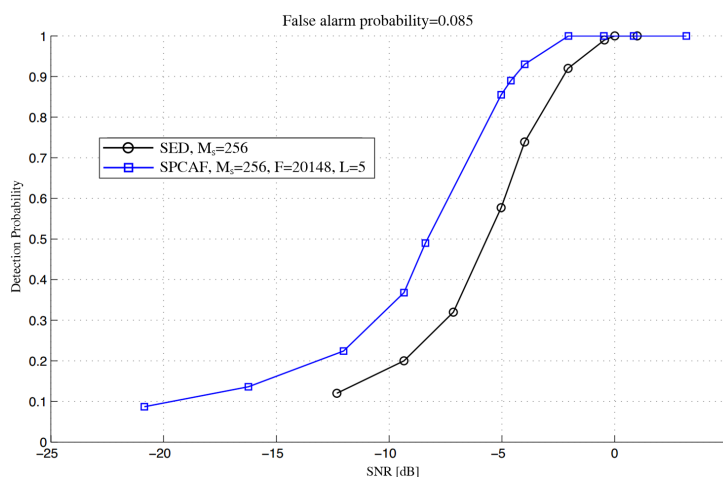


**Figure 2.9:** Probability of detection  $P_d$  vs SNR for Primary User OFDM signal ( $P_f = 0.085$ )

In the first scenario, a Frequency Modulated signal is used as Primary User's signal. In the experiments, the central carrier frequency is set to  $f_c = 560$  MHz. Under Constant False Alarm Rate (CFAR) with probability of false alarm equal to  $P_f = 0.08$ , the detection probability ( $P_d$ ) vs SNR has been analysed (Fig. 2.8). Proper SNR estimation is based on the noise power  $\hat{\sigma}_n^2$  estimation conducted at the receiver *a priori* with no transmitted signal. Then, the transmitter power is appropriately tuned in order to obtain a desirable SNR. The parameters of the SPCAF detector are as follows: the maximum value of the lag parameter is  $L = 5$  and the FFT size is  $F = 2048$ . In Fig. 2.8 the detection probability of the SPCAF is higher at about 0.1 than for SED in the range of the SNR from  $-13$  to  $-3$  dB. The number of samples processed by the SPCAF is equal to  $M_s = 256$ , while in the SED the minimum number of samples is  $M_s$ .

In the second scenario, the Primary User signal is an OFDM signal. Fig. 2.9 shows the detection probability achieved by the Secondary User for SPCAF and SED, while maintaining the false alarm probability below 0.08. Based on the Fig. 2.9, it can be concluded that the  $P_d$  for SPCAF is significantly higher than for SED, about  $0.1 - 0.3$  for  $\text{SNR} = (-12, -2)$ .

These results may lead to the conclusion that cyclostationary-based sensing guarantee higher detection rate than ED-based techniques. This is true for the low SNR region, which is a key area in signal detection. However, for substantially high signal-to-noise ratios, which are also the case in detection, it is not worth adopting feature-based detection. Energy-detection based solution guarantee sufficient detection level. The key question is how to distinguish the case where there is a low SNR, and an advanced but costly technique is desirable from high-SNR case where energy and time-efficient ED-based technique may be applied. The answer is the concept of a hybrid structure of the spectrum sensing algorithm introduced in Section 2.1.3. In such a case, the low-complex double-threshold algorithm should be applied in the first phase, followed by the cyclostationarity-based one. When the PU signal is strong enough or the observed signal variance is close to the noise variance, the sequential energy detection algorithm is going to make a reliable and time-efficient decision. On the other hand, if the energy-detection procedure is not able to produce a reliable decision after collecting  $M_s$  signal samples, the feature-based algorithm shall be applied for final decision. It is also, however, important to check other parameters which classify the aforementioned algorithms apart from detection quality. The first is to calculate the efficiency of sensing method understood as, e.g., a number of operations needed for producing sensing decision. It is directly connected with energy efficiency and medium sensing time.

## Conclusion

Above, in this section, details and results of practical implementation of the energy and cyclostationary-based sensing techniques have been presented, conducted by the author of the thesis in cooperation with partners from Supelec, France [118]. Two sensing techniques have been implemented using the USRP platforms and GNU Radio software. The processed results show that the cyclostationary-based solution guarantees a higher detection rate than the energy-based one but is characterised with higher computational complexity. However, if SNR is sufficiently high, there is no reason to apply cyclostationary feature detection, thus, it is beneficial to adopt the *hybrid* approach presented in the following subsection.

### 2.1.3 Hybrid Approach for Spectrum Sensing Using USRP and GNU Radio

As ED imposes very low complexity burden to the CRT, other noise-independent methods that are based on, e.g., cyclostationarity property or angles-of-arrival are characterised by high complexity, which is the price of enhanced reliability. This existing trade-off between the reliability and complexity leads to creation of the hybrid approach. When the detected signal is strong, the SED method could be used, while for low SNR region, cyclostationary-based sensing is conducted.

This connection allows one to sustain advantages of the two methods, overcome their drawbacks and, with the use of the latter scheme, guarantee total reliability at substantial level while minimising energy consumption and sensing time. Thus, in the proposed hybrid approach (Fig. 2.10), the detection is conducted by the SED algorithm first and for a very weak or very strong PU signal (see eq. 1.4), it guarantees reliable and fast sensing decision. However, if the reliable decision cannot be taken after reaching maximum of  $K$  sequential phases, the SPCAF algorithm is applied to proceed with the already collected signal samples. Intuitively, the performance

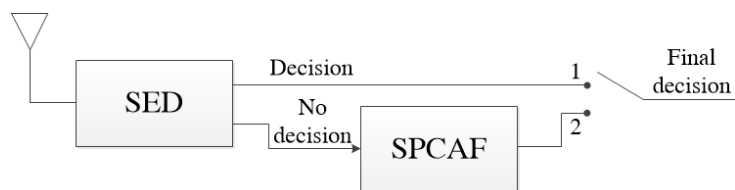


**Figure 2.10:** Scheme of the hybrid spectrum sensing detector

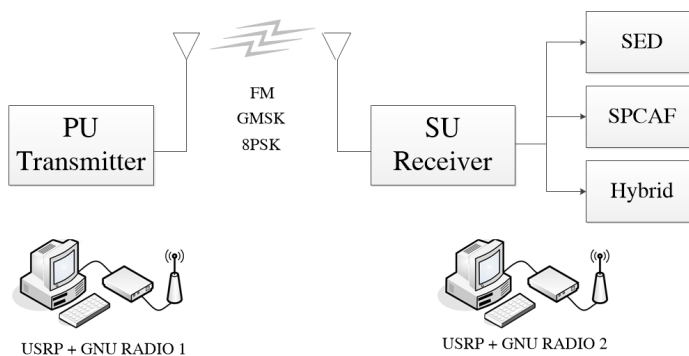


**Figure 2.11:** Experimental setup diagram

of the proposed solution should be close to the results obtained by the cyclostationarity-based algorithms; however, the sensing time shall be reduced.

### Brief Hardware/Software Overview

The applied experimental setup used for hybrid approach verification is based on the one described in Section 2.1.2. The experiments were conducted by means of USRP boards connected with Personal Computers via a Gigabit Ethernet cable. The PU signal was generated in the first board, as distinct from the previous set, in three cases: the Gaussian Minimum Shift Keying (GMSK) signal, the FM signal, and 8PSK signal. In the second board, a SU receiver was working in three modes (Fig. 2.11). The whole software processing was realised in the open-source GNU-Radio environment. More details about the USRP board, its parameters and implementation details may be found in Section 2.2, while the explanation of GRC blocks with illustrations of exemplar programs is drawn in Section 2.1.2.

### Transmitter/Receiver Chain

The transmitter part of the experimental setup is implemented in the GNU-Radio Companion (GRC) environment. This transmitter has three processing chains, where the random sources are connected to FM, GMSK and 8PSK modulators, respectively. The modulated signals are selected by means of the selector block, amplified and sent to the USRP board. In all cases, the centre radio frequency was set to 560 MHz, the complex sampling frequency was defined to be equal to 1 MS/s. The bandwidth of the generated signals are as follows: FM signal – 144 kHz, GMSK – 600 kHz, and 8PSK – 800 kHz. The receiver side is also implemented in the GRC environment. Four parallel processing chains indicate the simultaneous processing of the same samples by different algorithms. For comparison purposes, stand-alone SED and SPCAF algorithms were

used together with the hybrid solution. In the hybrid algorithm, both the sequential energy detector and SPCAF solutions were merged. In the first sensing phase, a decision can be made by the sequential algorithm every time the next  $M_s/K = 128$  signal samples are collected. If the total number of samples  $M_s = 512$  is collected and a reliable decision cannot be made, the SPCAF processes the same set of samples.

### Simulation Results

The simulations have been conducted with the use of the setup described above. The sensing decisions were made within dedicated GNU-Radio blocks, designed for the purpose of this research. In Fig. 2.12 the probability of detection ( $P_d$ ) as a function of signal-to-noise ratio (SNR) for various PU signals is shown.

In every plot, the curve representing the detection efficiency of the proposed hybrid approach is located between the curves of the SED and the SPCAF. This phenomenon can be explained as follows: for certain predefined values of probability of a false alarm, two decision thresholds are calculated and used in the sequential energy detector part (see eq. 1.4). Too restrictive thresholds (i.e., when in most cases the average power of collected samples lies between thresholds  $\epsilon_{LO}$  and  $\epsilon_{HI}$ ) may lead to the case where all decisions are shifted to the second and next phases of the proposed hybrid algorithm. In such a case, the final achieved efficiency is identical as for the cyclostationarity-based algorithm. Such a situation may provide precarious time reduction, thus, the decision thresholds have to be properly matched to guarantee time reduction and possibly low performance degradation. Moreover, it can be observed that the performance of the SPCAF algorithm is persistent, irrespective of the bandwidth of the PU signal. However, in other cases, one may observe that the wider the PU signal bandwidth, the better performance of energy-based algorithms.

Apart from detection quality comparison, it is important to evaluate and compare the sensing time results. While in correlation-based solution time duration is substantial, for SED it may be significantly reduced. In Fig. 2.13, the probability of reaching ‘no decision’ after collection of  $M_s$  samples is presented. The decision thresholds used in the sequential energy detection algorithm were calculated according to a fixed value of  $P_{f,LO} = 0.001$  and various values of  $P_{f,HI}$  as highlighted in Fig. 2.13. For very low and very strong signals, the decisions are made mainly during the first phase, thus, the probability of ‘no decision’ is small. In the mid-SNR region, where the reliable decision cannot be easily made, the probability increases.

Concerning the proposed hybrid spectrum sensing architecture, substantial time reduction is achieved compared to the classical SPCAF architecture. A shorter sensing time is preferable in order to improve the throughput of the cognitive radio network. This phenomenon is the sensing time vs spectrum access trade-off and is highlighted in Section 1.3. Let  $t_H$ ,  $t_{SED}$ , and  $t_{SPCAF}$  denote the sensing time of the hybrid, the SED and the SPCAF detectors, respectively. Then, the sensing time of the proposed architecture, which influences the overall throughput of SU is:

$$t_H(\text{SNR}) \approx \begin{cases} t_{SED} & \text{if } f(\text{SNR}) \ll 1 \\ t_{SED} + f(\text{SNR}) [t_{SPCAF} - t_{SED}] & \text{otherwise,} \end{cases} \quad (2.4)$$

where  $f(\text{SNR})$  is the theoretical probability of ‘no decision’ after SED processing as given in Fig. 2.13 and defined in (2.5):

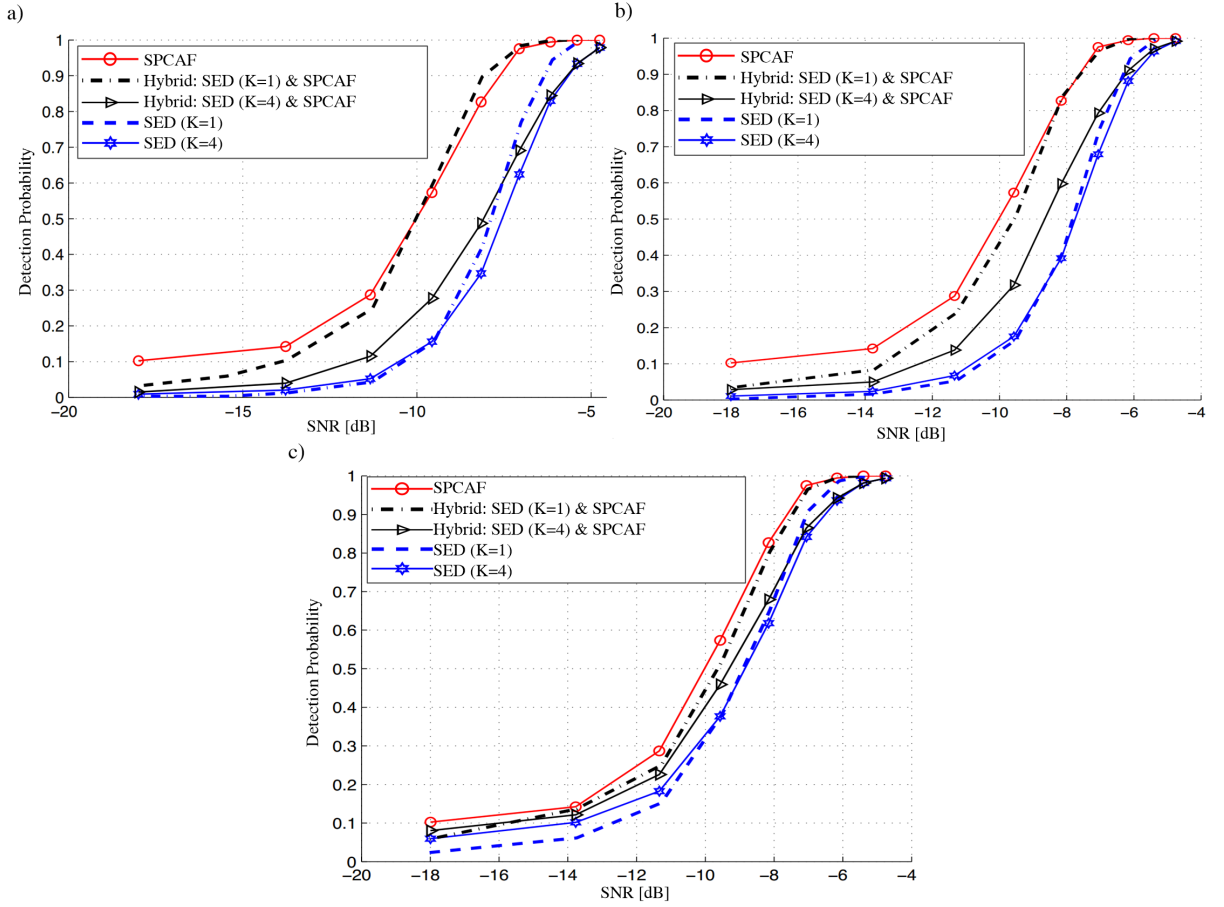


**Figure 2.12:** Probability of detection  $P_d$  vs SNR for various PU signals: a) FM signal, b) GMSK signal, c) 8PSK signal.  $M_s = 512$ ,  $P_{f,LO} = 0.001$ ,  $P_{f,HI} = 0.1$

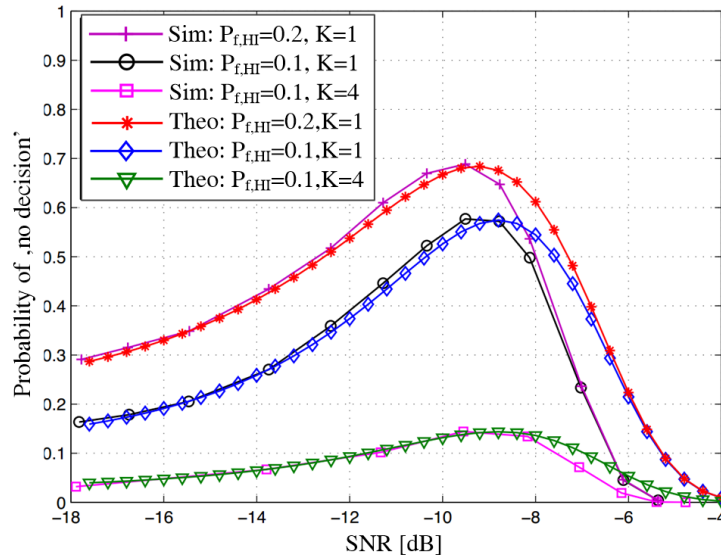


**Figure 2.13:** Probability of 'no decision' state in Sequential Energy Detection scheme after collection of  $M_s/K$  samples.  $P_{f,LO} = 0.001$ ,  $M_s = 512$ , FM PU signal

$$f(\text{SNR}) = \frac{P(P_{M_s} > \epsilon_{\text{LO}}) - P(P_{M_s} > \epsilon_{\text{HI}})}{K}. \quad (2.5)$$

Fig. 2.13 shows the theoretical and the simulated probability that, after the first phase, no sensing decision is made by the SED detector. The tiny difference between the theoretical result and experimental result might be caused by the real experimental environment which differs from the considered theoretical Rayleigh fading channel. Moreover, it can be observed that if just one phase ( $K = 1$ ) is considered in SED, then the probability of no decision increases dramatically in mid-SNR range. In that case the SPCAF detector is often applied, thus, the sensing time  $t_{\text{H}}(\text{SNR})$  is increased. On the other hand, if  $K$  phases is considered, and each contains  $M_s/K$  samples, then the probability of no decision decreases and consequently the sensing time diminishes.

## Conclusion

The idea and performance of the hybrid spectrum sensing algorithm has been presented above, focusing on the quality of detection and sensing time as major factors of reliability and energy efficiency of spectrum sensing. The presented results were achieved in practical experiment implementation conducted with USRP platforms and GNU Radio environment, where the dedicated block for the hybrid sensing scheme was modelled. The presented results show that the hybrid approach merges the assets of the energy and cyclostationary-based schemes. Therefore, it is reliable enough even in low-SNR conditions, and additionally fast for a high-SNR region resulting from applied SED scheme.

## 2.2 The Impact of Hardware Implementation on the Performance of Energy-based Spectrum Sensing Algorithms

Various results of the energy-based methods have been presented in the previous sections, after which ED and SED seem to be solutions with the mediocre complexity and short detection time, but also with high sensitivity to noise power fluctuations [34]. As every noise-variance dependent technique, the ED requires detailed knowledge of the exact value of noise power, which is then used for the determination of the decision threshold. The performance of the energy-based method can be improved by increasing the data collection time (thus number of samples), however, for a given SNR value, an upper bound for the value of  $M_s$  exists, above which no improvement in certainty level can be made (the problem of the so-called *SNR-wall* [159]). Moreover, the longer the sensing time, the shorter the data transmission period and the lower the achievable data rate, as well as lower energy efficiency. Thus, the spectrum sensing phase should be as short as possible to guarantee the assumed decision reliability. Clearly, there are many other ways of increasing the robustness of spectrum sensing algorithms, e.g., through the implementation of more sophisticated solutions (for the price of higher computation complexity) or the application of more processing chains (such as more receive antennas, cooperative sensing, etc.).

However, proper noise power approximation is not a trivial issue, since beside the thermal noise floor, various unwanted effects can also be observed (such as spurious emission, harmonics, I/Q mismatch, leakage of local oscillator, etc.) that influence the behaviour of the implemented algorithms. In this section a detailed analysis of the impact of various observed phenomena on

the performance of ED algorithms is presented. The research is intentionally limited to the ED case; in particular, its sequential version (SED) is analysed and its pragmatic version is proposed.

In order to get the estimated yet accurate value of noise power observed in the given frequency band, the Cognitive Radio Terminal (CRT) should have a possibility of its detailed approximation. The detailed description of noise power estimation problem is presented in Section 2.3. Regardless of the agreed noise estimation method, the problem of other unwanted phenomena also has to be taken into account – the aforementioned ambient noise does not cover all disturbances that can appear in the observed frequency segment. For example, relatively high spikes (a couple of decibels higher than the noise) in the frequency domain can be the product of intermodulation. Moreover, the imperfection of hardware modules used by CRT manufacturers can result in local-oscillator leakage or I/Q mismatch.

The subsequent subsections analyse the influence of the observed effects on the efficiency of the sequential energy detection method.

### 2.2.1 Hardware Implementation Details

The foundation of proper spectrum sensing utilising ED algorithms is a good estimation of the power of noise  $\hat{\sigma}_n^2$ . The detection thresholds used in the considered sequential sensing algorithm (but also in other energy-based solutions) are usually slightly higher than the noise power (about 0.7 – 1.5 dB—see Fig. 1.5). Therefore, the inaccuracy of noise power approximation even at the level of 0.25 dB may cause a high number of false alarms or misdetections. It had been decided to analyse the impact of various unwanted phenomena in a possible practical scenario, where the secondary user would like to perform a transmission in a vacant TV-band. In consequence, in the conducted experiments, the CRT, implemented by means of an USRP N210 board [1], needs to detect the Primary User signal generated by a wireless microphone (being an example of a PMSE device that can operate legally in the TV band). The signal originating from the microphone is frequency-modulated with the deviation set to 75 kHz resulting in the PU signal bandwidth of around 150 kHz. However, with fully charged batteries, the microphone was able to generate signals of the power up to 10 mW. Thus, due to undoubtedly too high generated power, the microphone was kept in an anechoic chamber in order to lower the transmitted power (Fig. 2.14a). The centre frequency of the generated FM signal was set to 540 MHz.

The presented Sequential Pragmatic EnERgy Detection (SPEED) algorithm was implemented by the author of the thesis with an USRP N210 platform (Fig. 2.14b) with a WBX daughterboard and GNU Radio environment. According to the manufacturer [2], the WBX (2.14c) is a wide bandwidth transceiver (50 MHz to 2.2 GHz) equipped with a reception filter of the 40 MHz bandwidth. The noise figure is equal to around 5 dB, while third-order intercept point—to 0 dBm. The phase noise of the WBX board measured at 1.8 GHz is set to  $-80$  dBc/Hz for the offset of 10 kHz. After processing in the WBX board, the analogue I/Q samples are shifted from radio to intermediate frequency and—after analogue-to-digital sampling—processed in the digital domain. The 14-bit Analog-to-Digital Converters (ADCs) work with the speed of 100 MS/s. Next, the signal samples are processed in the Field Programmable Gate Array (FPGA) module (Xilinx Spartan 3A-DSP 3400), where they are digitally down-converted, decimated and managed by the provided network drivers. The decimation coefficient can assume values between 4 and 512. In this work, 8 was applied, which produces a sampling frequency of 12.5 MHz. It should be noted

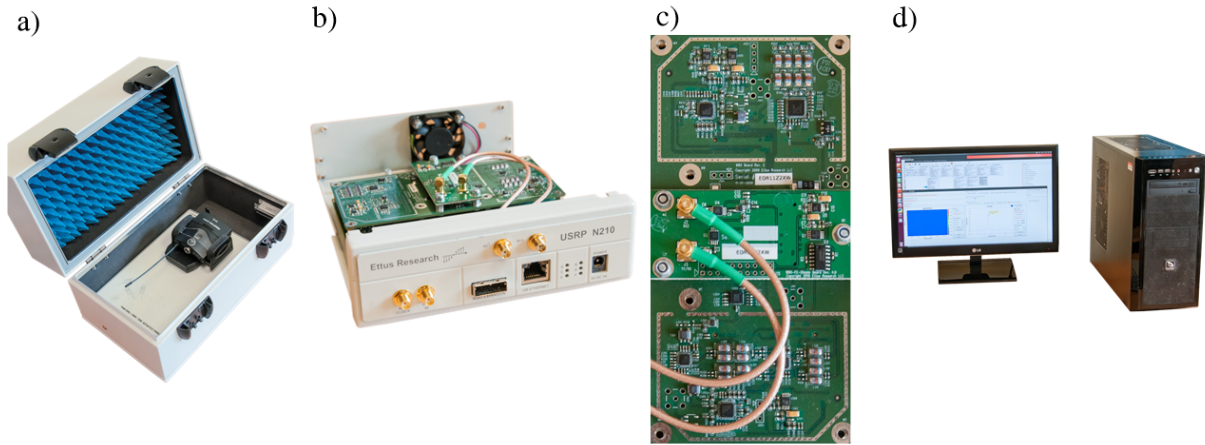


**Figure 2.14:** Hardware employed in the practical implementation experiment: a) PMSE equipment (PU signal) stored in anechoic chamber, b) USRP N210 device, c) WBX daughter-board, d) Personal Computer where sample processing has been conducted

that the band of interest is equal to the effective sampling rate, since the complex sampling is applied. Finally, data is sent via the Gigabit Ethernet cable (offering a maximum bandwidth of 25 MHz) for further software processing. The samples received by the USRP platform are transferred to PC to allow fast software processing (Fig. 2.14d). The 12.5 MHz-wide frequency band with the centre frequency of 541 MHz is considered. At the PC side, the received IQ samples are managed by the USRP Hardware Driver (UHD) [3] and can be processed in GNU Radio. In the application, a 256-point FFT of IQ samples is computed, resulting in the subcarrier bandwidth of  $\sim 48.8$  kHz. Then the counted power for each FFT carrier is collated with lower ( $\epsilon_{LO}$ ) and higher ( $\epsilon_{HI}$ ) thresholds used in the sequential energy detection algorithm. Please note that all collected samples, as well as other important results and parameters achieved by software means (such as samples' distribution etc.), are saved in output files and processed afterwards.

In order to get the most accurate results, the WBX daughter-board was self-calibrated by exploiting built-in procedures provided by Ettus Research LLC. This enabled the correction of IQ imbalance and DC offset at the receiver side. Furthermore, the receiving device was calibrated by application of the following procedure. The USRP was connected to the signal generator which emits a sine (single tone) signal of a known power in dBm. Taking into account all of the losses in the connectors and front-ends, it was possible to compare the original signal power with the one observed in GNU Radio. This way, the values observed in GNU Radio can be translated to dBm.

Moreover, there is a possibility in the USRP to move the DC offset out of the observed band since the power of the Local Oscillator (LO) leakage is relatively high. It is done by adding a frequency offset to the LO in the daughter-board and thus changing the intermediate frequency [4]. The maximum value of the DC-offset shift is 40 MHz.

## 2.2.2 Measurement Analysis

In this section, the measurement results are analysed from the perspective of spectrum sensing methods. First, the problem of DC offset existence is discussed, followed by the analysis of

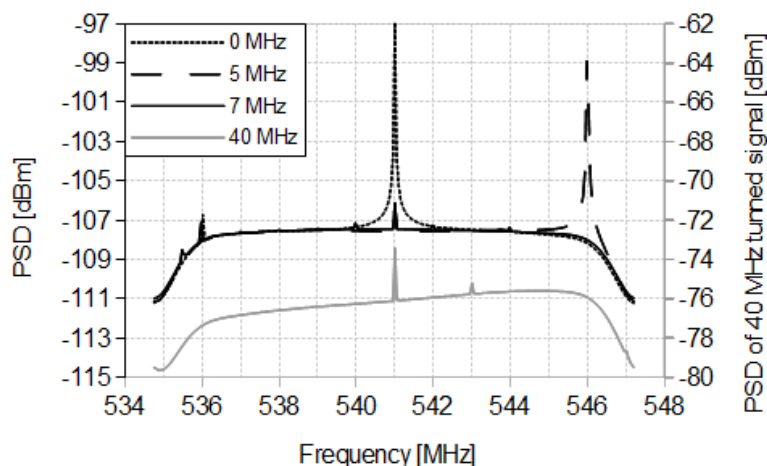


**Figure 2.15:** Noise power for different frequency of tuning  $f_w$

temperature and ambient noise influence on algorithm reliability. Finally, the impact of unwanted effects that appear and change over time is presented.

### DC offset

First, the effects related to the LO leakage are analysed. The presence of high spikes in the middle of the observed band can lead to a higher false alarm probability, thus increasing virtual spectrum occupancy (i.e., when the CRT decides that the spectrum is not free due to the presence of high-power unwanted signals, such as harmonics). In Fig. 2.15, the noise power within the observed 12.5 MHz-width band is presented when the frequency is tuned by  $f_w$  equal to 0, 5, 7 and 40 MHz. For the case of no tuning ( $f_w = 0$  MHz), one can observe a 10 dB peak of the DC offset at the centre frequency. Tuning at the level of 5 MHz results in a DC bias at the frequency of 546 MHz, i.e., 5 MHz away from centre frequency (thus as expected). 7 MHz tuning guarantees no DC offset in the observed band (the DC offset falls just behind the observed frequency segment) but results in some spurs, among which the most significant may be observed at 536 MHz. The selection of an accurate tuning level is not simple, because using nearly every tuning frequency results in some spurs in the observed noise mask.

However, one can observe an unexpected phenomenon related to the measured noise power. In particular, the power level for a strongly-tuned DC offset is much higher than for a small or no shift (see Fig. 2.15). For a 40 MHz shift, the noise is tuned, as well as input signals. As a result, the Power Spectral Density (PSD) of tuned signals is at the level of  $-75$  to  $-80$  dBm. Moreover, the noise characteristic is slightly increasing with frequency. This is caused by a band-pass filter characteristic used at the daughter-board. In Fig. 2.16, one can observe the spectrum mask of noise for the exploited hardware as the function of the DC offset shift. The plot was created by merging a series of measurements with shift values of the DC-offset from  $-40$  to  $40$  MHz. As a result, one can observe a 100 MHz band where the power is presented in *Normalised PSD* which is the power of the samples observed in the PC. In the centre of the band, one can see 40 MHz of relatively flat bandwidth, which is guaranteed for the daughter-board by the designing company [5]. However, one can see many undesirable frequency bins in the bandwidth which are created

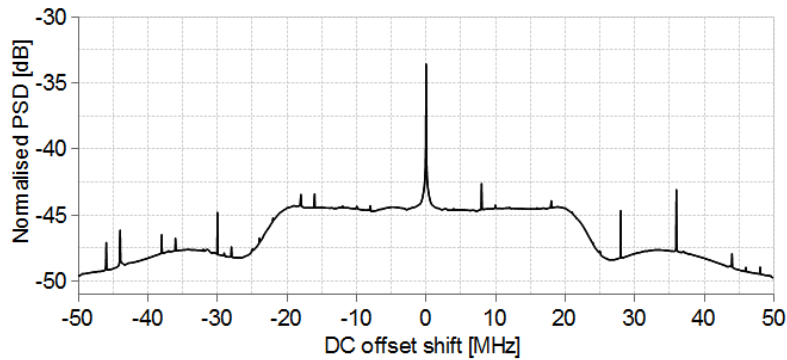


**Figure 2.16:** Spectrum mask of noise for exploited hardware as a function of the DC offset shift

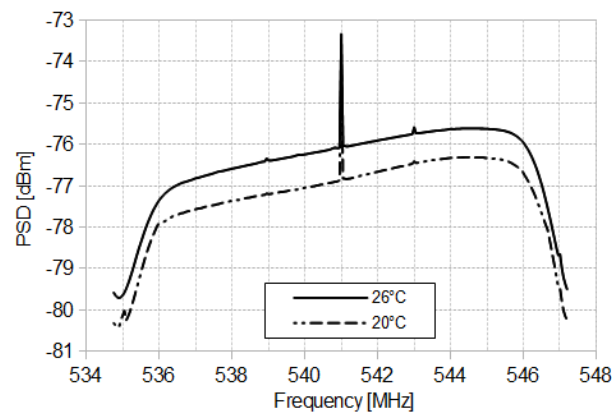


**Figure 2.17:** Influence of temperature on the noise power

in the analogue part of the receiving chain (in the daughter-board) where amplifying, filtration and IF conversion are realised. Due to these impairments, it is decided to use the DC offset shift of 40 MHz.

### Temperature

One of the reasons of noise variability is the changing of hardware temperature. In Fig. 2.17, these are two curves of the measured noise power. Please note that the presented temperatures were measured in a laboratory, not inside the platform, but according to carried theoretical calculations, the temperature inside the platform could even exceed  $70^{\circ}\text{C}$ . The difference of 0.7 dB between the curves leads to the conclusion that noise approximation should be performed not only at the beginning but also during the sensing procedure in order to detect noise variability caused by hardware heating.

### Ambient noise

Other aspects that have to be taken into account are: first, the influence of the reception antenna, and second, the addition of the so-called ambient noise. The measurements of a noise mask presented in Fig. 2.15 were conducted for the USRP with terminators plugged at antenna ports. Identical conditions were guaranteed while obtaining the results illustrated by the bottom line in

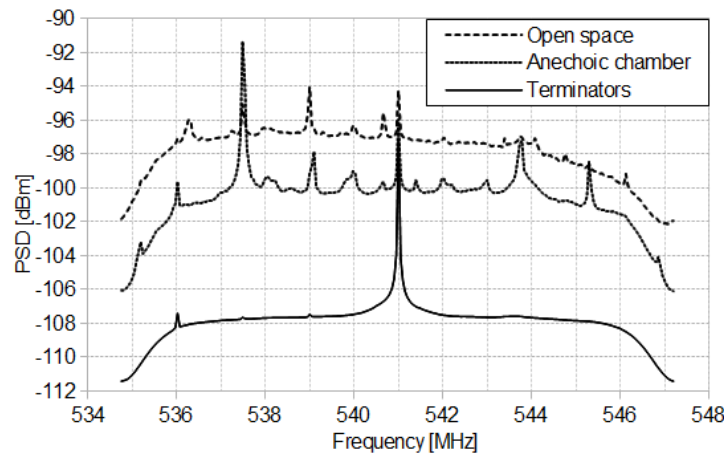


**Figure 2.18:** Noise floor for measurements conducted in three various scenarios

Fig. 2.18. Here, the stable noise power at the level of  $-108$  dBm has been obtained. However, the measured noise power is significantly higher when the terminators are replaced with antennas. The difference is at the level of 8 dB for the measurement where the antenna was kept in an anechoic chamber, and 11 dB for the measurement in open space. One can observe that these two curves are unstable and have a few significant spikes. The biggest one is at the frequency of 537.5 MHz and probably is an interference from the PC signal bus. The spikes seen on other frequencies could also have come from outside radio environment or could have been generated in the hardware due to inaccurate mixing and filtering of signals in the analogue part. Thus, the CRT should somehow approximate the real level of noise in the radio environment. This cannot be done by simply taking the measured power because there is no guarantee that there is no Primary User in the observed band. In this work, spectrum sensing was performed with 40 MHz tuning. For this value, the noise power for measurements with terminators or with an antenna is comparable. In practice, however, one of the approaches presented in the introduction of the Section has to be applied.

### Effects that appear over time

The next Figure illustrates the presence of other unwanted signals that change their features during the sensing time—Fig. 2.19. Here, one can see four curves, each created for the range of 200 thousand consecutive detected samples. All samples were received in one measurement: case P considers the first 200 thousand samples, then Q, R and S represent the next 200 thousand samples, respectively. In Fig. 2.19, one can observe nonlinear effects around the frequencies 544 – 545.5 MHz. The measurement was conducted with connected terminators, which may suggest an internal cause of the distortions, but outside interference cannot be excluded—it is possible that the signal has penetrated through casing. The presence of such effects results in the degradation of algorithm performance.

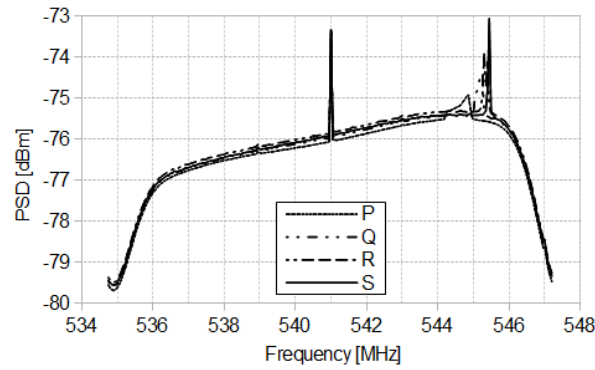


**Figure 2.19:** Non-linear effects that appear over time

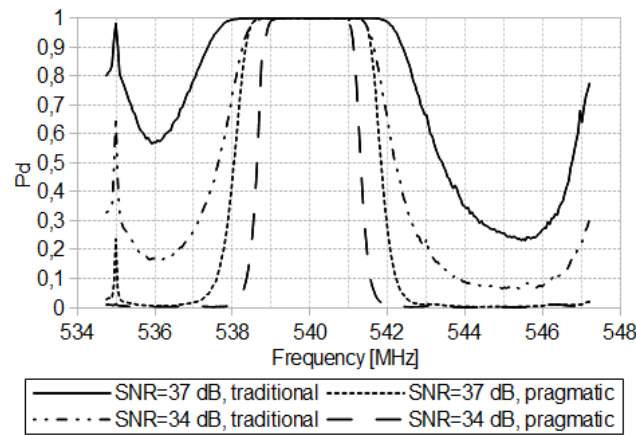


**Figure 2.20:** Comparison of traditional and pragmatic approaches for high-power incoming signal

### The effect of a close high-power signal

During the measurements, the impact of a high-power incoming signal was checked (Fig. 2.20). A frequency-modulated signal of a wireless microphone was located 3 metres from the receiver, which gave an SNR at the level of over 34 decibels. The real signal of the microphone occurred at exactly 540 MHz and had a bandwidth of about 150 kHz. However, due to the nonlinear behaviour of the Low Noise Amplifier, significant power growth was observed at a wide part of the spectrum, leading to many decisions about signal presence. It is worth mentioning that the presence of nearby signals (not only high-power ones) can result in the presence of numerous peaks, being the  $n$ -th harmonics, but also in the increase of the noise floor observed in the observed subband. These aspects have already been discussed in this section.

### Sequential algorithm performance discussion

The analysis of the presented figures leads to the conclusion that unwanted effects have to be taken into account, or otherwise, simple ED or sequential ED algorithms will result in a much higher number of false-alarm decisions. The conducted measurements have revealed a high vulnerability of the sequential ED algorithm to the aforementioned phenomena, since the real noise variance in a practical scenario will be much different from the internal noise power. Thus, the

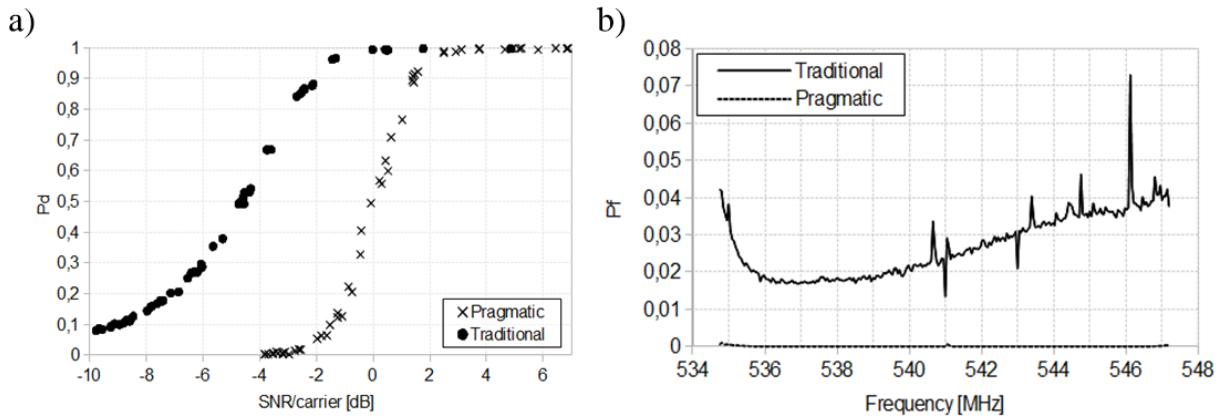


**Figure 2.21:** a) Probability of detection and b) probability of false alarm for traditional and pragmatic approaches

so-called pragmatic approach has been proposed by the author of this thesis. In order to minimise inaccurate noise power estimation, it is proposed that  $\epsilon_{LO}$  and  $\epsilon_{HI}$  thresholds should be placed 2 and 3 decibels above the noise power, respectively. This guarantees the independence of thresholds from the probability of false alarm and the number of collected samples.

In Fig. 2.21a, one can observe the probability of detection in the function of a signal-to-noise ratio per one FFT subcarrier. One point in the plot is the mean value of 100 thousand measurements for one subcarrier with guaranteed PU presence in the observed frequency bandwidth. The traditional solution (i.e., pure energy detection) outperforms the pragmatic one in terms of detection. However, the pragmatic solution guarantees much lower probability of a false alarm (see Fig. 2.21b). In the traditional algorithm, the probability of a false alarm is between 0.015 and 0.075, which corresponds to the value of  $P_f$  taken for sequential thresholds. On the other hand, the pragmatic approach guarantees the probability of a false alarm not higher than 0.01. The traditional algorithm has many more false alarms, which is connected with much better detection. Besides, in the traditional algorithm, the false alarm ratio depends on the subcarrier index. The number of false alarms rises with the subcarrier index (excluding the beginning of the spectrum). The unstable level of false alarms is caused by nonlinearities in the USRP. The pragmatic approach lowers the number of false alarms and provides its stable value in the domain of frequency.

The pragmatic (SPEED) and traditional (SED) approaches have been also compared in the high incoming power case. In the results presented in Fig. 2.20, one can see the probability of detection for two SNR cases. As it is shown, for the traditional approach curves, the decision about PU presence is determined for all carriers, while in the pragmatic approach, it is positive only for carriers 60-153 and 6. The real high-power PU signal is at frequency of 540 MHz.

## Conclusion

An analysis of the impact of hardware implementation parameters and conditions on the performance of noise-dependant algorithms has been presented above. It has been stated that there is a considerable problem with accurate estimation of the real value of the noise power, since ambient

noise should also be included. Moreover, based on the conducted experiments, during which a few unwanted effects were observed, it can be stated that the performance of the solutions, that are based on noise power only, can be significantly reduced. Although the pragmatic approach was proposed, in which the decision thresholds were arbitrarily increased in order to cope with unwanted effects, the performance degradation was significant. The impact of the spurious emission or ambient temperature was compensated by changing the decision threshold values, but the presence of spikes and influence of digital algorithms (DC offset shift) cannot be mitigated. Such an observation, however, leads to the conclusion that the impact of various deterministic phenomena (such as intermodulations) on the noise-independent algorithm should also be verified. Moreover, the number of such unwanted effects grow with the width of observed frequency band. Thus, a cognitive radio terminal equipped with spectrum sensing modules should be aware of such phenomena. Finally, if the reliability of spectrum sensing algorithms depends so strongly on the quality of the electronic elements used for the manufacture of a CRT device, the question of accuracy and real performance of collaborative sensing solutions has to be addressed, and the degradation of reliability in such approach, due to hardware implementation issues, should be analysed.

### 2.3 The Problem of Noise Power Estimation in practical Energy-Detector Implementation

In order to get the estimated yet accurate value of the noise power observed in the given frequency band, CRT should have a possibility of its detailed approximation [40]. In this context, various approaches are possible.

First, the value of the power of internal noise power existing inside the device can be prefabricated and stored inside the device; such values will consist of, e.g., the thermal noise, phase noise at given frequencies, and in general noise figure, etc.; in that case, however, the device should adjust the stored values to current circumstances, such as ambient temperature, carrier frequencies of the input signal, etc.; moreover, such values are device-specific, and dedicated calibration algorithms should be delivered by the manufacturer.

Second, taking into account the drawbacks of noise power prefabrication in each CRT, another solution would allow the device to measure the noise power exclusively. In that case, the device should be able to switch from the transmission/reception mode to the dedicated calibration mode where no RF signal is observed. In the laboratory conditions, such values can be measured with the use of a matched RF terminator; in everyday practice, however, such a goal can be reached with the application of, e.g., an isolated switch, as illustrated in Fig. 2.22. Due to the application of an internal switch, the device will be able to assess the current value of the noise power in a given temperature and ambient conditions. Unfortunately, the power measured by a CRT equipped with such a module will be affected by the possible strong signals penetrating the chassis. Moreover, the impact of the antenna system installed in a particular device will not be included, and neither will the ambient noise apparent in a given location, at a given frequency band. Such an ambient noise could originate from, e.g., nearby high-power transmitters causing high out-of-band emissions.

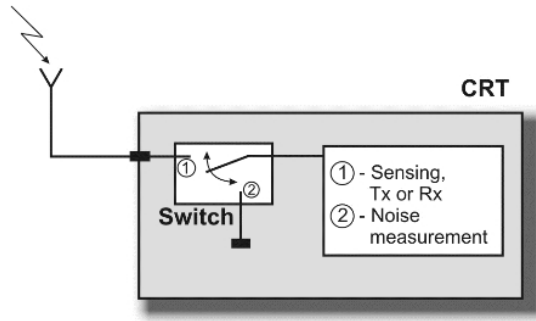


**Figure 2.22:** Measurements of internal noise with the use of a dedicated switch

Finally, the approximated noise power level can be assessed while observing a frequency spectrum that is certainly vacant. However, the CRT has no knowledge about the spectrum occupancy. Thus, the approximate solution could be applied, as presented in [90]. Assuming that the CRT knows the range of the sensed spectrum, it can possess the knowledge on the types of possible signals that could be observed. The CRT can define the analysis window that will be wider than the highest bandwidth of the possible signal spectrum and perform a detailed analysis of the observed data. Taking, for example, five percent of the lowest observed values, it can be stated with high certainty that the measured value is close to the real noise observed by the device in its location, including thermal noise, impact of the antenna and the whole front-end, as well as ambient noise.

### 2.3.1 Noise Uncertainty

In energy detector, the noise power estimate  $\hat{\sigma}_n^2$  is found in the receiver by the averaging of a number of noise samples. However, for a given noise uncertainty there exists a boundary SNR, below which a robust sensing decision would not be taken even if the number of collected samples could be infinitive. This phenomenon is known as *SNR wall* and is given by the formula:

$$\text{SNR}_{\text{wall}} = (\rho^2 - 1) / \rho, \quad (2.6)$$

where  $\rho$  is noise uncertainty in linear scale. If  $x$  would be the noise uncertainty in decibel scale, then  $\rho = 10^{x/10}$ . In Fig. 2.23, the plot of SNR wall versus noise uncertainty  $\rho$  is shown.

According to [88], noise uncertainty depends on four factors: calibration error, thermal variation, changes in Low Noise Amplifier (LNA) gain, and interference. If every of these factors is treated individually, as an independent noise source, then the signal acquired by the receiver is not a ‘pure’ noise but the noise with interferences. Applying the Central Limit Theorem (CLT) it can be assumed that the noise measured in the receiver is a Gaussian one. It is known that the error in CLT is as close to zero as  $\frac{1}{\sqrt{\nu}}$ , where  $\nu$  is the number of summed independent random variables. In reality, the  $\nu$  is not sufficiently large, and the error in Central Limit Theorem should not be ignored [158].

However, even if in the above considerations the error of too low number of summed random variables is considered, then it is assumed that the received noise is white and has (after averaging) flat spectral density. Nevertheless, in [159] it is underlined that in practice this assumption is

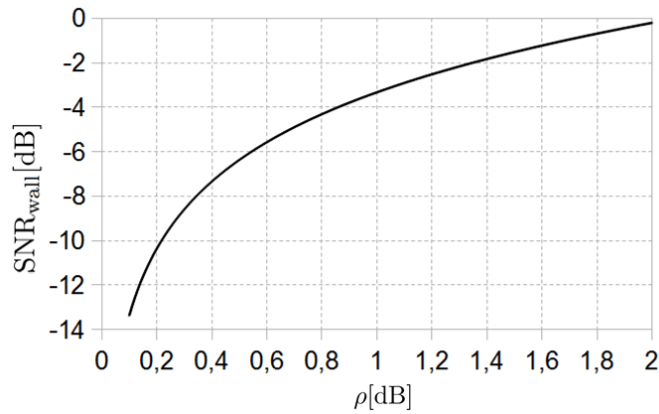


**Figure 2.23:** SNR wall vs noise uncertainty

unrealistic. In reality, noise uncertainty is caused by unknown interference signals generated by sources in various locations. Thus, the received interference power depends on the distance from the source of interference and the wireless conditions such as multipath fading, fast fading, shadowing influencing the radio channel between the source of interference and CRT. Thereupon the received noise should be treated as a *coloured* noise rather than *white* [159].

### 2.3.2 Noise Estimation Methods with Elimination of the Narrow-band Signals

The above observation that the received noise has a *coloured* nature in comparison with the fact that the noise estimation should be done just before or even during the sensing procedure, is the basis for noise estimation methods with elimination of narrow-band signals. As it is underlined in Section 2.2.2, the estimation has to be conducted neither with terminators, nor in laboratory conditions. However, the reliable noise estimation should take into account *coloured* character of the noise and, thus, possible interferences and spurs. As a result, three different noise estimation techniques with spurs elimination are presented below and tested.

#### Estimation ranges

In [45], the noise estimation method has been applied which is based on the division of the observed spectrum portion  $B$  on the subbands of width  $B/m$ , where  $m$  is the total number of subbands. For each subband consisting of  $M$  samples, the estimated value of noise has been found by taking the  $k$ -th sample, counting from the lowest.

The above approximation method is insusceptible of taking the narrow-band signal as noise for small  $k/M$  ( $k/M < 1/2$ ). However, its relevant drawback is the significant approximation error, especially at the ends of approximation subbands, which is increasing with the value of  $B/m$  [45].

### Median value

In order to cope with the approximation errors at the end of subbands, it is proposed not to divide the bandwidth into subbands. Instead, the approximation can be conducted for the subsets of  $M$  samples from the observed bandwidth. The value of estimated noise sample for  $i$ -th sample is calculated as a median from the set of  $M$  samples surrounding  $i$ -th value, as in eq. (2.7). The drawback of this method is inaccurate estimation for  $M/2$  samples on the ends of the whole bandwidth.

$$\hat{x}_i = \begin{cases} x_{(\frac{M+1}{2})} & \text{for odd } M \\ \frac{1}{2} \left( x_{(\frac{M}{2})} + x_{(\frac{M}{2}+1)} \right) & \text{for even } M. \end{cases} \quad (2.7)$$

### Least Median of Squares (LMS) Estimator

The basis of the third estimation method is the observation that unwanted narrow-band signals are the values quite different from the rest (the so-called *outliers*). It was observed that the *outlier detection* is possible with use of estimator. For the purpose of the analysis, the regression analysis has been applied where the classical linear model assumes the relation of the type:

$$y_i = x_{i1}\theta_1 + \cdots + x_{ip}\theta_p + e_i \quad \text{for } i = 1, \dots, M, \quad (2.8)$$

where  $M$  is the sample size,  $e_i$  is the regression error. The real values of  $\theta_i$  are unknown, however,  $\hat{\theta}_i$  as a result of the linear regression allow to have:

$$\hat{y}_i = x_{i1}\hat{\theta}_1 + \cdots + x_{ip}\hat{\theta}_p, \quad (2.9)$$

where  $\hat{y}_i$  is the estimated value of  $y_i$ . The  $r_i$  is the *residual* between what is actually observed and what is estimated:

$$r_i = y_i - \hat{y}_i. \quad (2.10)$$

The most popular regression estimator found by Gauss and Legendre\* is the *least squares* estimator:

$$\min_{\hat{\theta}} \sum_{i=1}^M r_i^2. \quad (2.11)$$

The reason of its popularity is fast computation speed and the fact that it fits data very well, however, it is vulnerable to the values that are not the part of the estimated set (are *outliers*), e.g., are the transmission errors. The *least squares* estimator is susceptible to even one outlier in a sample set. In other words, its lowest outliers percentage which does not influence the result of the estimation (thus its *breakdown point*) is 0. However, there exist estimators that can deal with data containing a certain percentage of outliers. It was proved that the highest possible

---

\*The dispute about the discovery of least squares method is one of the most famous in the history of statistics. Gauss probably possessed the method before Legendre, but the French was the first who crystalized the idea and gained public attention [153].

breakdown point is 50% [143]. The Least Median Squares estimator can guarantee this border value:

$$\min_{\hat{\theta}} \text{med}_i r_i^2. \quad (2.12)$$

However, the median estimator is highly computationally complex, and the finding of the regression coefficients is not obvious at all. In [144], the efficient method for calculation of the regression coefficients for median estimator has been proposed. Assuming sufficiently low number of samples  $M$ , the regression coefficients in the algorithm are calculated per each pair of samples. Then, the line connecting these points is taken and the median of residuals  $r_i$  is calculated. After processing all cases, the approximation with the lowest median of residuals is selected.

Following this way, for each set of  $M$  points the regression coefficients with the lowest median error have been proposed. Then, for these coefficients the approximation error is found per each point. As a result, error value for each analysed sample is generated.

The calculated errors are then compared with an assumed threshold. In the case when calculated error for a given sample is lower than the threshold, the sample is considered as a noise sample; in other cases it is recognised as outlier which should be eliminated and not included in noise mask. For such values the noise power is calculated as a mean of first neighbouring trusted values. After such estimation, most of samples remain unchanged, while the outliers are changed by estimated values.

### 2.3.3 Experiments outcome

#### Brief setup overview

The noise estimation methods were validated on real devices in operating frequency. As it is underlined in Section 2.2.2, the noise estimation should be conducted in operating conditions, neither with terminators, nor by producer in an anechoic chamber. The implementation details are as follows: USRP platform with dedicated WBX daughterboard operating at the centre frequency of 550 MHz, the analysed bandwidth is 25 MHz. Due to the input filter slope, the analysis covered central 20 MHz of observed bandwidth. Thus, the samples from 540 to 560 MHz were analysed. The adopted 256-point FFT gives 256 subbands, for which the sensing decision is considered and noise estimate should be provided. For more details regarding the USRP, WBX and applied GNU Radio please be referred to Section 2.2.1.

#### Experiments Outcomes

As it is highlighted above, the observed 20 MHz is divided into 200 subbands where per each subband 100 thousand samples have been collected. In the first analysed estimation method, called estimation ranges, one may find that the following parameters have been assumed:  $m = 10$  which is the number of subbands in the whole bandwidth (each of 2 MHz). The sample set size is  $M = 10$  and the selected estimate is  $k = 5$  sample.

The key parameter in noise estimation is the quality of estimation measured by the error of estimation. However, one may pose the question how to find the reference value of noise, the ‘real’ noise estimate. In this work the reference value of noise has been found by averaging a huge number of samples equal to one million per subband. On this basis, the estimation error is

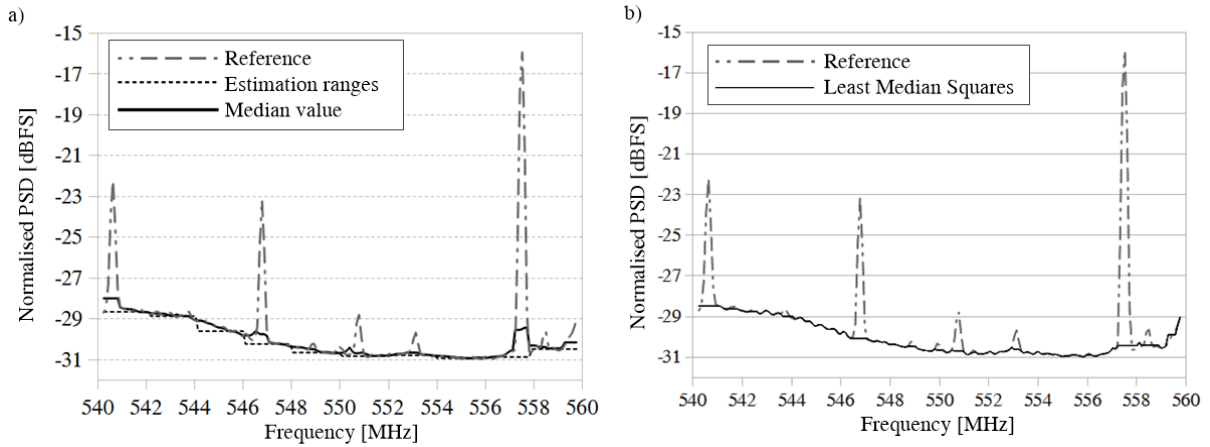


**Figure 2.24:** Noise power estimation for a) estimation ranges and median value, and b) Least Median of Squares methods

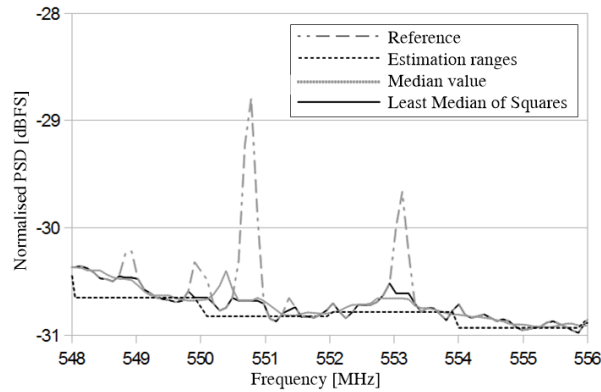


**Figure 2.25:** Noise power estimates for selected spectrum portion for all analysed methods

the difference between the reference value and the result of estimation. The estimation error for each proposed method is illustrated in Fig. 2.26, while the results of estimation for all analysed methods are presented in Figs. 2.24 and 2.25.

None of the methods is drawback free. However, the most promising is the Least Median Square method, which has quite low estimation error in most of the observed spectrum with the exceptionally high error in the ends of range. On the other hand, median is not good enough at the places where narrow-band signal is observed but apart from this, it has good overall results with difference to range estimation which is the most primitive method. It has the highest error rate and is vulnerable to non-equal slope of noise mask.

## Conclusion

Noise power estimation is the crucial issue in energy-based spectrum sensing. The conducted measurements have confirmed that the noise distribution is not flat within observed bandwidth, thus, it cannot be modelled as white Gaussian noise. It has been also proven that in order to guarantee reliable results of energy-based spectrum sensing, the noise should be estimated on

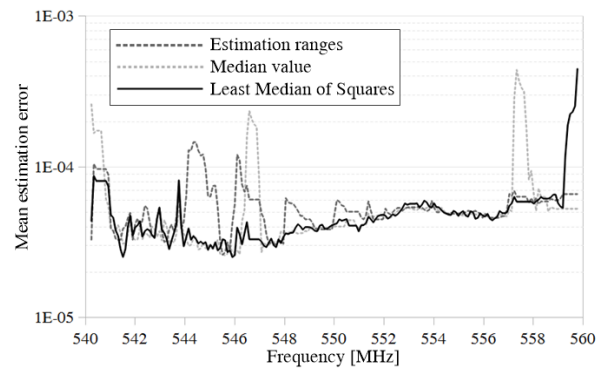


**Figure 2.26:** Mean estimation error vs frequency for analysed noise estimation methods

the basis of the measurement conducted by the device just before or even during the experiment. However, such a condition creates the possibility of having narrow-band signals and interferences in the observed spectrum portion. Thus, the efficient estimation should be aware of such phenomena. As a result, three methods have been analysed and proposed for the purpose of noise power estimation with narrow-band signal elimination. It was proven that Least Median Square and Median criteria guarantee lower estimation error than the *range estimation*.

## Chapter 3

---

# Cooperative Spectrum Sensing

---

Spectrum sensing can only be adopted if reliable information can be gathered. Several investigations have pointed out that sensing carried out locally by autonomous devices is not accurate enough for safe coexistence between primary and secondary users [63]. Thus, reliable spectrum sensing requires cooperation between nodes. In a widely adopted scenario, every node in a cognitive network senses the spectrum, and spreads the observation to the other nodes or fusion centre where the global decision is made. Thus, the nodes need to cooperate to increase the sensing reliability. It was shown that the greater the number of cooperating nodes, the higher the global probability of detection.

The need of exchanging the data between nodes in order to guarantee the quality of detection at acceptable level is, however, burdened with great overhead. A great number of exchanged messages between a significant number of nodes consume much energy. Therefore, intensive research about the energy-efficient cooperative spectrum sensing has been conducted recently. In this thesis, chapter 4 is devoted to the issue of EE in Cooperative Spectrum Sensing.

In this chapter, devoted to Cooperative Spectrum Sensing, the emphasis is put on implementation issues in cooperation and maximisation of detection rate and minimisation of false alarm rate. First, in Section 3.1 some remarks about the practical implementation of Cooperative Spectrum Sensing are put. Then, in Section 3.2 the correlation-based grouping scheme is described with the mobility-aware leader selection method proposed by the author of the thesis is presented.

### **3.1 Considerations about the Cooperative Spectrum Sensing regarding the Implementation Issues**

#### **3.1.1 Practical Implementation of the Cooperative Spectrum Sensing**

In Section 2.2 one may find the description of various phenomena which may significantly limit the performance of spectrum sensing conducted by single device. It is highly possible that the observed effects may degrade the performance of the cooperative sensing. Thus, the motivation

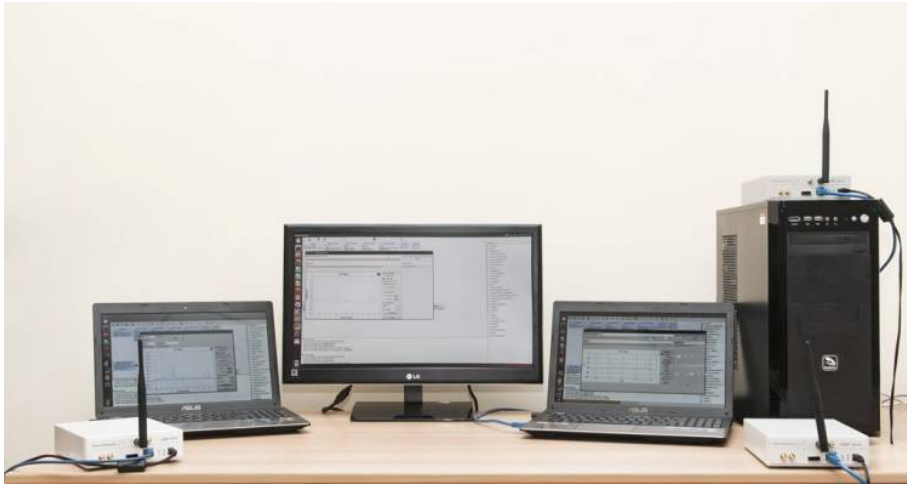


**Figure 3.1:** Illustration of all three sensing devices equipped with the same set, containing USRP with WBX daughter-board and transferring complex base-band signal samples to the computers via Gigabit Ethernet

behind the research presented in this section is to verify the detection performance in the practical implementation experiments of CSS.

### Implementation Setup Details

Similarly to the non-cooperative setup described in Section 2.1, the cooperative scheme was verified using sequential energy detector. Its effectiveness was verified during measurement campaign conducted in the building of the Faculty of Electronics and Telecommunications [45]. The measurement setup consisted of three identical device setups (all three are shown in Fig. 3.1). The signal samples were received in each set by USRP N210 device and transferred via Gigabit Ethernet to the computer (PC or notebook) with applied GNU Radio program.

The measurements were conducted in two scenarios (Fig. 3.2). In the first, three receiving entities were located in two rooms while the transmitter (PU) located in the corridor, all in the second, the highest, floor of the building. In the second scenario, two Primary Users were active and located in different parts of the building, while from three receivers two stayed at the same locations when compared to previous scenario and one was moved to a different room, at the opposite side of the corridor.

The configuration of each receiving entity was identical, i.e., each receiver was equipped with USRP N210 device with WBX daughter-board and had the same transmission parameters. Signal samples received by antenna and amplified in analogue part of the daughter-board were transferred to the base-band frequency and then converted to digital form in fast ADC. There they were processed to a computer and there full software processing was conducted. In the applied open-source environment GNU Radio, the dedicated *cooperative sensing* block was created. Thus, it was possible to process all data in real-time for applied sampling frequency 25 MS/s and make all sensing decisions in real-time.

The observed portion of bandwidth is 25 MHz which is equal to the sampling frequency (the Nyquist bound is hold due to complex sampling applied in USRP). However, the central 20 MHz

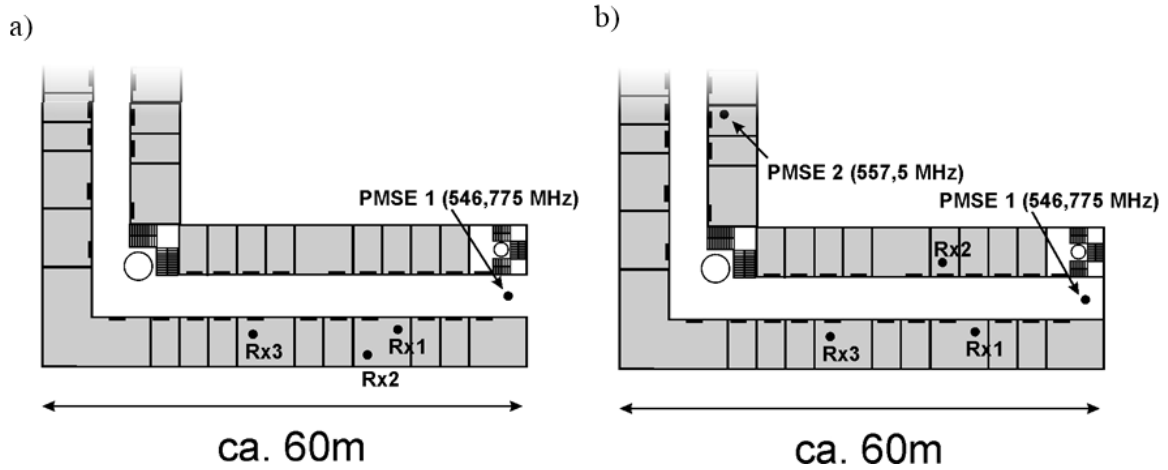


**Figure 3.2:** Position of receiving and transmitting entities on the premises of the Faculty of Electronics and Telecommunications in a) scenario I, b) scenario II

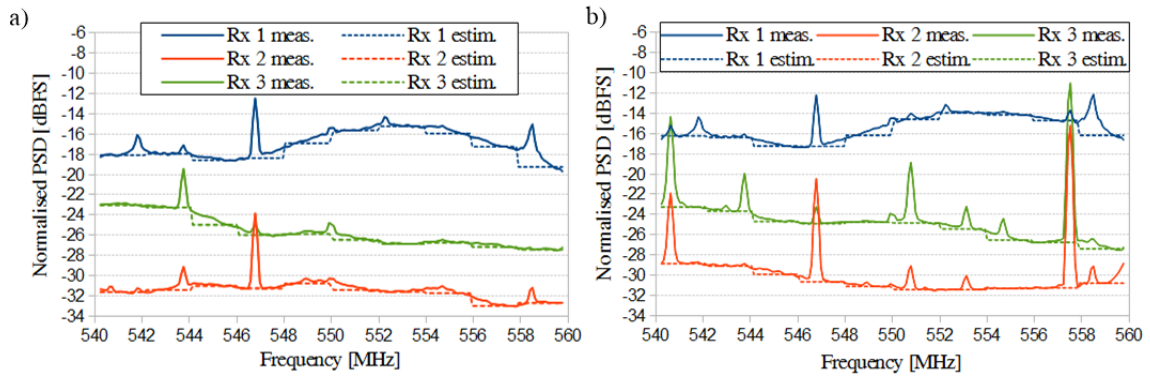


**Figure 3.3:** The results of noise power measurements and noise estimations for three receiving entities in a) scenario I and b) scenario II

out of 25 MHz was used due to the slopes of the input filter characteristic in analogue part of receiving chain. As a result, the analysed range of frequencies was from 540 to 560 MHz. The applied 256-point FFT divided the observed bandwidth to subbands of the width 97.7 kHz each. The sensing decision resolution was equal to the width of one subband.

Accurate energy detection is possible since the accurate noise estimation is properly provided. In Section 2.2.2 it has been shown that noise power estimation should be done in open space conditions, i.e., the typical conditions in which sensing device operates. Thus, noise power estimation cannot be conducted with plugged terminators or inside the anechoic chamber. However, the noise samples taken from the open space have to be properly processed since they may include narrow-band signals. According to the former classification presented in Section 2.3.2, the applied noise estimation method is the *estimation ranges* one with the following parameters:  $m = 10$ , subband width  $B/m = 2$  MHz,  $k = 5$ .

In Fig. 3.3, the results of noise power measurements and applied estimation for three receivers have been presented. The values of noise power for each receiver are different despite the fact that identical hardware and software configuration has been applied in each receiving entity. The

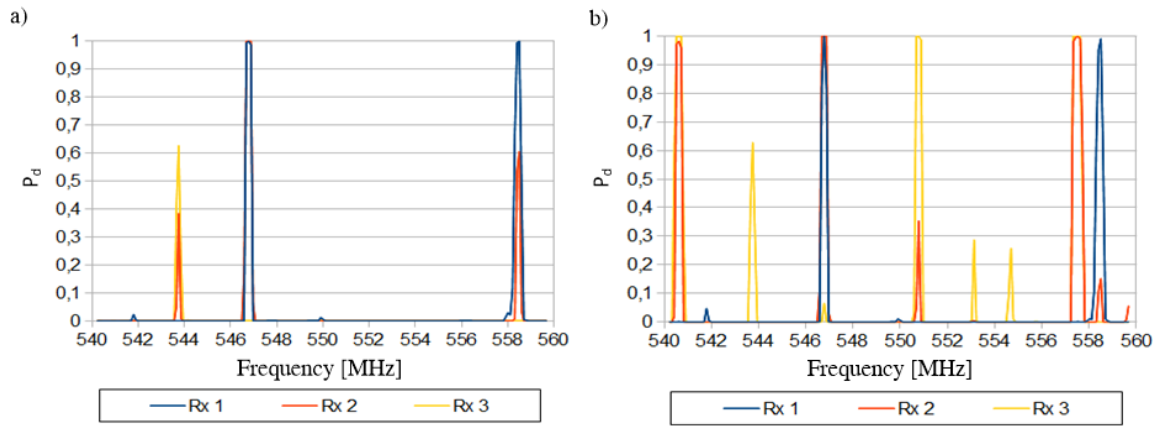


**Figure 3.4:** Probability of detection  $P_d$  vs frequency for each receiving entity separately in a) scenario I and b) scenario II

difference may be caused by different locations and therefore various wireless vicinity and due to possible difference in analogue components in applied entities.

The key topic in implementation is the synchronous operation of all devices. The synchronisation issue was solved as follows: first, in all computers the system time was normalised according to Network Time Protocol (NTP), second, by the use of option possible in Python language, the beginning of measurements was set in each device in advance. The results showed in next figures have been averaged over 100 thousand measurements conducted in 10 series. A measurement is understood as one sequential procedure for one subband which finishes with sensing decision.

### Measurements results

In Fig 3.4, the results of spectrum sensing for all nodes have been shown. In scenario I (Fig. 3.4a) wireless microphone operated at frequency of 546.775 MHz and was detected by two sensing devices located in the same room (Rx 1 and Rx 2). Moreover, these nodes detected the signals at the frequencies of 543.75 and 558.5 MHz, although the PU transmission at different frequency. Thus, the sensed signals may be: *i*) the outside narrow-band signals, *ii*) the local interference, produced, e.g., by the computer or fluorescent lamp, *iii*) the effect produced in receiving chain, i.e., in USRP or in WBX daughter-board.

In Scenario II (Fig. 3.4b), two PUs were transmitting narrow-band signals at frequencies 546.775 and 557.5 MHz and were located in two separate parts of the building. Sensing nodes detected the presence of both PU signals and also the extra signals mentioned in Scenario I. However, the sensing nodes detected additionally other signals despite the fact that measurements in Scenario II were conducted a few hours after the measurements of scenario I. Thus, it is possible that these signals appeared in wireless vicinity during this short period or, more probably, were the products of non-linear effects observed in receiving chain [44].

Let, however, check the detection parameters in the case when sensing nodes cooperate and, instead of local decisions, produce joint global decision. The result of the cooperative operation of three sensing entities is shown in Fig. 3.5. Three most common decision rules have been applied: OR, AND, MAJORITY. As it is explained in Section 1.2.3, decision rules OR and AND are the

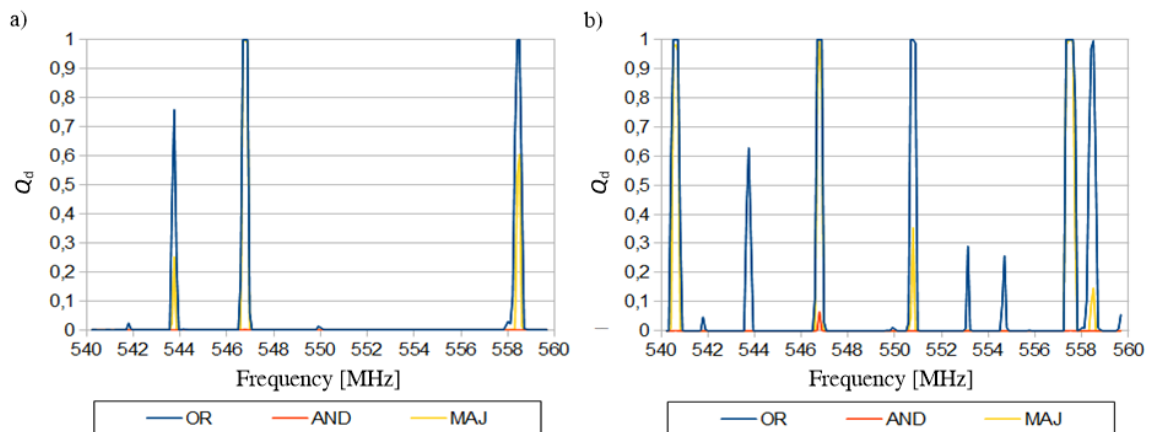


**Figure 3.5:** Global probability of detection  $Q_d$  vs frequency for cooperative spectrum sensing while three fusion rules are adopted in a) scenario I and b) scenario II

border cases, i.e., OR is aimed on guaranteeing the highest detection probability, while AND minimises the false alarm rate. Thus, as it is observed in Fig. 3.5, OR rule curve guarantees the highest global probability of detection—the PU is detected if at least one node notifies its presence. In the opposite case, while AND rule is employed, the PU is detected since all nodes decided so. The MAJORITY rule is a kind of trade-off looking as most reasonable solution when the voice of the *most* nodes is definitive.

In theory and simulations it is straightforward to apply a given decision rule, and predict the detection and false alarm metrics, yet in a real measurements scenario it becomes difficult. In the presented experiment the OR detection rule has allowed to detect many signals including the most uncertain ones, being the product of hardware impairment, as stated in previous paragraph. Thus, the false alarm rate has been significantly increased and as a result there are not so many spectrum portions where cognitive entities could transmit data. The AND rule is the opposite case, where very few signals have been detected and there exist a risk of miss-detection. The key issue is the great uncertainty about the signal character: whether they are the licensed signals which should be carefully protected by the cognitive entities or they are the outcomes of the non-ideality in the applied receivers. The answer to this question may be the reasonable results of the MAJORITY rule, which marked the signals as present in case of being detected by two nodes out of three.

In Fig. 3.6, the medium number of samples needed in the sequential process of making the decision is presented. The definition and initial results of the medium sensing number of samples (time) may be found in Section 2.1.1. The presented results are the extension of the single-node-case results. One may observe that the greatest number of samples is needed at the slopes of signal where the detection uncertainty is the highest.

## Conclusion

In the section above, the results of the CSS implementation conducted by the author of the thesis have been shown. Conducted experiments have proved that in wireless environment the cooperative spectrum sensing results may be actually unreliable. First, a proper and accurate noise

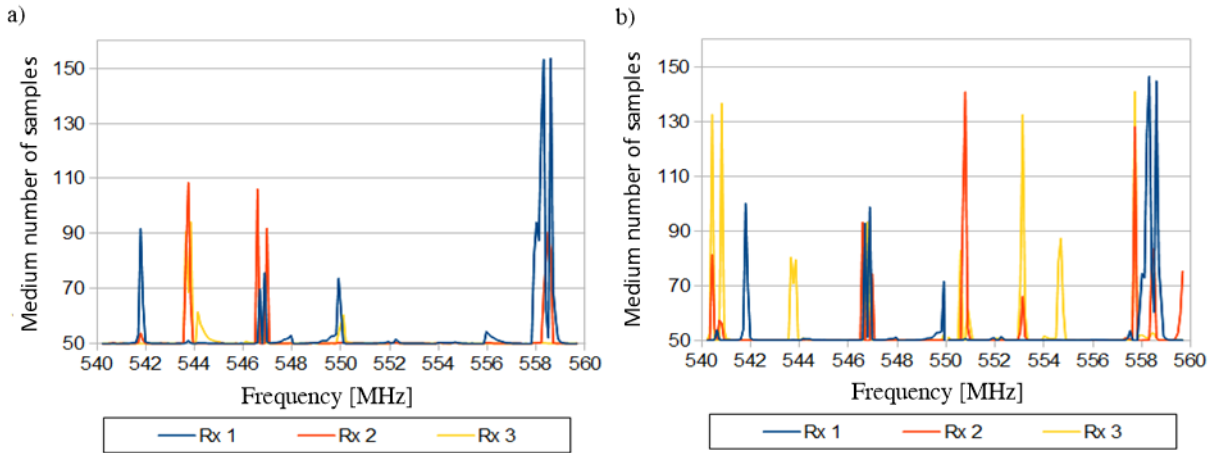


**Figure 3.6:** Medium number of samples (medium sensing time) vs frequency for three receiving entities in a) scenario I and b) scenario II

estimation is needed; second, sensing thresholds should be carefully and properly set in order to make reliable sensing decisions. Even then, the acquired spectrum decisions may be distorted by hardware imperfections. As a result, the cooperative spectrum sensing is susceptible to these phenomena and does not bring the effect, as in the theoretical considerations. However, the observation of the spectrum by a few nodes is still more desirable than single-node spectrum sensing. In this case, however, some post-processing of the observed data is needed. This observation has motivated experimental research described in the following section.

### 3.1.2 Signal Analysis in Cooperative Spectrum Sensing

Although the cooperative approach has gained significant approval from telecommunications community recently, it was shown in the previous section that after implementation its gain may be significantly reduced. Thus, it is proposed to employ signal analysis as a post-processing method in order to overcome performance degradation.

#### Brief setup overview

The experiments have been conducted with similar devices settings, as it is stated in previous section, i.e., in each receiver the signal is received by USRP equipped with WBX daughter-board and processed to computer where full software processing is done. The selected measurement parameters are as follows: observed bandwidth:  $B = 25$  MHz (centre 20 MHz is utilised), FFT size:  $F = 256$ , subband width: 97.7 kHz.

The experiment scenarios were, however, modified. In Scenario III, three receivers were located in two rooms on the premises of the Faculty of Electronics and Telecommunications (Fig. 3.7a). No PU transmission was active. In Scenario IV, the receivers were put at the same places, but the transmission of two PU devices (PMSE) was active (Fig. 3.7b). Two wireless microphones were transmitting narrow-band signals at frequencies 546.775 and 557.5 MHz.

The first part of the proper sensing procedure is an approximation of noise. In Fig. 3.8 one can see the noise power and the estimated noise thresholds. The applied method is *estimation*

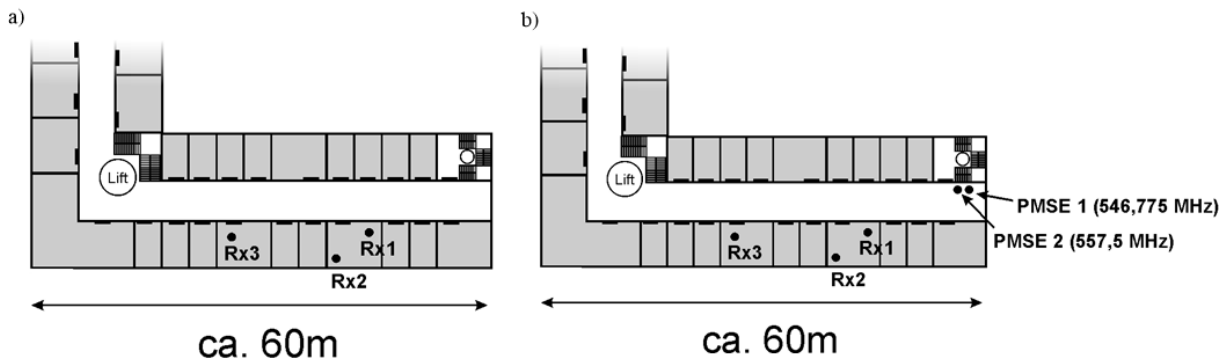


**Figure 3.7:** Location of receiving entities and PMSE during measurements in a) Scenario III (PU transmission disabled) and b) Scenario IV (two PU devices active)

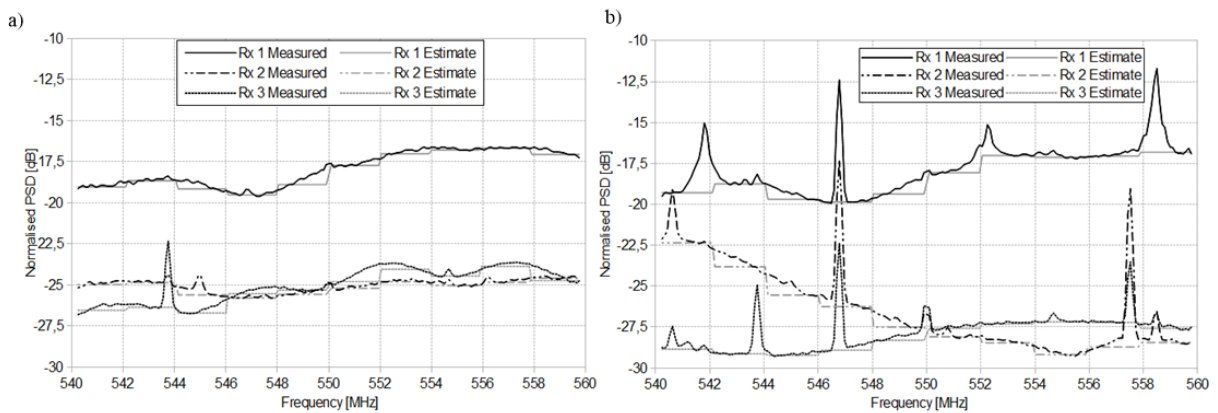


**Figure 3.8:** Measured noise power for each receiving entity with corresponding noise estimation results conducted with *estimation ranges* method in a) Scenario III and b) Scenario IV

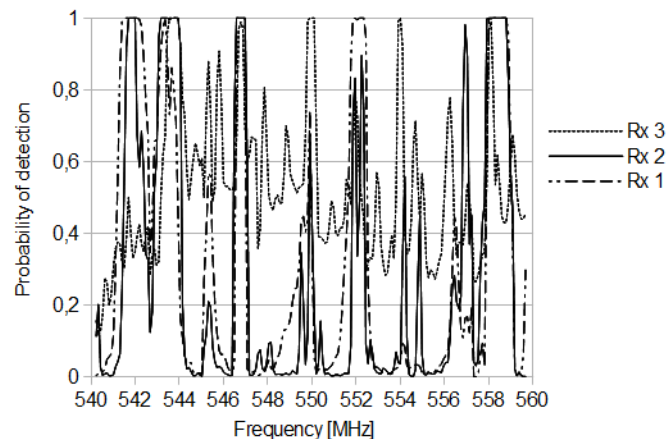


**Figure 3.9:** Detection rate for theory-based thresholds

*ranges* with subband width of  $B/m = 2$  MHz. It should be noted that the level of measured noise power in every receiving device is different, since it may be time-variant and location-dependent due to various radio environment and differences in receiver's internal hardware [34].

The key issue in the sequential algorithm is the determination of the decision thresholds. Based on noise estimates, as in eq. (1.5), thresholds  $\epsilon_{LO}$  and  $\epsilon_{HI}$  are determined for  $P_{f,LO}$  and  $P_{f,HI}$  equal to 0.1 and 0.001, respectively. Then, the mean power of collected samples is compared with these thresholds. The example of the results of the sequential detection is shown in Fig. 3.9. Many signals are decided as busy although just two PMSE devices are active. Thus, the detection in real devices on the basis of the theory-based thresholds provides a high false alarm rate, and it is impossible to make a reliable false alarm-free cooperative decision. Two main reasons of this phenomenon should be pointed out: *i)* simple and inaccurate noise estimation method, *ii)* the impact of hardware limitations such as too large input power causing improper work or distortions in the RF chain [34]. Thus, in the measurements presented below, SPEED method has been applied (introduced in Section 2.2). The sequential thresholds have been increased. Although this may lower the detection rate, allow, however, to overcome the practical implementation impairments and allow to make sensing at all.

### Measurements results

In the typical cooperative spectrum sensing, global decision is determined by adoption of a selected fusion rule in a blind way. However, due to inaccurate noise estimation and signal distortions, which was proven by the real-environment measurements, a high number of false alarms is observed [35]. In Figure 3.10a, the probability of detection for Scenario III is presented, where no PMSE transmission is active. In this case only receiver 3 sensed the signal at the frequency of 543.75 MHz. Contrarily, in Figure 3.10b the results of measurements are shown which were conducted while two PMSE devices were active (i.e., 546.775, 557.5 MHz). Measurements for both presented scenarios were conducted on the same day, one after another. Interestingly, in Figure 3.10b, one can observe two peaks of PMSE signals observed in Scenario III and surprisingly a few other signals which probably were generated inside the receiving entity. Note that in Scenario IV (Figure 3.10b) very low amount of the observed bandwidth could be adopted for cognitive transmission. This effect could be enhanced if guard bandwidth of every sensed transmission was applied. A guard band is the portion of bandwidth adjacent to every detected signal in a sensing procedure in order to increase protection of PU. Adopting an exemplary guard band of 1 MHz may result in a high number of busy subcarriers and a lack of bandwidth devoted for cognitive-radio secondary transmission.

In Fig. 3.11, the result of decision fusion is presented. Similarly to the results shown in Fig. 3.5, the results where fusion rules are adopted are shown. As stated before, OR and AND rules are the extreme cases where one or all nodes are needed to finalise the decision that the spectrum is utilised. While OR rule is adopted, a great part of spectrum is decided as detected due to many detections provided by single devices. The most reasonable is the majority rule (in the applied case 2-out-of-3 rule), which guarantees the detection if two nodes detected the PU signal. It also enables to exclude some signal images in hardware and is not as restrictive as AND rule.

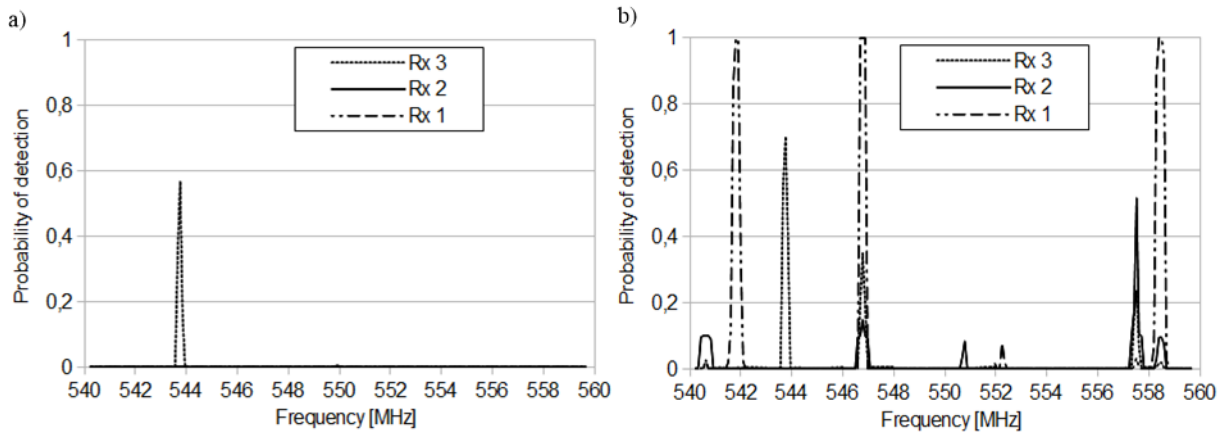


**Figure 3.10:** Measurements sensing results in a) Scenario III and b) Scenario IV

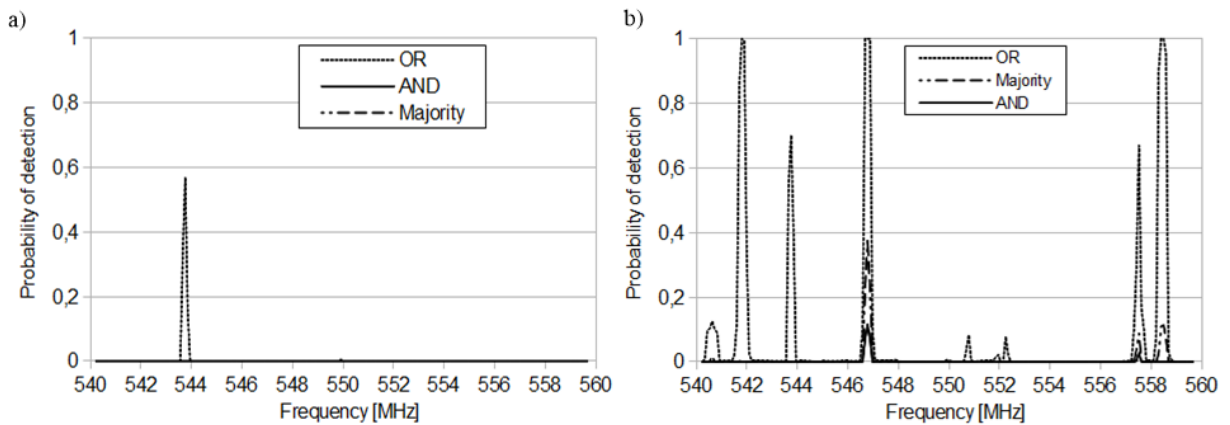


**Figure 3.11:** Probability of detection vs frequency while three decision rules are adopted in a) Scenario III and b) Scenario IV

## Signal Analysis

The detailed analysis involving hardware impairments and radio environment influence should be adopted [36]. Employment of knowledge about radio environment and the so-called context awareness information should increase the reliability of conducted spectrum sensing.

First, it would be useful to have knowledge about the types of possible licensed signals in the observed frequency bandwidth. In the analysed scenario, two types of signals may be sensed. First, 8 MHz-wide Digital Video Broadcasting–Terrestrial (DVB-T) signal, second, narrow-band signals occasionally generated by PMSE devices such as microphones and cameras with an impulse shape width not greater than 250 kHz. This knowledge employed in noise estimation process may result in adjustment of noise estimation subbands and guaranteeing more accurate noise estimation.

Another possibility is to make the analysis of decision in a frequency manner. For example, if many adjacent subcarriers are decided as busy but a few among them are decided as vacant, then it is possible to use context awareness knowledge. In this example it may be the information that the expected portion of bandwidth is 8 MHz block devoted for digital television transmission. As a result, contiguous 8 MHz portion of bandwidth should be decided as busy, thus reversing

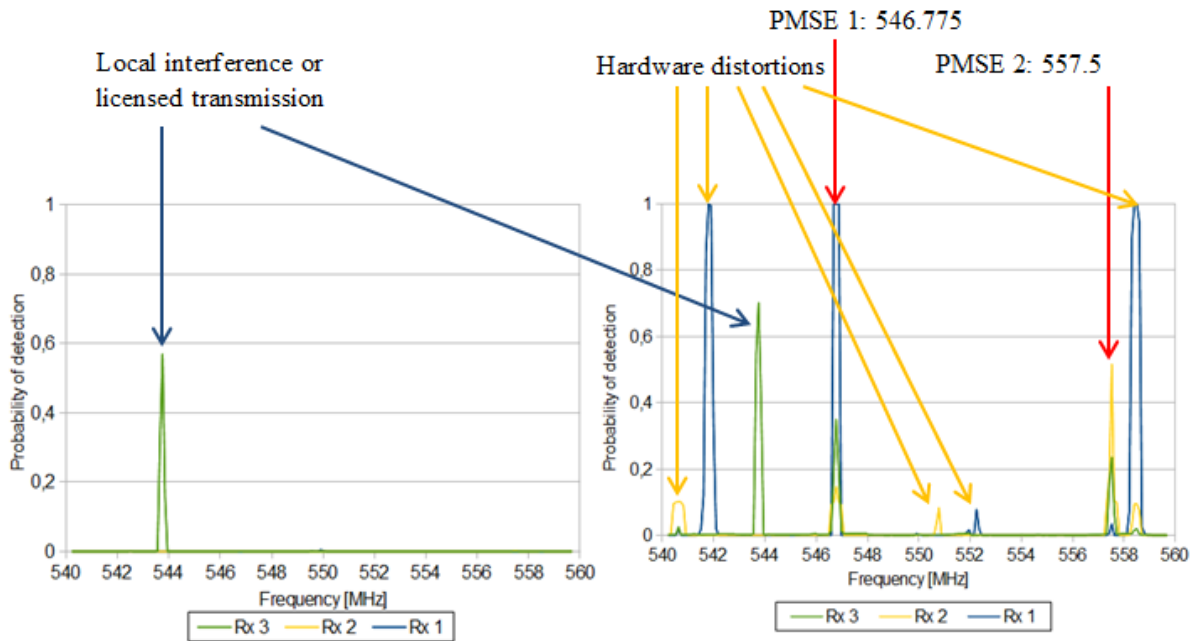


**Figure 3.12:** Signal analysis in a) scenario III and b) scenario IV

decisions for a few free subcarriers. Similar rules are possible for narrow-band signals, e.g., if two busy subcarriers are disjointed by one free, then all three subcarriers should be decided as occupied.

Large amount of knowledge is possible with the use of temporal correlation. Observation in the period of 24, 48 or 72 hours may give great knowledge about sensed signals and radio environment. It would be useful to use the knowledge that wireless microphones cannot transmit signals continuously longer than 8-12 hours due to limited battery lifetime. Temporal analysis and temporal correlation may highly discredit narrow-band signals which are observed in the bandwidth continuously for several days. With a great probability they may be assumed as local interferences from, e.g., computers or fluorescent lamps. Information of such detected interference may be kept in the memory of the device and used in the learning process. In the future, the overall detection quality could be improved by using such context awareness information. For example, the information kept in memory which could be useful is the frequencies of detected signals in the past: both the signals classified as interferences or licensed transmissions.

In distributed systems, it is often beneficial to know positions of sensors. For example, if fusion centre possesses information that two nodes are positioned close to each other, and if one senses strong signal and the other does not, then it may assess it is node's internal hardware distortion and decide the spectrum portion at this specific frequency is vacant. The position awareness may help in the global decision process. If the nodes are far apart, then their decisions may be not correlated. Contrarily, the nodes which are close are correlated and the correlation may be used for distortion exclusions.

In the measurement experiment provided for this work, it was possible to turn on and off the signal of Primary User. Thus, it is possible to analyse the observed signals where no PMSE was transmitting and compare it with the situation where devices were transmitting. In Figure 3.12, one can see a possible analysis of the received signals. The only signal observed in both scenarios is classified as licensed transmission or local interference. It should be noted that a signal sensed at 543.75 MHz has another probability of detection in both scenarios: in Scenario III it is 0.57 while in Scenario IV it is 0.7. The difference can be induced by fluctuations of signal power or slightly different noise estimations. The other signals were decided as licensed transmission if at least two from three nodes detected signals with probability of detection greater than 0.2.

In signal analysis it would be beneficial to adopt a learning phase. In the learning phase, a simple procedure of transmission training signals in the following order. A node selected by fusion centre transmits the training signal while other nodes sense the spectrum implying the training signal. The procedure is repeated for selected nodes. After that it is possible to assess if distortions are produced in receiving entities and in which frequencies. The analysis could involve generation of training signals of different power levels. However, the receiving entities should be isolated efficiently in order not to interrupt the licensed transmission outside the observation area.

## Conclusion

In this section it has been shown that hardware limitations observed in real time measurements result in a large number of false alarms, decreasing the performance of sequential energy detector. The proposed signal analysis may improve the detection performance in cooperative spectrum network and lower the number of false alarms. However, appropriate signal analysis involves context awareness information, which has to be provided to cognitive devices. Moreover, it requires additional computational complexity as well as additional sensing time, e.g., for executing a learning phase.

## 3.2 Mobility-Aware, Correlation-Based Node Grouping and Selection for Cooperative Spectrum Sensing

Cooperative spectrum sensing requires explicit information exchanges between nodes. Minimising the overhead introduced by such exchanges, so to guarantee energy efficiency and low complexity, is an important aspect to be considered in the design of a cooperative spectrum sensing algorithm. Therefore, the solution presented below could be classified as an energy-efficient solution and included in Chapter 4, which is devoted for EE in Cooperative Spectrum Sensing. However, the author of the thesis classifies the solution in cooperative spectrum sensing-devoted chapter due to the emphasis put on the reliability in the solution and the lack of detailed analysis in energy-efficiency area like the lack of EE metric. Thus, in this section the solution concerning the correlation-based node grouping with introduced mobility of nodes is described although it is somehow related with energy-efficient algorithms of node selection. Following this way, one may find in Section 4.4 solutions regarding the energy-efficient node grouping with the following classification: *node selection*, *node censoring* and *voting schemes*, and deep analysis.

An aspect that is seldom considered in the definition and performance evaluation of cooperative sensing schemes is mobility. There are in fact only a few papers tackling the role and impact of mobility in cooperative spectrum sensing. In [112], the authors present a theoretical analysis confirming that node mobility increases spatial diversity and as a consequence improves the sensing performance. The results presented in that work show the trade-off between the number of sensors and the number of measurements taken by each sensor. The authors in [18] base their work on [112] but introduce more accurate assumptions and provide more detailed results. Moreover, the expression for the number of measurement required for a given velocity, probability of detection and probability of false alarm is derived. The research in [53] compares results obtained on the basis of the aforementioned works and presents results obtained by simulation under more realistic conditions, showing that relaxation or removal of some of the assumptions taken in previous research has a significant influence on performance.

In the above context, here below, a cooperative sensing scheme is proposed based on the measure of correlation in sensing decisions for node grouping and on a mobility and sensing aware metric for the selection of group leaders [33]. The concept of node grouping based on correlation is leveraged from [157], and combined with a novel metric for group leader selection—proposed by the author of the thesis—that takes into account mobility and sensing performance to guarantee adequate sensing performance for extended periods of times. The proposed approach is then compared with previous solutions by means of computer simulations, implementing accurate models for the mobile radio channel, taking into account spatial and temporal correlation for both fading and shadowing components.

### 3.2.1 Correlation-Based Node Selection

Correlation-based node selection has been introduced in [150] where a network of nodes is considered. All nodes are grouped in an active set at the beginning of the algorithm, while after selection a subset of nodes may remain in the active set while the rest is moved to the passive set which includes all nodes that are not allowed to vote. In order to make a proper selection, the correlation measure is computed for pairs of nodes in the network. Then, the node with the highest summed correlation with the remaining sensors is removed from the active set and moved to the passive set. The *correlation measure* used in [150] is based on the positions of nodes and associated positioning uncertainty. The following correlation function (3.1) is an example of correlation measure:

$$R(d) = e^{-ad}, \quad (3.1)$$

where  $a$  is a decay constant related to the environment and  $d$  is the distance between sensors.

An example of the correlation-based approach is described in the paper written by Yanzan Sun et al. [157]. In this approach the correlation measure is computed based on the node decisions only. Thus, no additional information, such as position of nodes, is needed. Correlation-based node selection presented in [157] is based on similarity in decision making.

The performance evaluation that supports the approach in [157] is however quite preliminary, as it relies on several simplifying assumptions. For example, authors state that sensing information was "generated randomly according to the probability of correct detection between 70 and 90%" [157], implying that the radio channel model was not taken into account in the results. The

authors also assume that by putting the value of correlation threshold  $\alpha$  to 0.96 the nodes can be divided into 10 groups. This assumption would not hold in general in the real world, as the selected number of nodes resulting from the approach in [157] constantly changes and depends on several parameters, e.g., on actual propagation conditions or nodes positions. Finally, the simulation results in [157] were obtained in a low-correlation scenario for an average signal-to-noise ratio equal to 10 dB, while one would reasonably expect a CSS scheme to be tested in a low SNR regime, where its improvement over local sensing is expected to be most relevant.

Despite the lack of thorough experimental verification, the approach proposed in [157] is appealing, since it inherently takes into account the role of spatial positions of nodes and channel conditions in determining the best set of nodes. A solution inspired by this approach, but also taking into account the role of mobility, is introduced in Section 3.2.3, and its performance is evaluated in Section 3.2.4.

### 3.2.2 System Model

The adopted model foresees  $N$  nodes randomly distributed in a square area of side equal to  $R$  meters. Every node is assumed to have the same desired probability of false alarm (under CFAR requirement) and therefore the same sensing threshold computed according to equation 1.2.

The generic node moves with a randomly selected direction of movement  $\phi_i$  and velocity  $v_i$ . Angles of movement and velocities are uniformly distributed, with  $\phi$  taking values between 0 and  $2\pi$  radians, and velocities  $v$  between  $v_{\min}$  and  $v_{\max}$  meters per second. Whenever a node hits the border of the square area, it bounces back from it according to a total reflection model, while keeping the same velocity.

The following power attenuation model is assumed for the mobile radio channel between a mobile node and the Primary User:

$$\text{channel}|_{dB} = \text{pathloss}|_{dB} + \text{fading}|_{dB} + \text{shadowing}|_{dB}. \quad (3.2)$$

The path loss depends on carrier frequency  $f_c$  and on the distance  $d$  between the node and the PU according to the well-known Friis' formula. The carrier frequency is assumed to be constant for all nodes, while the distance changes in time proportionally to the node velocity. However, it is assumed that during the single sensing phase the path loss does not change due to relatively small possible variation of nodes' locations.

Fading coefficients are modelled according to Rayleigh fading channel. Doppler shift is proportional to the node velocity, and in the presented model it varies according to the following equation:

$$\Delta f = 3 \cdot v_i. \quad (3.3)$$

In the model, every node experiences an independent fading channel (as suggested in [124]), resulting in uncorrelated fading between different nodes, but correlated channel coefficients in time for a given node.

Regarding shadowing modelling, the decorrelation distance  $d_{\text{corr}}$  was set according to Gudmundson model [67] and Min and Shin work [112]. Hence, the square area of side  $R$  meters was divided into  $q$  smaller (pixel) squares containing different values for shadowing. The values are constant in time for a given location according to [149], so during the observation time the shadowing value for every shadowing centre does not change. The values are randomised with the

normal distribution  $N \sim (0, \sigma_s)$ . However, one can find more sophisticated shadowing models. Kasiri and Cai in the work [85] applied NeSh (Network Shadowing) model taken from [128]. The model allows one to determine correlation values between links of different users, while in Gudmundson case it is possible only for links coming from one node. Since the scenario considered in this paper focuses on correlation between measurements involving the same primary transmitter, the Gudmundson model is deemed sufficient to the purpose of this work.

In the considered system, every node takes  $M_s$  sensing decisions and sends them to the fusion centre, under the assumption that radio coverage between the nodes and fusion centre is always guaranteed. One can reasonably expect that mobility will also significantly impact the topology of the secondary network and thus the radio coverage between nodes and fusion centre; for the sake of simplicity the analysis of such impact is left for future research, while in the present paper the impact of mobility is restricted to the results of sensing.

Nodes in the network share a common time reference, and time is organised in frames of duration  $T_{\text{tot}}$ . Sensing information is gathered and exchanged during the sensing phase of duration  $T_{\text{se}}$  that takes place at the beginning of each frame. The remaining time in the frame  $T_{\text{dt}}$ , equal to  $T_{\text{tot}} - T_{\text{se}}$  is dedicated to data transmission if the presence of PU is excluded (see Fig. 1.11).

The frame duration  $T_{\text{tot}}$  is also used as the reference period for updating the positions of nodes and determining the new values for shadowing. Note that a smaller update period could easily be adopted, but this would have no impact on sensing performance, as sensing is also performed with period  $T_{\text{tot}}$  and network wide synchronisation is assumed.

### 3.2.3 Mobility-Aware Correlation-Based Spectrum Sensing

The proposed sensing scheme organises network operation in two states: a *training* state, used for node grouping and selection, and an *activity* state, during which nodes selected in the training state perform sensing, and all nodes transmit data packets whenever the network sensing decision excludes the presence of the PU.

While in the *training* state, each node takes  $M_s$  signal samples during the sensing phase, with a sampling period  $t_s = T_{\text{se}}/M_s$  seconds. The samples are compared with the sensing threshold, with  $M_s$  decisions taken at each sensing node (one decision per one sample). Each node sends the  $M_s$  decisions to a FC that uses them to compute the correlation measure. The number of decisions  $M_s$  should be thus large enough to allow for a reliable estimation of the correlation between different nodes. As a result of the selection procedure (detailed below), a set of active nodes is determined, and the network switches to the *activity* state, during which the active nodes perform sensing and report their decisions to the fusion centre, where a network decision on the presence of the PU is taken.

The selection procedure used during the training phase is the following one. Let be  $S_i(k)$  the  $k$ -th decision out of  $M_s$  taken by the  $i$ -th node, and define it as follows:

$$S_i(k) = \begin{cases} 1, & \text{when } \mathcal{H}_1 \text{ is declared} \\ -1, & \text{when } \mathcal{H}_0 \text{ is declared} \end{cases} . \quad (3.4)$$

Given the decisions taken by two SUs,  $i$  and  $j$ , the  $\gamma_{i,j}$  correlation measure for the two nodes is defined as [157]:

$$\gamma_{i,j} = 1 - \frac{\sum_{k=1}^{M_s} |S_i(k) - S_j(k)|}{2M_s}, \quad (3.5)$$

where  $\gamma_{i,j} \in \langle 0, 1 \rangle$ . If all decisions for the  $i$ -th and  $j$ -th nodes are identical  $\gamma_{i,j}$  is equal to 1; in general, the higher the number of common decisions, the greater the value of correlation measure.

After computing correlation measures between all pairs of nodes, the  $\Gamma$  matrix of size  $N \times N$  is built:

$$\Gamma = \begin{bmatrix} \gamma_{1,1} & \gamma_{1,2} & \cdots & \gamma_{1,N} \\ \gamma_{2,1} & \gamma_{2,2} & \cdots & \gamma_{2,N} \\ \vdots & \vdots & \ddots & \vdots \\ \gamma_{N,1} & \gamma_{N,2} & \cdots & \gamma_{N,N} \end{bmatrix}. \quad (3.6)$$

It is assumed that correlation coefficients are reciprocal, so  $\Gamma$  is a symmetric matrix. The diagonal elements of matrix are the auto-correlation coefficients. Therefore,  $\Gamma$  can be represented as upper triangular matrix  $\tilde{\Gamma}$  [39]:

$$\tilde{\Gamma} = \begin{bmatrix} 0 & \gamma_{1,2} & \cdots & \gamma_{1,N} \\ 0 & 0 & \cdots & \gamma_{2,N} \\ \vdots & \vdots & \ddots & \vdots \\ 0 & 0 & \cdots & 0 \end{bmatrix}. \quad (3.7)$$

After evaluating the correlation measures for all possible pairs of nodes, the grouping procedure is executed. First, the value of a correlation threshold  $\alpha$  is defined. Next,  $\gamma_{i,j}$  coefficients above  $\alpha$  threshold are determined. If more than one  $\gamma$  coefficient is higher than  $\alpha$ , then two cases may occur:

- the pairs of correlated nodes are disjoint. In this case nodes are grouped by correlated pairs,
- one node is correlated with more than one node. In this case three or more nodes are grouped together only if all mutual correlation measures are larger than  $\alpha$ . Nodes that do not meet this condition are not included in the group.

The procedure is performed repeatedly until there are no further nodes that can be grouped together.

When the grouping procedure is complete, some groups are formed while other nodes remain uncorrelated. Note that the above algorithm, first described in [157], does not require a predetermined number of nodes and groups to be selected as an input parameter. The output number of groups and the total number of selected nodes depend on the correlation environment.

Following the division of nodes into groups, a group leader for each group is selected according to the Leader Suitability (LS) parameter, defined as follows for the generic group member  $i$ :

$$LS_i = c_1 P_{d,i} + c_2 \exp\left(\frac{v_i - v_{\min}}{v_i - v_{\max}}\right), \quad (3.8)$$

where  $c_1$  and  $c_2$  are weight coefficients that can be used to adjust the relative importance of the two terms that form the LS parameter. The first term is the probability of detection of node  $i$ , while the second term models the stability of the node, defined as its ability to stay as long as

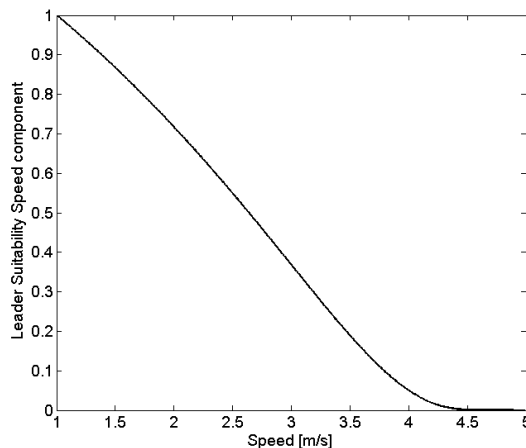


**Figure 3.13:** Behaviour of the term related to node velocity used in the Leader Suitability formula

possible at a given location. The stability coefficient is equal to 1 when  $v_i$  is equal to minimal velocity and 0 if  $v_i = v_{\max}$ . The behaviour of the stability parameter is presented in Figure 3.13 for  $v_{\min} = 1$  m/s,  $v_{\max} = 5$  m/s.

The goal of the proposed metric is to ensure that selected group leaders are able to guarantee good sensing performance not only at present time, but also in foreseeable future, thanks to their low mobility. As a result of the selection procedure, the set of active nodes allowed to participate in sensing is determined, and is composed by one group leader from every group and all the uncorrelated nodes. The network switches then to the *activity* state for a predetermined amount of time, before switching back to the *training* state for updating the set of active nodes.

### 3.2.4 Simulation Results

The performance of the mobility-aware correlation-based cooperative sensing scheme introduced in Section 3.2.3 was investigated by means of computer simulations carried out in the Matlab environment. In the simulations a square area of 200 m side was divided into 16 pixels of  $d_{\text{corr}} = 50$  m side [112] and  $N = 100$  SUs were randomly distributed in the area. The same area was covered by the transmission of a PU. The PU signal was characterised by a carrier frequency of 300 MHz, transmit power of 1 W, and distance to SUs in the range 1.41 – 1.86 km. In order to observe the benefit of the grouping algorithm, it was assumed that the PU is always present. A list of key simulation parameters and corresponding values is presented in Table 3.1.

According to Ofcom (the British spectrum regulator) rules, sensing should be executed at least once a second and occupy no more than 10% of the total frame length [125]. Thus, in the simulations a frame of duration  $T_{\text{tot}} = 1$  s was divided in  $T_{\text{se}} = 0.1$  s and  $T_{\text{tot}} - T_{\text{se}} = 0.9$  s. During the sensing part every node collected  $M_s = 1000$  samples, corresponding to a sample time equal to 0.1 ms. The decisions were generated by comparing the power of each sample to a constant sensing threshold. Such decisions were then provided as an input to the CSS algorithm for group formation and leader selection. As mentioned in Section 3.2.3, any fusion rule could be adopted to take the network decision; in the performance evaluation presented in this Section an OR fusion rule was adopted. The CFAR requirement was adopted in the system, with a global

**Table 3.1:** Key parameters of simulation

Param.	Description	Value
$M_s$	Number of samples used for correlation approximation	1000
$N$	Number of nodes	100
$P_f$	Local probability of false alarm	0.001
$Q_f$	Global probability of false alarm	0.095
SNR	Averaged signal-to-noise ratio	2 dB
$T_{se}$	Sensing phase duration	0.1 s
$T_{tot}$	Frame duration	1 s
$d_{corr}$	Decorrelation distance	50 m
$t_s$	Sample time	0.1 ms
$v_{min}$	Minimal velocity of nodes	1 m/s
$v_{max}$	Maximal velocity of nodes	5-50 m/s
$\Delta f$	Doppler Shift	3-150 Hz
$\alpha$	Minimal correlation coefficient	0.95
$\phi_i$	Direction of movement of nodes	0- $2\pi$ rad
$\sigma_{SU}$	Noise power at SU	3.01e-13 W
$\sigma_s$	Shadowing variance	4.6 dB

probability of false alarm equal to 0.095, implying thus local probabilities of false alarm equal to 0.001, assuming that all nodes participate in the sensing process. Identical  $P_f$  and noise power at SUs imply, as a result, constant sensing threshold in every node (see equation 1.2).

All of the simulations have been done under the assumption of an average SNR between the PU signal received at an SU and the noise at the same SU equal to 2 dB. The results were averaged over 20 thousand iterations, and in each iteration the state of the system was recorded every second for a 70 seconds observing time. As already pointed out, mobility is expected to play an important role in sensing performance. As a consequence, all simulations were performed in presence of mobility.

An example of the state of the system after node grouping and group leaders selection is presented in Fig. 3.14 (node velocities in the range 1 – 20 m/s). In the figure, different markers correspond to different groups, while filled markers identify the leader of the corresponding group. The figure shows that from every group, only one node is selected as a group leader except for a group marked by circles. These are uncorrelated nodes—the nodes which are not correlated enough to join another group. Therefore, all of these nodes are allowed to vote. In the situation presented in Fig. 3.14, 11 nodes out of 100 are selected to vote: 6 uncorrelated nodes and 5 group leaders. In general, it can be observed that in the low-SNR-scenario, the received power is often below the sensing threshold, due to strong shadowing and/or fading. Thus, in such a scenario many nodes with bad channel conditions take the decision that the PU is not present. As a result, these nodes are associated with the same, large, group. Therefore, only a few groups are eventually formed. This effect may prove a significant advantage of correlation-based sensing when AND or majority rules are adopted, as it significantly reduces the impact of individual missed detections by grouping all nodes likely to generate such missed detections in a single group. This result was

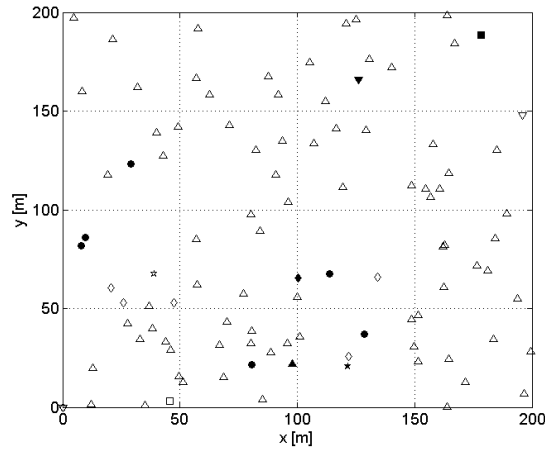


**Figure 3.14:** Exemplary state of the system after node selection procedure. Triangles, squares, circles, diamonds and stars reflect belonging to particular group. Nodes marked with filled symbols are selected by the procedure.

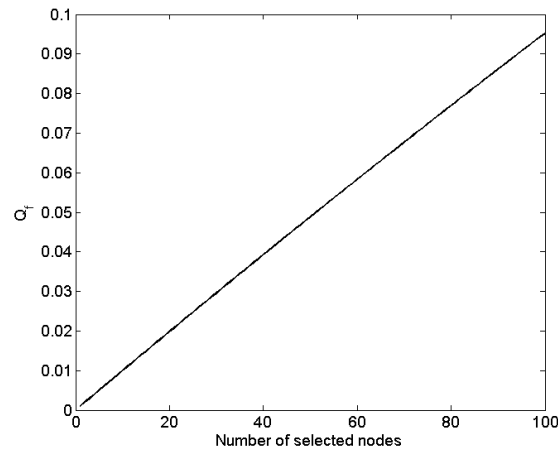


**Figure 3.15:** Global probability of false alarm  $Q_f$  in the function of the number of selected nodes

not observed in previous works on correlation-based sensing, most probably due to the lack of detailed modelling for channel correlation.

The results have also showed that the number of selected nodes influences the value of  $Q_d$ . In general, the lower the number of selected nodes, the smaller  $Q_d$ , with actual value depending on the average SNR, as expected from the adoption of an OR decision rule. The loss in global probability of detection  $Q_d$  has been observed due to the reduction of the number of group leaders. The first case is the  $Q_d$  when all nodes in the system are allowed to send their decisions to fusion centre. The second case, referred to as *ideal selection*, corresponds to executing the grouping procedure at the beginning of each sensing phase, so at every second. The  $Q_d$  for all nodes is equal to 1, while for the optimally selected set of nodes it is around 0.9992. So the selection of a smaller number of nodes introduces a penalty in terms of a slight reduction of the global probability of detection, mainly as a result of the selected fusion rule. On the other hand,

**Table 3.2:** Global probability of detection  $Q_d$  values for *ideal selection*

Leader selection method	$Q_d$ value
$maxP_d$	0.9992
$mixed$	0.9975
$maxST$	0.9925

the global probability of false alarm was also significantly reduced, which is a strong advantage from the point of view of the secondary network. In fact, as under the CFAR requirement, the local probability of false alarm for every node is kept constant, the global probability of false alarm depends on the actual number of nodes taking part in decision making process. Figure 3.15 shows the relation between  $Q_f$  and the number of active nodes. One can see that, e.g., selection of 10 out of 100 nodes lowers the  $Q_f$  from 0.095 to 0.01. This implies that for the SNR used in experiments, the proper node grouping causes barely visible fall of  $Q_d$  and sensible fall of  $Q_f$ .

The above results prove that correlation-based node grouping can improve performance under realistic channel conditions and go beyond the results in [157] since, as already discussed in Section 3.2.1, in that work performance evaluation of the correlation based solution was limited to a scenario with randomly generated local probabilities of detection with no connection to relative positions and correlation of channel responses between secondary nodes.

The analysis focused next on the impact of the new leader selection metric. Three strategies for the group leader selection were investigated, corresponding to three coefficient sets for the metric. The first strategy selected the node with the highest local probability of detection to act as a group leader (corresponding to weight coefficients for eq. (3.8):  $c_1 = 1, c_2 = 0$ ), as proposed in [157], referred to in the following as  $maxP_d$  strategy. The second strategy aimed to select the group leader on the basis of both the local  $P_d$  and the stability coefficient ( $c_1 = 0.5, c_2 = 0.5$ ), and is referred to as the  $mixed$  strategy. Finally, the third strategy,  $maxST$ , only rewards stability ( $c_1 = 0, c_2 = 1$ ).

The results for  $maxP_d$ ,  $maxST$  and  $mixed$  strategies are shown in Figure 3.16. In every figure one can find three plots: the top curve is the *ideal selection* update strategy previously defined; the bottom curve corresponds to an update strategy named *starting selection* in which the grouping and selection procedure is executed only once, in the first second of simulation. Finally, the middle plot corresponds to the *periodic selection* update strategy, in which grouping is carried out every  $n$  seconds where  $n$  is selected so to keep the 0.95 threshold.

One can see that when adopting the *ideal selection* update strategy, the best result is guaranteed by the  $maxP_d$  strategy. In the  $mixed$  strategy  $Q_d$  value is slightly lower, while the  $maxST$  strategy leads to the worst result (see Table 3.2). The *ideal selection* values (presented in Table 3.2) are matched exactly by the *starting selection* at the beginning of each simulation, and by the *periodic selection* immediately after each update.

Maximum  $Q_d$  values are doubtless relevant for evaluating the performance of grouping and selection algorithms, but the stability of received measures is important as well. Figure 3.17a presents results for the *starting selection* update strategy for the three leader selection strategies introduced above. One can see that in the  $maxP_d$  strategy, which guarantees the highest  $Q_d$  value for *ideal selection*, the  $Q_d$  value decreases quickly in time, while for the stability-involved strategies the slope is significantly less steep. The least steep slope and the highest values of  $Q_d$

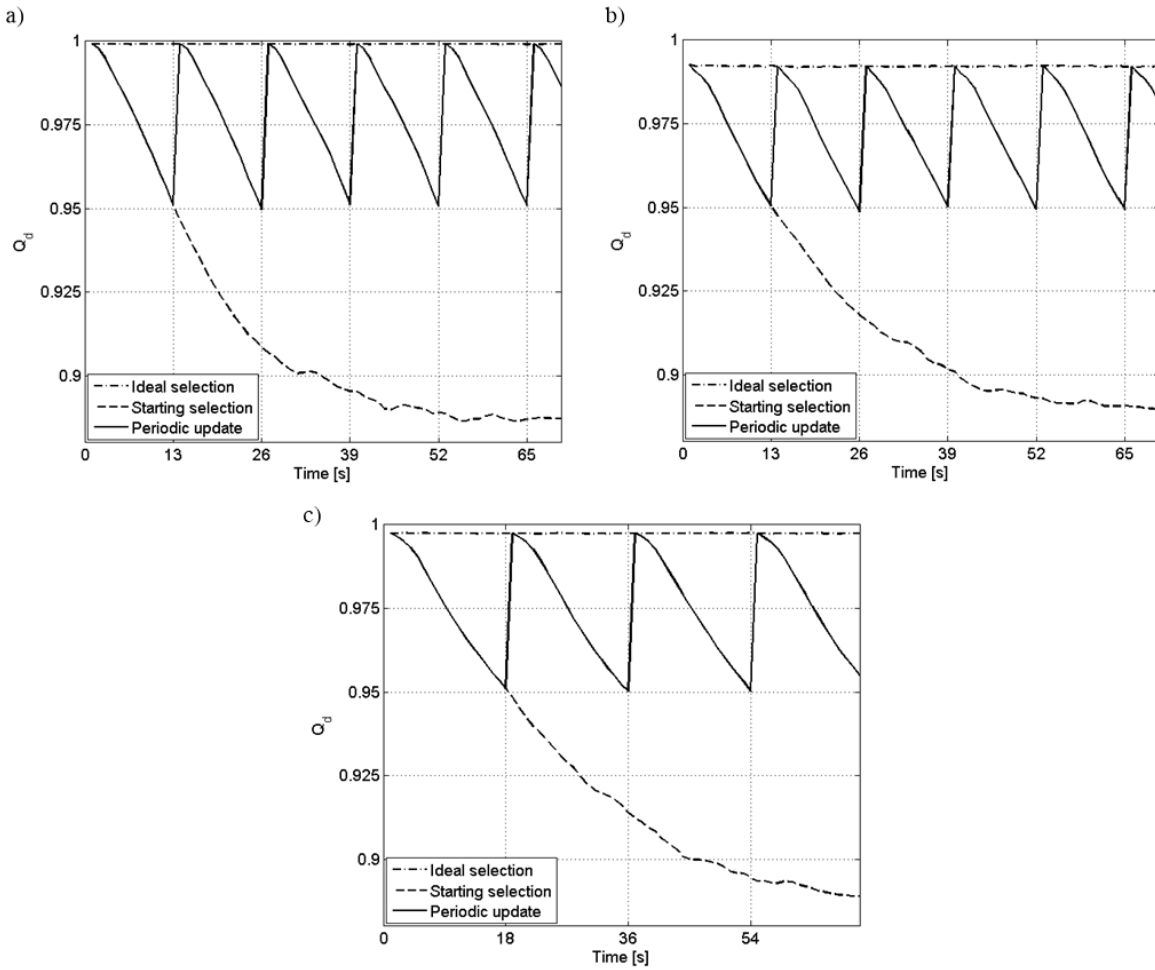
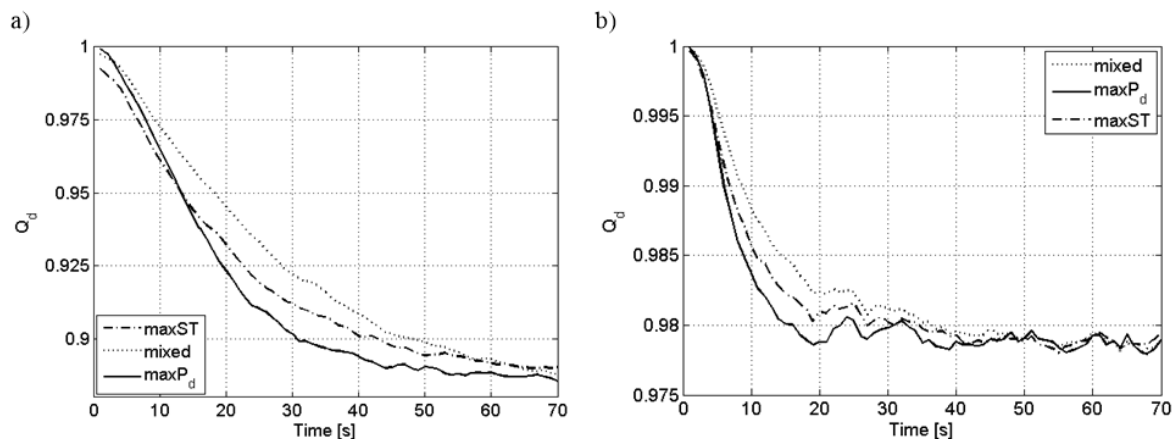


**Figure 3.16:** Global probability of detection  $Q_d$  vs time for a)  $\max P_d$  strategy,  $n = 13$  s, b)  $\max ST$  strategy,  $n = 13$  s, c)  $\text{mixed}$  strategy,  $n = 18$  s

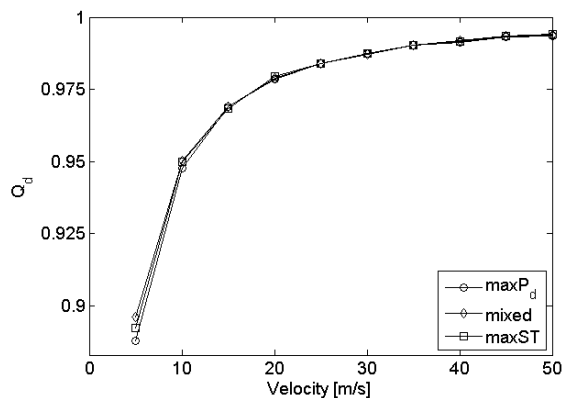
after two seconds were obtained for the strategy involving both stability and  $P_d$  in the selection of the group leader.

Fig. 3.17a shows that the global probability of detection might be acceptable not only immediately after the leader selection but also some time after the grouping and selection procedure. Since grouping and leader selection require significant information exchanges between nodes and thus introduce significant overhead in the network, one might want to perform such a procedure as seldom as possible while guaranteeing the desired probability of detection.

The beneficial effect of taking into account stability in group leader selection can be observed by comparing the *periodic selection* curves in Figure 3.16 that shows results assuming a minimum acceptable  $Q_d$  equal to 0.95. In fact one can observe that the periodic update time differs in the three cases, with the *mixed* strategy requiring an update only every  $n = 18$  seconds, while the other strategies require an update at most every  $n = 13$  s. The combination of node's  $P_d$  and stability introduced in the proposed leader selection strategy guarantees thus an increase of the minimum update time from 13 to 18 seconds corresponding to 38% gain. The price paid to get such an improvement is a slightly lower  $Q_d$  value in the very first seconds after each



**Figure 3.17:** Global probability of detection  $Q_d$  for *starting selection* for terminal velocities in the range of: a) 1 – 5 m/s, b) 1 – 20 m/s



**Figure 3.18:** Floor value of the global probability of detection  $Q_d$  vs maximum node velocity for three leader selection strategies

selection procedure. Although further studies are required to quantify the overall impact of the two phenomena on overall performance in the secondary network (e.g. in terms of throughput), the results strongly suggest that the proposed strategy may provide a significant advantage.

The trend of  $Q_d$  as a function of time strongly depends on the mobility of SUs. In Fig. 3.17b, one can observe results for nodes velocities in the range of 1-20 m/s. The results in Fig. 3.17 show that the floor value in the *starting selection* update strategy is significantly higher in the  $v_{\max} = 20$  m/s case. Min and Shin in [112] pointed out that the sensing scheduling gain rises proportionally as node's velocity increases. One could thus predict that wider range of nodes velocities lowers correlation between nodes and thus improves global sensing results.

In order to verify this assumption, the floor value of global probability of detection was evaluated as a function of the SU maximum velocity  $v_{\max}$ , with minimum velocity  $v_{\min}$  set at 1 m/s (Fig. 3.18). One can see that the higher the node's maximum velocity, the higher floor value of  $Q_d$ . This is determined by correlation between the sensors. In low-velocity scenarios, decisions of nodes are highly correlated so there are a few large groups of nodes. Therefore, only a few nodes are selected and allowed to vote. In a high-velocity scenario, the correlation between

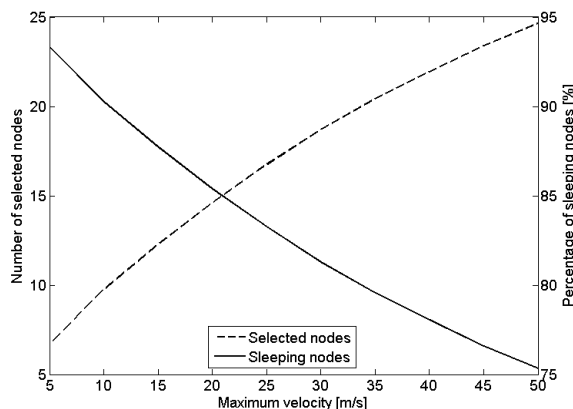


**Figure 3.19:** Number of selected nodes and percentage of sleeping nodes versus maximum node velocity

nodes' decisions is small. As a result, there are more groups of nodes and more uncorrelated nodes. The higher the number of active nodes and the higher the average velocity, the higher the probability that one or a few nodes experience reliable channel conditions. This is confirmed by Figure 3.19, showing the number of active nodes (dashed curve): the higher the mobility of nodes, the higher number of active nodes. Moreover, the higher number of active nodes provides lower overhead reduction. In Figure 3.19, in solid line, one can also observe the percentage of sleeping nodes which were not selected by the procedure. These nodes may sleep and thus lower the overhead information exchange as well as reduce energy consumption. For high-correlated scenario the reduction in the number of updates and the corresponding overhead is the most significant. Even in the low-correlated scenario, the reduction of number of the active nodes is however still prominent (75% for  $v_{\max} = 50 \text{ m/s}$ ) thus justifying the adoption of a grouping and selection procedure even at relatively high speeds.

### 3.2.5 Conclusion

In this section, a novel correlation-based node grouping and selection algorithms have been proposed by the author of the thesis, that take into account both sensing performance and mobility of secondary nodes. This is obtained by introducing a leader selection metric that combines node's individual detection probability  $P_d$  and its stability. The performance of the proposed algorithm has been evaluated and compared with previous work by means of extensive computer simulations carried out in Matlab environment. Simulation results show that by including stability in the group leader selection criteria correlation-based sensing can operate with larger time intervals between the periodic updates, with a 38% decrease in the number of updates while guaranteeing a network probability of detection above the 0.95 threshold, at the price of a slight reduction in the maximum value of the same probability. It has been also proven that adopted selection procedure guarantees usage of only 9% and 25% of nodes in high and low-correlated scenario, respectively.

The proposed algorithm requires the availability of information about the nodes velocities; it should be noted however, that this information can be derived by means of outdoor (e.g., Global Positioning System (GPS)) and indoor positioning systems based on technologies like Wi-Fi or

Radio Frequency Identification (RFID). Furthermore, the algorithm can equally operate based on relative velocities of nodes, rather than on their absolute speed. This relative information can be obtained by monitoring the rate of topological change observed by a node (e.g., average number of neighbours varied per second). One could thus argue that this assumption is overall more realistic than the one of knowing exactly the local probability of detection of each node. Nevertheless, most of the solutions for cooperative spectrum sensing presented in the literature make the latter assumption.



## Chapter 4

---

# Energy-Efficient Cooperative Spectrum Sensing

---

### 4.1 Considerations on Energy Efficiency for Spectrum Sensing Algorithms

#### 4.1.1 Identification of the Figure of Merits

One can find several metrics related to power consumption in devices or networks [37]. The basic one is the *bits-per-Joule* [b/J] which is essentially a throughput-per-energy usage metric. Throughput is understood here as the total number of bits transmitted in a network. In the case of CSS, where a number of steering and control messages are often interchanged, the metric of *effective bit-per-Joule* can also be considered, where only the transmitted information-data bits are counted, and the bits transmitted in supporting channels are not included. Alternatively, the *bit-per second-per-Watt* metric can also be taken into account.

The next group of energy efficiency indicators is connected with network coverage, such as the *Watt-per-square kilometre* denoted as [W/km<sup>2</sup>]. This indicator is adequate for systems covering large areas, e.g., in macrocells used in rural areas or in sensor networks designed to cover a given area [145]. However, in urban areas, where a system is traffic-demanded, a more fair indicator is one related to the number of serviced users. Such a metric is defined as the number of users served in the busy hours measured in *users-per-Watt* [60]. An energy-related metric taxonomy may be found in [71]. Note that for cooperative sensing, these metrics have to be adapted to a specific CSS case. Contrary to cellular networks, in CSS, the coverage has to be understood as the area for which a decision made by the fusion centre is valid, or—alternatively—the area over which sensing nodes are deployed.

Although the coverage and capacity-related metrics are important and widely used, they are in fact not comprehensive enough in the cooperative spectrum sensing reality. It is suggested to introduce energy efficiency metrics related to the *quality of sensing* understood as the *global*

*probability of detection-per-Watt* and the *global probability of false alarm-per-Watt* [32]. Such metrics can be defined mathematically as:

$$EE_{Q_d} = \frac{Q_d}{P_{\text{tot}}}, \quad (4.1)$$

and

$$EE_{Q_f} = \frac{1 - Q_f}{P_{\text{tot}}}, \quad (4.2)$$

respectively. Here,  $Q_d$  and  $Q_f$  stand for the global probability of detection and the global probability of false alarm in the network, which have been defined in Section 1.2.3. Moreover,  $P_{\text{tot}}$  represents the total power consumed by the network in one sensing and data-transmission period. The energy efficiency increases when the detection quality increases, and when the consumed power decreases, which are usually contradictory goals in the network.

### 4.1.2 Single Sensing-Node Power Optimisation

Because energy efficiency may be measured with the use of a number of metrics, these considerations are focused on the reduction of the consumed power with as low a degradation of performance as possible. Thus, the first step in finding reliable solutions for energy reduction is to identify the possible opportunities where such optimisation can be achieved.

The power consumption in a sensing node  $P_{\text{node}}$  in a network of cooperatively sensing nodes consists of the energy devoted for sensing  $P_{\text{sensing}}$ , for the processing of gathered data and the preparation of the reporting message (e.g., quantisation)  $P_{\text{processing}}$ , and finally, for the transmission of this reporting message  $P_{\text{transmission}}$ :

$$P_{\text{node}} = P_{\text{sensing}} + P_{\text{processing}} + P_{\text{transmission}}. \quad (4.3)$$

Therefore, the optimisation of energy efficiency should include the reduction of the power related to each component from formula 4.3. In other words, the sensing energy may be reduced by shortening its duration, and the processing power usage depends on the complexity of adopted sensing method, as well as on the adopted quantisation algorithm applied for sensing-information representation (see Section 1.2.1). The power consumed on the transmission of the reporting message depends then on the transmission distance and the environment in which the transmission is performed (described by the path loss coefficient). Besides,  $P_{\text{transmission}}$  may be reduced by lowering the size of the transmitted message.

One may try to analyse, in a more detailed way, which factors influence the average power consumed by each sensing node in each phase. The amount of power consumed in the first phase, i.e., spectrum sensing  $P_{\text{sensing}}$ , depends on the electric and electronic components of the terminal front-end. In particular, in order to effectively sense a wide range of a frequency spectrum, the wireless terminal should be equipped—depending on the selected architecture (homodyne, heterodyne, low-IF etc. [77, 140])—with a wideband (possibly tunable) aerial, wideband and steerable filters and Low Noise Power amplifiers. Next, the received signal should also be shifted to the baseband, thus appropriate wideband mixers and voltage-controlled oscillators with phase-locked loops have to be used. Finally, such a signal has to be converted from the analogue to digital domain, and the power consumption by such tunable converters strongly depends on the

processed bandwidth. Clearly, instead of wideband elements mentioned above, a set of parallel processing chains may be used. In order to estimate the power consumed by the analogue front-end of the sensing node, one should apply relevant models proposed in the rich literature, e.g., in [49, 50].

The power consumed during data processing  $P_{\text{processing}}$  strongly depends on the computation complexity of the selected sensing algorithms. Such computation complexity can be represented by the number of operations (e.g., complex multiplications, complex additions and the number of accesses to the memory) required for the preparation of the reporting message containing a local sensing decision. By getting the number of operations, one may assess the average power consumption by the Digital Signal Processor (DSP) or FPGA modules. A detailed comparison of selected single-node spectrum sensing algorithms (including computational complexity) can be found in [102].

Finally,  $P_{\text{transmission}}$  represents the power required for reporting the message delivery to distant nodes (e.g., to the fusion centre). Depending on the situation (environment type, e.g., urban, suburban), appropriate channel models can be used for an accurate assessment of the power consumed by this data transmission.

Note that, in fact, the energy consumption within a given time also has to be considered during the optimisation process. This is due to the fact that the time devoted for each phase is also one of the parameters that can be optimised. For example, the selection of a specific sensing algorithm (such as energy detection) influences both the average power used for sensing, and the time required for it. Let  $T_{\text{sensing}}$  denote the sensing time,  $T_{\text{processing}}$  the processing time,  $T_{\text{transmission}}$  the reporting time. The energy consumed by a single node in a CSS network equals:

$$E_{\text{node}} = P_{\text{sensing}} \cdot T_{\text{sensing}} + P_{\text{processing}} \cdot T_{\text{processing}} + P_{\text{transmission}} \cdot T_{\text{transmission}}. \quad (4.4)$$

### 4.1.3 Energy Efficient Optimisation From the Network Perspective

Each energy-efficient sensing node improves the overall energy efficiency in a cooperative network, but the total energy consumption may be further reduced if the energy consumption is analysed from a network-level point of view. In particular, the energy consumed in a centralised network of  $N$  cooperating nodes (in a network where a central entity collects sensing information and then announces a global decision by a broadcasting message) is given by:

$$P_{\text{network}} = \sum_{i=1}^N P_{\text{node},i} + P_{\text{fusion}} + P_{\text{broadcast}}, \quad (4.5)$$

where  $P_{\text{node},i}$  is the power of sensing, processing and transmitting (reporting) the sensing information by node  $i$  in the network,  $P_{\text{network}}$  is the power devoted for CSS consumed in the whole network,  $P_{\text{fusion}}$  is the power devoted for the process of decision fusion, and  $P_{\text{broadcast}}$  is the power for broadcasting the message by the fusion centre. Let us note that this formula can be easily adopted to other network topologies used for CSS. For example, in the approaches known as censoring or node sleeping (both described in Section 4.4), the number of nodes used for sensing and data reporting can be reduced. Moreover, the value of  $P_{\text{broadcast}}$  depends mainly on the distance between the fusion centre and the most distant node awaiting its decision. In a centralised

network, especially for large  $N$ , this component will be relatively small compared to the first one, i.e., the  $N$ -fold included power consumed by sensing nodes. Again, the time used for report delivery to the fusion centre and data broadcasting is also one of the parameters for optimisation. Thus, instead of the total power consumed in the network, one should concentrate on the energy consumed. The formula for energy consumption in a CSS network is the following:

$$E_{\text{network}} = \sum_{i=1}^N P_{\text{node},i} \cdot T_{\text{node},i} + P_{\text{fusion}} \cdot T_{\text{fusion}} + P_{\text{broadcast}} \cdot T_{\text{broadcast}}, \quad (4.6)$$

where  $T_{\text{node},i}$  is the time required for sensing, processing and transmitting (reporting) the sensing information by node  $i$  (assumed as a single activity time-period),  $T_{\text{fusion}}$  is the time required by the fusion centre for collected information processing and taking the global decision, and finally,  $T_{\text{broadcast}}$  is the time of broadcasting the global sensing decision.

One can observe that the energy in the network may be saved by the reduction of the following factors: *i*) the number of cooperating nodes (e.g., by selecting only substantial representative nodes), *ii*) the power consumed by the nodes (e.g., in the sensing, sensing-information processing or in the transmission phase for a selected subset of nodes), *iii*) the energy cost of data fusion and decision delivery to the interested nodes (being a mixture of the two previous factors), *iv*) or network topology.

To sum up, energy efficiency may be provided to the CSS network with several possible methods. A variety of propositions which may be found in the literature, and which are proposed by the author in the thesis, show that the overall energy efficiency depends on the operating radio environment and desirable performance.

## 4.2 Energy Efficiency in Cooperative Spectrum Sensing: Classification

The aforementioned analysis of cooperative spectrum sensing has set a solid background for the possible directions of energy savings. In the literature, one can find a number of diverse energy-efficient techniques which may be grouped according to several possible classifications. In this thesis, the classification is proposed based on four main directions (or branches) of possible energy savings (see Fig. 4.1). They are as follows:

- Branch A: energy reduction in the (local) spectrum sensing phase,
- Branch B: optimisation of the number of cooperating nodes,
- Branch C: proper selection and application of fusion and decision rules,
- Branch D: energy-efficient network organisation.

Below some general observations for each branch are provided which will be discussed in detail in the following sections.

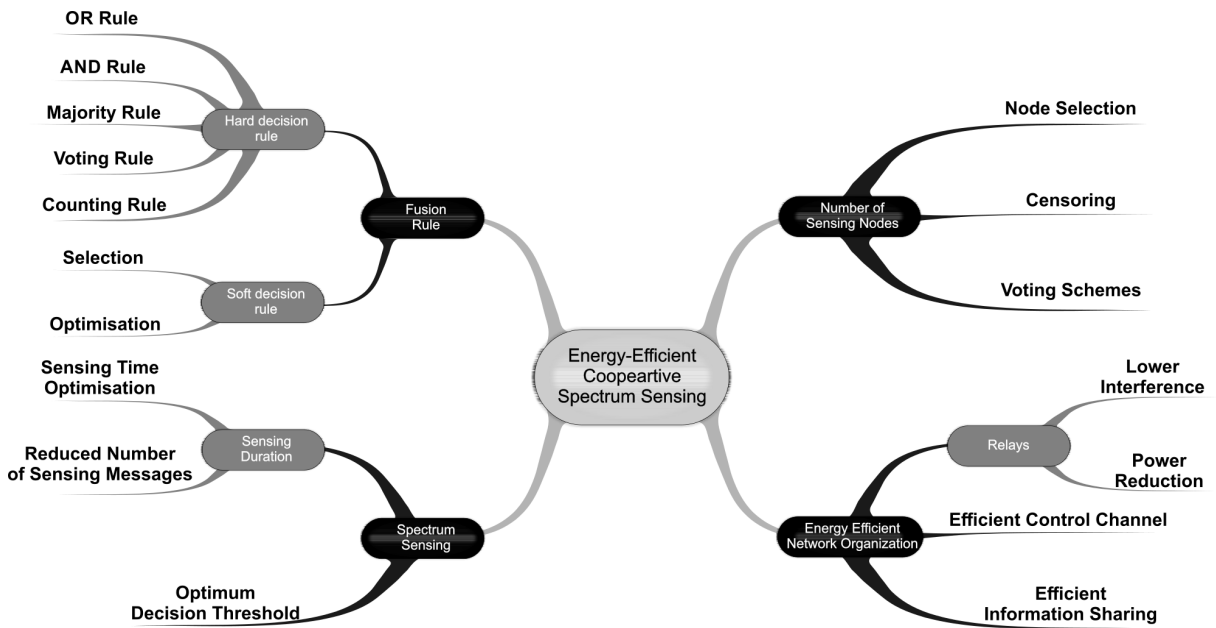


Figure 4.1: Classification of energy-efficient cooperative spectrum sensing

### Branch A

Focusing on the first branch, one can state that an immediate and natural option of saving energy is to go inside the sensing device for the proper selection of energy-efficient components. The application of advanced and flexible radio-frequency front-ends, where some portions of digital or analogue elements can be switched off or shifted into stand-by mode, may result in overall energy consumption reduction, especially if the number of sensing nodes is high. Exemplary discussions on such solutions may be found in [25, 64, 65].

Furthermore, one of the basic ideas of energy efficiency in local spectrum sensing is to reduce the sensing time or the number of collected samples regardless of the adopted sensing method. Certainly, the lower the number of acquired samples, the lower the energy consumed. However, this comes at the cost of decreased performance. Solutions which optimise the sensing time (or the number of acquired samples) are described in Section 4.3. Although this may be done simply in a non-cooperative network scenario, the sophisticated cooperative adjustment of sensing times may also be provided.

A further increase of energy efficiency may be achieved by optimisation of the decision threshold,  $\epsilon$ , shown in Fig. 1.8, which is used for the differentiation of decisions reported in soft- and hard-decision scheme. However, taking into account network cooperativeness, joint optimisation of the decision threshold may bring even higher a gain than the one obtained with individual (distributed) optimisation.

### Branch B

Another possibility of introducing energy efficiency in CSS comes from the observation that there may be some nodes in the network which bring a marginal profit to the overall detection performance. Therefore, it is beneficial to lower the number of active nodes when they encounter

bad channel conditions in the sensed channel or their sensing results are highly correlated with other (neighbouring) sensors. In such a case, these nodes offer a relatively small added value to the network EE metrics at the high cost of consumed energy. Thus, it is beneficial to reduce the activity of some nodes. One may pose two questions: *i*) selection of which nodes is the most beneficial, and *ii*) how to organise such a selection.

Dozens of authors have tried to ask the first question and find the optimum sets of selected nodes for various topologies and network configurations. The general rule is that it is optimum to select the sensing nodes on the basis of the signal-to-noise ratio (in the primary- to secondary-user link) [129]. However, the possibility of proper selection depends on the radio propagation conditions. It is not always possible to estimate an SNR accurately. Moreover, the transmission of all approximation results consumes much of the spectral and energy resources.

As the nodes are recommended for active participation in the sensing process, the following cases can be considered. First, a subset of nodes from a group can be selected, i.e., be active in the sensing phase, while the other ones turn to the sleep mode, and do not sense the frequency-band occupation or report any sensing information. The nodes may also be censored, i.e., may sense the licensed signal but have no reporting rights, i.e., do not report local sensing observations to the other nodes. Although a limited number of active nodes lower the overall energy consumption, the node selection process may be inefficient energy-wise, or incorrect (if wrong nodes are selected for a sensing or sensing-and-reporting group).

### Branch C

Further energy savings are possible if an efficient fusion of sensing messages is considered. For example, for the hard decision reporting mode, it is possible to adapt the decision fusion threshold on the basis of the observed wireless channel conditions (e.g., [130]). When soft or quantised-soft metrics are taken into account, further energy efficiency improvements are possible.

### Branch D

The consumed energy may also be limited by efficient network organisation. Clearly, if the number of interchanged steering messages in CSS is high, the energy devoted to this process should definitely be considered more carefully. Thus, the question about cooperation gain and associated overhead in the centralised and decentralised CSS topologies is crucial. Recently, much attention has been given to the topic of relaying technologies. One may find papers tackling the problem of how relaying is energy efficient, and when it is more beneficial (in terms of the saved energy) compared to direct transmission (e.g., [68]). Apart from relays, the other solution for energy efficiency in Branch D is a cluster-based one.

Please note this is one of possible classifications. An other would be a division according to the provided sensing procedure parts. In Fig. 1.7, one can see an illustrative diagram of cooperative spectrum sensing. Here, energy efficiency may be introduced for each state, e.g., in “Local Decision Reporting”, energy may be saved by a proper selection of cooperating nodes or a neat network organisation. Note that some solutions described in that work introduce energy efficiency by combining two different *branches* shown in Fig. 4.1.

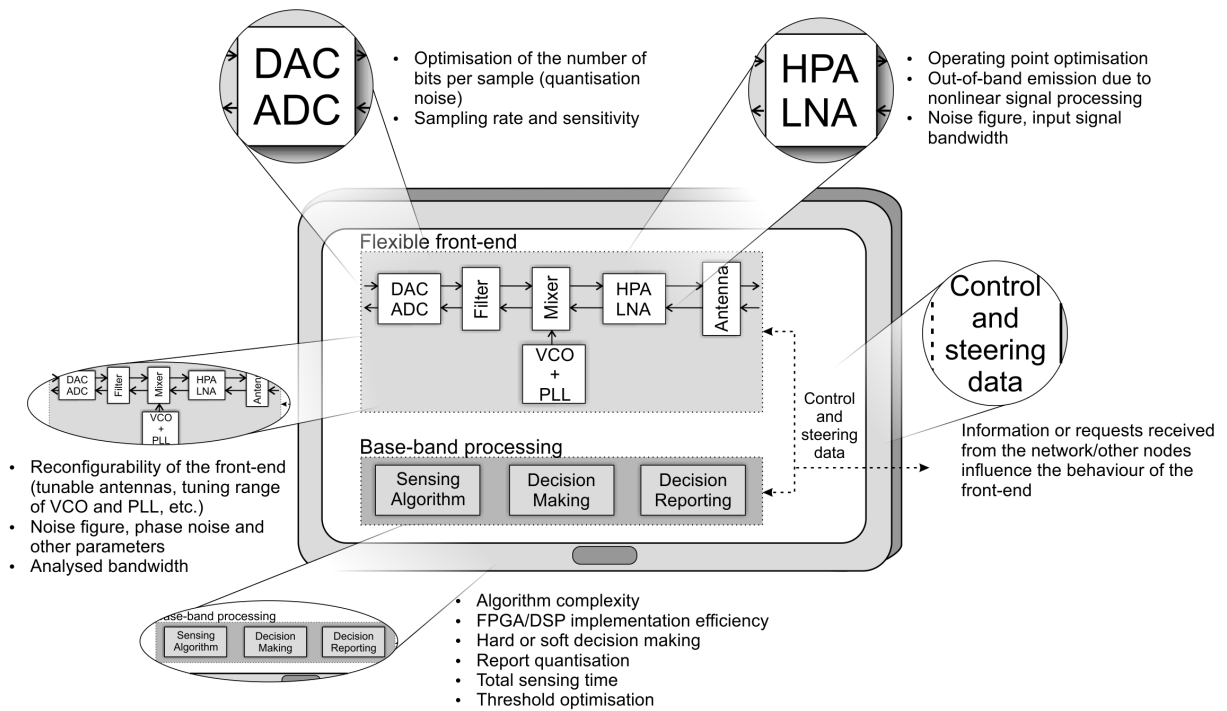


Figure 4.2: Energy saving areas in a single node

### 4.3 Energy Savings in Local Spectrum Sensing

Energy-efficient design and algorithms are possible inside a sensing device. The aforementioned energy-efficient hardware (e.g., power amplifiers) may significantly reduce the power consumption. This may also be done if the spectrum sensing procedure is optimised. The first possibility is to reduce the number of acquired samples or, in other words, reduce the sensing time. Although the number of samples may theoretically always be reduced when the desired sensing reliability should be achieved, the minimum number of collected samples can be found for each sensing method. Regardless of the number of samples required for further processing, specific features of the applied analogue elements in the transceiver front-end have to be defined (Fig. 4.2). For example, one of the key contributors to the energy consumed by the terminal front-end is the power amplifier. Optimisation of its operating point also optimises its energy efficiency, and can lead to the reduction of nonlinear effects (like intermodulation products) which are not allowed in practical systems, especially in the context of cognitive radio. Moreover, beside the total number of samples needed for the sensing algorithm, the frequency of their collecting, as well as the number of bits used to represent each sample influence the energy consumed by the ADC and DAC. For example, in [70], it has been shown that for a given architecture, the power consumed by a DAC varies from 10 nW achieved for the sampling-frequency of 1 kHz to 26  $\mu$ W at the 10 MHz sampling frequency.

The sensing nodes should be able to operate in various frequency bands. Thus, all the necessary elements should be reconfigurable, and very often such tuning possibility is provided to the user at the cost of complexity, thus, higher energy consumption. It is then even more meaningful to optimise the energy consumed by the wireless terminal front-end. The analysis of the energy

consumed by particular elements of the radio transceiver front-end can be found in [11, 66]. In particular, in [66], the total power consumption at 1.1 V for various system architectures (Global System for Mobile Communications (GSM), Digital Video Broadcasting–Handheld (DVB-H), WCDMA, MIMO WiMAX and MIMO WiFi) varies from 60 W to 230 W.

Note that the number of required samples strongly depends on the selected sensing algorithm. For example, cyclostationary-based detection involves hundreds or even thousands of samples in order to observe periodicity in the sensed signal. In energy detection, this number may be reduced even to one sample, however, too small a number of samples (or too short sensing time) leads to performance degradation. Therefore, there is a trade-off: on the one hand, lowering the number of samples leads to detection degradation, while on the other, it guarantees lower power consumption, and results in a higher throughput because more time may be devoted to SU's data transmission (for more details see Section 1.3).

Moreover, the selection of the spectrum sensing algorithm can also impact the energy consumption by the radio-frequency front-end. The application of the pure energy-detection algorithm entails a high dependency of the final sensing decision on the noise variance. Thus, in order to improve the reliability of detection, the sensitivity of the device should be as low as possible, also meaning that the resultant noise figure or the impact of the phase noise should be minimised. It also means that the bitwise representation of each sample should be possibly high in order to minimise the impact of the quantisation noise on the sensing procedure. Furthermore, the application of more complex algorithms typically results in more sophisticated hardware realisation (using FPGAs or a digital signal processor), and this entails a higher power consumption by these chips. An interesting discussion on the FPGA implementation of selected spectrum sensing algorithms can be found in, e.g., [92, 172].

Discussion on sensing time optimisation may be found in [131], where it is shown that there exists an optimum sensing time which guarantees a maximum throughput. Interestingly, the sensing time is similar irrespective of the transmitted power level. In [111], the sensing time was analysed from the perspective of time per bit. It was proven that the longer the transmission time related to one bit, the higher the energy efficiency. However, when the circuit energy in a realistic implementation is taken into account, there exists an optimum point of time per bit for which the energy per bit is the smallest. However, in such an optimum point, the delay constraint has not been taken into account [154]. Finally, in [89], a sensing time allocation scheme for two PUs is proposed, while in [151], a neural-network-based optimisation is delivered. It has to be underlined that the individual optimisation of the sensing time may affect the transmission throughput performance. In Section 1.3, the idea of the joint optimisation of the sensing time and spectrum access is described.

Another possibility of increasing the energy efficiency is to optimise the sensing threshold. In [58], the threshold for energy detection is optimised. The algorithm in its two versions requires instantaneous or averaged SNR, and it has been proved that the total energy may be reduced and is supported by sensor-selection in the first step. Another threshold optimisation scheme is described in [82]. Here, the optimum threshold for energy detection has been found for a cooperative network in which the nodes send their binary decisions to the fusion centre adopting the OR-rule. This solution also proves that a combined use of energy efficient *branches* improves

the overall efficiency. Thus, the energy in CSS may be reduced for a single device, but a higher number of possibilities is opened when the energy is saved in a cooperative way.

Finally, note that in the context of the relaying nodes (or even cluster heads), the above discussion has to be slightly extended to the detection process performed before the signal is forwarded. Thus, the energy devoted to signal detection (and potentially decoding followed by re-encoding) has to be considered.

## 4.4 Number of Cooperating Nodes

The strength of the cooperative spectrum sensing solutions lies in the diversity of node locations and thus, in the variety of channel conditions and spectrum observations. Thus, the effect of faded and shadowed signal in one place for a single node is mitigated if a number of nodes cooperate in order to make a global decision. However, too high a number of the sensing devices may not bring relevant detection improvement while still consuming a high amount of power. Therefore, many authors try to find the optimum number of cooperating nodes and/or give a recipe for proper selection. For example, in [16], the number of nodes is optimised under specific time constraints. It is assumed that the duration of a frame and its transmission part is fixed. The general conclusion is that there exists an optimum number of nodes that maximises the energy-efficiency. Moreover, the longer the time for sensing and reporting, the higher the number of nodes maximising the energy-efficiency.

The optimum number of nodes may be selected in many ways. One may distinguish three main approaches. In the first approach, known as *node selection*, a subset of SU nodes is not allowed to sense the spectrum and report relevant sensing information (local decisions on spectrum occupancy). These nodes turn to the sleep mode and thus save energy. The licensed signal is sensed just by another disjoint subset of nodes. Unlike in node selection, in a technique called *censoring*, all nodes are allowed to make sensing observations but some of them cannot report this information. In this technique, it is possible to censor nodes during the sensing process, i.e., on the basis of up-to-date local sensing results. These two situations are illustrated in Fig. 4.3.

Naturally, lowering the number of active nodes may degrade the overall probability of detection. Thus, although a lower number of nodes decreases the number of transmitted messages with reporting information, the power devoted to one link is higher due to the longer distance to its neighbour when the decentralised scheme is used. Moreover, the energy savings nearly always have an associated cost. One is the degraded performance through the decreased global probability of detection or increased global probability of a false alarm. The other is that the sensing and reporting nodes have to be somehow selected and informed about their selection. The additional messages and processing cost should also be taken into account, as they may reduce the energy efficiency of the algorithm.

### 4.4.1 Node Selection

The basic assumption in lowering the number of active nodes is to maintain the overall performance. This definitely depends on the criterion used for the selection of nodes in order to reduce the energy with an acceptable and possibly minimised cost of performance degradation.

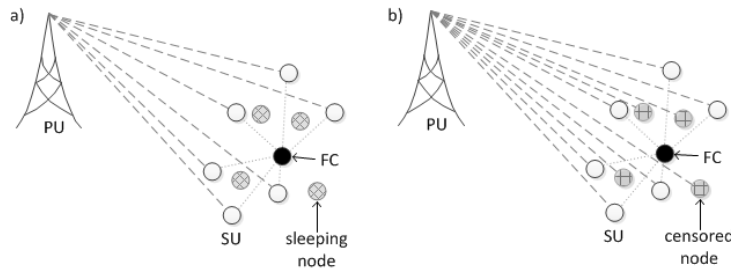


**Figure 4.3:** Model of a centralised CSS system where a) node selection or b) censoring is applied

The first criterion of efficient node selection is the observed signal-to-noise ratio. In [129], the authors propose such a selection and claim the solution is the optimum one. In this algorithm, the optimum value of  $Q_f$  (or  $Q_d$ ) is found by the selection of an optimum number of nodes with the highest signal-to-noise ratios. However, for the proposed algorithm, up-to-date information about the nodes' instantaneous SNR is needed, and has to be delivered to the fusion centre, while the fusion centre has to receive the information from every SU in the network. Variable channel conditions induce SNR variations that must be dealt with, for example, by periodic updates of the estimates of the SNR for each node. It was proven in the above-mentioned paper that the appropriate selection of only 19 out of 200 nodes provides promising results: under the CFAR with AND rule, the global probability of detection is improved from 92.04 % to 99.88 % and much energy for the decision interchange is saved.

Another algorithm based on the SNR criterion has been described in [166]. In this work, the secondary user with the highest SNR is chosen in the first iteration. Next, every other node compares the quality of its link to the fusion centre with the quality of its link to the formerly selected node and from the formerly selected node to the fusion centre. If a node determines that its own link is less reliable, then it joins the group of nodes experiencing the highest SNR. Otherwise, the next highest-SNR node among ungrouped nodes is selected, and then the procedure of comparing link qualities and grouping is repeated until all nodes are grouped. Again, reliable information about the SNR ratio is demanded. Moreover, the energy efficiency of the scheme depends on the number of selected group-heads: the lower the number of selected heads, the higher the energy efficiency, up to 76 %.

Another interesting SNR-based selection algorithm has been proposed in [20]. In this work, the nodes are classified either as leaders or followers based on the received SNR. The leading nodes have good detection performance and are allowed to sense the PU signal and broadcast their sensing information. The following nodes are considered unreliable due to a low SNR, so they do not broadcast their decisions, but rather wait for the broadcast packets from leaders. Thus, only the reliable information is broadcast. In addition, the information sent by the leaders is rather limited, only consisting of the PU-presence information. As a result, the approach proposed in [20] leads to low overhead information. However, the identification of nodes with the highest SNR is challenging, as it must rely on the presence of the PU during the training (measurement) periods.

A typical SNR-based node selection similar to the aforementioned work [129] has been described in [106]. In this paper, an adaptive double-threshold method is also introduced, and connected with noise uncertainty. The presented results show, as emphasised in [129], that it is

beneficial to select only a minor percentage of nodes with the highest SNR, thus guaranteeing an optimum global detection probability and important overhead reduction.

Although it is underlined that SNR-based node selection brings significant gains, in the literature, one may find another promising criterion of node selection. It is the correlation-based node selection algorithm which is based on nodes' decisions about PU presence. The idea is to select nodes whose sensing observations are uncorrelated. It relies on the assumption that the selection the uncorrelated nodes should result in high detection quality, while significantly minimising the energy overhead spent in the network for reporting.

The idea of correlation-based node selection comes from [150]. The selection of nodes is proposed to be conducted with the use of a correlation measure computed by the nodes. Starting with a randomly selected node, the nodes, one after another, compute the correlation of their own sensing decisions with the decisions of other nodes pair by pair. If the sum of correlation coefficients is high, the node becomes inactive and is removed from further correlation computing. The correlation measure in [150] involves location of nodes and distances.

Unlike in the aforementioned article, in [27], the correlation is based only on sensing messages received from nodes in the network. A randomly selected node broadcasts its sensing observation, while every other node listens to messages received from other nodes and calculates the correlation to that. If the correlation is above an assumed threshold, the node becomes inactive. Nodes which have a correlation below the threshold select a random delay and the one which has the shortest delay reports its data. The procedure is repeated until there are remaining uncorrelated nodes. After the procedure is completed, all nodes may specify the global decision because during the procedure they got the messages from all uncorrelated (i.e., selected) nodes.

In [157], the correlation between nodes is delivered only on the basis of decisions made by nodes. In the algorithm, a number of sensing decisions has to be delivered to the fusion centre. The FC then derives a correlation matrix and creates correlated groups of nodes according to the minimum correlation threshold. The information about the formed groups is sent to the network, and then, in each group of correlated nodes, a leading node is selected. In [157], the node with the highest detection probability is selected as a group leader.

In [33], basing on [157], a different selection of group leader has been proposed. It has been shown that in a mobile scenario, the formed group of nodes may quickly become obsolete. Thus, the leader selection metric considering both node mobility and sensing performance is proposed.

#### 4.4.2 Censoring

In the censoring algorithm, all nodes sense the spectrum band, however, only some of them are allowed to report their observations. Thus, the energy is saved during the reporting stage when some nodes do not transmit their observations. Moreover, censoring is more reliable than node selection because the censored nodes are selected after each sensing period.

An example of an algorithm based on censoring is introduced in [150]. In a network consisting of  $N$  nodes, all nodes are grouped to the active set at the beginning of the algorithm. After the selection, only  $X$  nodes may remain in the active set, while the rest is moved to the passive set, and that includes all nodes that are not allowed to vote for the global decision. In order to make a proper selection, the correlation measure is computed for pairs of nodes in the network. Then, the node with the highest summed correlation with the remaining sensors is removed from the

active set and moved to the passive set. The correlation measure used in [150] is based on the positions of nodes and associated positioning uncertainty.

In [109], the censoring scheme has been optimised. The authors put censoring into the global cost-function of sensing, and propose a solution for the selection process based on the double-threshold energy detection. The sensing decision is censored if the collected energy of the PU signal falls in between two thresholds. Under some constraints (the assumed global probabilities of false alarm and detection, and the OR fusion rule) it was shown that the censoring probability for an average node saturates rapidly and is not dependent on the number of cognitive radio nodes, leading to a lower consumed energy. The scheme can be easily adopted in a practical network.

The idea of censoring is further investigated in another article by the same authors [110]. There, a similar model of cooperative network is proposed, where censoring and sleeping are adopted under the constraints of minimum detection probability and maximum false alarm probability. Moreover, the authors provide a detailed analysis of energies consumed in the network. Two cases are compared: *A*) when the sensing and transmission energy are equal, and *B*) when the sensing energy is a minor part of the transmission energy. It is shown that the censoring rate in case *A*) is lower than in case *B*), and that the rate of turning to the sleep mode is higher in *A*) than in *B*). Moreover, the proposed solution is adopted in the real ZigBee transmission network. It is proved that it is possible to find the optimum censoring and sleeping rates and using these values may result in significant energy savings.

Finally, in [108], the idea of sequential censoring is introduced as a combination of traditional censoring with the sequential algorithm. Again, the authors find the optimum values for censoring thresholds both for the OR and AND rules. It is shown that for low-energy radios, sequential censoring outperforms regular censoring in terms of energy efficiency. Moreover, the AND fusion rule guarantees a lower energy consumption for medium values of PU presence probability (not higher than 0.8) than for higher values.

### 4.4.3 Voting Schemes

Note that it is not always possible to properly estimate the signal-to-noise ratio. Moreover, it may not be energy-efficient to interchange messages in order to find the specific SNR value. Therefore, voting schemes have been proposed, based on the observation that the conclusion of own and global decisions may be based on an SNR-like metric.

The first representative of voting schemes is the so-called *Confidence Voting* [95], in which the nodes build reliability-related measures. The idea is to limit unreliable decision transmissions. Every node is obliged to compute a confidence metric. In the hard decision scenario, the local and global decisions are collated. In the case of coincidence, the confidence metric is incremented, otherwise it is decremented. After the training period, in which the metrics are computed, only the nodes with the highest confidence metrics are allowed to report their decisions to the fusion centre. The authors claim that up to 40% of energy may be saved when using their algorithm.

The Collision Detection scheme, presented in [87], is based on node selection with the highest correctness measure. The measure notifies the number of a node's correct decisions when the global false decision is that the PU is not present. The nodes with the highest correctness are selected and involved in cooperative sensing.

The schemes based on voting have the advantage of being applicable in scenarios when there are no periods in which the presence of the PU is known in advance. However, these schemes have a major drawback. As they rely on the opinion of the majority, if most of the secondary users face bad channel conditions in their links between the PU and themselves, more confidence goes to unreliable nodes. As a result, the decision obtained in confidence voting may be worse than in the traditional scheme. Moreover, the voting schemes are not robust enough in the case of the presence of malicious SUs. A malicious SU is the one that sends untrusted decisions and makes the decision taken in the cooperative network unreliable [10].

In [120], the authors propose a scheme that combines energy efficiency and sensing performance in node selection. The scheme introduces a cost function that favours nodes with the lowest sensing and decision-transmission energy usage among those satisfying the quality of detection constraint. Furthermore, energy efficiency is increased by introducing the *Decision Nodes*, each acting as the collector of sensing results from a set of selected nodes, determining a common decision and sending it to the fusion centre. The scheme requires information about the nodes' signal-to-noise ratios and the distances between each node and the fusion centre in order to operate, leading to a significant control overhead.

In [59], the *multi-channel aware* algorithm is proposed. The nodes with the lowest energy consumed by sensing and reporting, and the lowest number of channel switches are selected. Moreover, the nodes experiencing higher SNRs (in the links between the PU and themselves) are chosen due to shorter demanded sensing time. There, the nodes' selection is performed with an occurring delay constraint. The algorithm results in low energy consumption.

## 4.5 Fusion Rule

As mentioned above, the decrease of energy consumption is possible if the fusion scheme is appropriately optimised. In Section 1.2.1, it is stated that there exist two basic types of decisions transferred from nodes to FC: hard- and soft-decisions. The main objectives are described and some references are proposed: [105, 156, 22, 164]. This essentially determines the effectiveness of decision fusion. The works presented below deal with the optimisation of the fusion rules, which for the hard-decision reporting are as follows: OR, AND and the majority rule (known as the  $k$ -out-of- $N$  rule).

In [15], the authors analyse the energy consumption and detection probability of three fusion rules under three parameters: frame length for each rule, the number of nodes and SNR. The results show that for the critical set of conditions (very short frame length, substantial number of nodes, low SNR), the Equal Gain Combining rule outperforms the Likelihood Ratio and Maximum Ratio Combining rules [15].

The majority of authors make the assumption that the reporting channel is ideal and error-free. This is, however, impractical in an actual CSS network. In [28], one may find an interesting analysis of the fusion rule performance where the reporting channel is not ideal. Hard decisions and soft decisions have been taken into account. It has been proven that the soft decision combination is more robust to channel impairments. However, the work has not covered the topics of the associated complexity and transmission overhead.

In [130], the authors propose optimisation of number  $k$  in the  $k$ -out-of- $N$  fusion rule together with energy detection threshold optimisation with the aim of energy efficiency maximisation in a network of cooperating nodes. The presented results show that the joint optimisation of  $k$  and the decision threshold may lead to energy efficiency up to 2 bits/Hz/Joule for different SNRs.

The *Adaptive Counting Rule*, which is in fact an optimisation of the majority rule, is proposed in [132]. There, a cooperative network of  $N$  SUs is considered. The adaptive rule is applied in the hard-decision fusion scheme. It optimises the number of sensing SUs  $k$  declaring the presence of the primary signal. It is shown that the optimum minimum value of  $k$  depends on the value of the calculated correlation of the nodes' decisions, as well as the number of detectors in the network and their detection performance. The authors also propose a continuous mechanism of selecting the optimum  $k$  value. However, the work lacks information about introduced overhead needed for the calculation of the optimum  $k$ .

An energy-efficient algorithm connecting the majority fusion rule with the sequential algorithm can be found in [179]. A two-stage algorithm was proposed, where in the first (coarse) stage, sequential sensing is applied with the modified majority rule. The stage is finished if more than a half of sensors declare the same decision. If the condition is not fulfilled, a fine stage is applied with the traditional energy detection algorithm and the accustomed majority rule. The proposed scheme may help in saving energy by up to 30 % for low SNRs and 60 % for high SNRs for most common settings.

In [136], optimum linear cooperative sensing is presented. The authors propose a method based on the combination of test statistics from the local nodes, instead of the full energy-detection reports with associated transmission overhead. The authors have conducted different optimisations for cases with different values of detection and false alarm probability. They claim that the optimisation of the fusion rule has to be provided for specific cases, e.g., for cases with a low possible false alarm rate and with a low detection rate.

## 4.6 Energy-Efficient Network Organisation

The energy-efficient network-organisation methods are presented that can be applied in CSS networks, allowing for energy-efficiency improvement. The topic of Medium Access Control with its details about spectrum access contention has not been addressed. Some details about spectrum access optimisation can be found in Section 1.3 and in the comprehensive works: [52, 170, 38].

In [68], the authors analyse the benefits of relaying the sensing information. They propose a two-stage algorithm consisting of the broadcasting and the relaying phase. The authors adopted the Bellman-Ford algorithm which for a given network-graph minimises the cost of transmission from a source to a sink in a distributed manner, taking the required transmission powers into account. The *optimum cooperative route* is found in an iterative way by exchanging a number of messages between the nodes, thus making the algorithm relevantly complex.

The same Bellman-Ford algorithm is used in an earlier work [78]. There, two solutions are proposed: first, minimising the power consumption in the route, and second, minimising the power under the constraint of achieving the assumed throughput. However, in that work, the power consumption is optimised only for single links, not for the whole network. Moreover, the scheme adopts a single-relay cooperation model due to an increased complexity for a higher

number of relays, although in that way simplifying the solution. The presented performance analysed for linear and grid networks shows significant power savings compared to the shortest-path algorithm.

An energy-efficient network with relays is also proposed in [169]. A wireless network of transmission pairs with the use of relays is analysed. There, it has been stated that for each transmission pair, one relay had been considered. With the introduction of virtual relay, the transmission mode selection has been simplified (direct vs cooperative). Then, the proposed iterative solution optimises the power allocation levels in order to find the minimum of the total power consumed in the network. However, the authors introduce a doubtful performance metric which is the *transmission reliability*, and adopt a limit of one relay per one transmission link. Finally, they present promising results of obtaining fairness in the network and solve the max-min fairness resource allocation problem. This fairness depends on the assumed transmission powers and the so-called transmission reliability being the probability that SNRs between source, destination and relay nodes follow a given criteria.

A similar single-relay scheme is proposed in [180]. The proposed protocol is based on request-to-send/clear-to-send (RTS/CTS) messages sent by a source and a sink, and on the contention phase in which relaying candidates compete. The contention is organised in a manner minimising the signalling overhead. Then, two solutions are proposed: minimisation of the total transmission energy and maximisation of the network lifetime. The presented results prove that direct transmission is outperformed by the proposed minimum-energy scheme, in terms of the consumed energy per packet and the network lifetime.

A similar cross-layer distributed algorithm can be found in [94]. As in some previously described schemes, here, the best relaying node and allocated power optimisation is found. Moreover, the authors not only present the prevailing min-energy total consumption but also introduce an interesting transmission rate-power trade-off. It is shown that under the energy minimisation constraint, the cooperative scheme outperforms the non-cooperative one, however, in the latter case, the gap in the defined utility-energy trade-off between cooperative and non-cooperative solutions is smaller.

In [163], an optimum routing strategy in a multi-hop network is proposed with identifying important delay constraints. The authors adopt a scheme where mutual information is accumulated after each packet transmission. Every node may send its information at any time after it receives the full packet composed of messages sent by other nodes. The authors propose a routing scheme minimising the total energy consumed in the transmission link under the constraint of a given delay. They show that this problem may be solved with the use of a greedy algorithm similar to the minimum delay routing. To this end, they introduce two heuristic algorithms presenting promising performance and underlining the fact of a limited overhead.

The authors of [155] present the analysis of energy efficiency in a system with one-way or two-way relaying. Although the proposed three-node scenario is quite simple, with a single relay positioned exactly between the transmitting and the receiving node and with a simplified channel model, the presented results are interesting. Generally, two-way relaying is more energy efficient than one-way relaying, since symmetrical transmission is considered. However, it is shown that relaying is not always more energy-efficient than direct transmission. If the channel attenuation is moderate, direct transmission is recommended. Otherwise, relaying is beneficial. Moreover, some

results related to the considered circuit power show that for a non-zero transmit, receive and idle power, energy efficiency has its non-zero maximum for medium spectral efficiency.

In [24], the authors present an optimisation of energy consumption in a network with some selfish nodes which may not be willing to relay other transmissions. The authors unveil the scheme of forming partnerships with selfish nodes under the condition that no central entity is employed. Finally, the presented results prove that the proposed bargaining technique guarantees about 50% of energy efficiency when compared to a centralised random scheme without selfish nodes.

In [101], a cooperative beamforming scheme is described. The authors analyse the energy efficiency of direct and cooperative schemes in the function of distance between the communicating entities. It is shown that the adaptive direct scheme, in which the transmission power is neatly adjusted, outperforms the cooperative schemes for transmissions on short distances (up to ca. 150 m to 200 m). For larger distances, cooperative relays are more energy efficient, however, the larger the distance, the higher the optimum number of the relaying nodes.

In [12], a scenario without any relays is analysed. The authors take two known algorithms into account: the *gossiping* and the *random walk*, and proposed improvements in order to decrease the information overhead in the network (resulting in an energy-efficiency increase). In the gossiping scheme, every node transmits information to a randomly selected node. In its enhanced version, it is done only if the usage pattern of a given band changes. In the random walk algorithm, only some nodes communicate to randomly selected neighbours while in the incremental version of it, the procedure is started if an information update occurs. The authors present the results which prove that the proposed enhancements decrease the number of overhead information up to 2.5 times. However, the definition of update is dubious, so is the number of collisions which may occur in the presented schemes, e.g., when a node cannot transmit in the same time as it receives the information signal.

In [75], the trade-off between sensing performance and its energy efficiency has been discussed. The authors present a scheme in which a larger number of samples increases the detection probability. However, if the minimum detection probability is satisfied, the energy consumption increases linearly with the number of samples. The authors analyse the scheme with a simple amplify-and-forward scheme. The presented analysis shows that it is possible to find the optimum pair of the amplifying gain and the number of samples in order to get the best trade-off between sensing performance and energy efficiency.

Another solution which is not based on the idea of relays is presented in [121]. There, two heuristic models are presented in order to optimise network utility and energy efficiency. In the network model, the authors assume several licensed signal spectra present in several fragmented frequency bands. They adopt the economic concepts of social welfare and net revenue to the communication network scenario. It is proved that the optimum trade-off between energy consumption and social welfare may be found by allowing for the interference-dependent competition for links and source nodes.

The next solution proposed for a network with multiple-license signals is described in [141]. Here, the proposed solutions aim at maximising the energy efficiency and transmission rates. It is achieved by allowing the node to use vacant channels with the upper-bounded transmit power, and to transmit multiple packets in one transmission.

In [167], the *cluster-and-forward* scheme is presented, where the nodes are dynamically put into cluster groups. In each group, a node with the best channel gain is selected as the Cluster Head. Then, it collects local decisions from cluster members, forwards them to the Fusion Centre and, in order to improve the energy efficiency, also serves as the fusion centre for cluster members. In the paper, it is shown that for a given number of nodes, there exist an optimum number of clusters for which the amount of saved energy is the most significant.

A similar clustering scheme is described in the aforementioned article [95]. There, the total transmit energy in clustering and broadcasting is compared, proving that the clustering may provide significant energy savings due to shorter transmission links. Moreover, there exist an optimum number of clusters for a given number of nodes which guarantee most of the energy savings. A similar conclusion has been drawn in [168]. The transmit energy may be reduced compared to the traditional scheme, especially when the transmission takes place over large distances (1000 m and more).

A cluster-based efficient protocol has been described in [171]. First, a MAC mechanism is proposed in order to reduce the number of collisions. Then, a channel sensing scheme is designed to reduce the total consumed energy. It is proved that there is a relationship between the energy efficiency and the number of sensed channels, and the best overall performance is guaranteed by cluster-based sensing for three channels.

Walid Saad et al. propose in [146] an interesting attitude to cluster formation. Although usually clusters are formed during a centralised procedure where the key role is performed by the central entity, in the cited work, node collaboration is provided in a distributed way. Two coalition-formation approaches have been proposed. In the first one, under the false alarm requirement, the nodes may form clusters (coalitions) by pairwise negotiations between them, followed by the sequential *merge-and-split* procedure in order to maximise detection probability and keep the false alarm rate sufficiently low. The second one aims at forming coalitions under the minimum-detection constraint, while keeping the false alarm rate at a given level, thus guaranteeing the achievement of detection probability with a minimum overhead. This is provided by forming *minimal winning coalitions*. One may find promising results where the miss-detection rate has been significantly reduced and the detection rate relevantly increased for the first and second algorithms, respectively.

## 4.7 Final Classification of Energy-Efficiency Options for Cooperative Spectrum Sensing

In the previous sections, the ways to increase the energy efficiency in CSS have been analysed. Here, the discussed methods are summarised in the form of a table, which should guide the reader through the papers for further reading. The analysis of Table 4.1 allows us to identify the best ways for global energy consumption minimisation in CSS depending on various optimisation constraints. Following the overall chapter structure, the table is split into four separate (yet mutually related) parts which reflect the four branches defined in Section 4.2. Within each part, the key CSS aspects have been identified which can be subject to optimisation. However, the key challenges in accurate energy consumption modelling and optimisation for CSS networks arise from the fact that there exist a great variety of elements that have to be considered in the

Table 4.1: Classification of energy saving approaches

		Feature	Pros	Cons	Ref.
<b>Branch A</b>	Energy reduction in the (local) spectrum sensing phase	A1. Reduction of the number of collected samples	<ul style="list-style-type: none"> <li>• Less data to send and process</li> <li>• Shorter sensing time</li> </ul>	<ul style="list-style-type: none"> <li>• Potentially less reliable decision</li> <li>• Good candidate only for strong PU signals or lack of transmission</li> </ul>	[89, 97, 131, 151, 154]
		A2. Application of an advanced, energy efficient front-end	<ul style="list-style-type: none"> <li>• Better energy utilisation</li> <li>• Front-end adapted to current requirements</li> </ul>	<ul style="list-style-type: none"> <li>• Mass-production of electronic chips limits the degree of freedom in energy-efficient front-end design for spectrum sensing purposes</li> <li>• More advanced chips typically lead to higher prices</li> </ul>	[25, 64, 65, 103, 175]
		A3. Message quantisation	<ul style="list-style-type: none"> <li>• Reduction of the data volume to send (reduced traffic in the CSS network)</li> <li>• Optimised number of quantisation levels can guarantee the agreed level of QoS in CSS</li> </ul>	<ul style="list-style-type: none"> <li>• Insufficient number of quantisation levels reduces the reliability of global decisions made in CSS</li> </ul>	[21, 22, 28, 134, 156, 164]
		A4. Optimisation of the decision threshold	<ul style="list-style-type: none"> <li>• Reduction of the processing load</li> <li>• Optimisation of sensing time</li> </ul>	<ul style="list-style-type: none"> <li>• Wrong threshold selection influences CSS reliability</li> </ul>	[58, 82]
		A5. Selection of a simpler sensing algorithm	<ul style="list-style-type: none"> <li>• Reduction of processing load in each sensing node</li> <li>• Reduction of energy consumption in each node</li> </ul>	<ul style="list-style-type: none"> <li>• Poorer (e.g., less reliable) spectrum sensing algorithm can breach the assumed QoS</li> </ul>	[92, 172]
<b>Branch B</b>	Optimisation of cooperating nodes number	B1. Node selection	<ul style="list-style-type: none"> <li>• Reduction of the sensing node number</li> <li>• Sleeping nodes do not consume energy</li> <li>• Proper selection of the reporting node can improve the quality of the reported message</li> </ul>	<ul style="list-style-type: none"> <li>• Possible detection probability degradation</li> <li>• Proper selection of reporting nodes possible when additional data is acquired (e.g., nodes' SNRs)</li> </ul>	[16, 20, 33, 106, 129, 150, 157, 166]
		B2. Node censoring	<ul style="list-style-type: none"> <li>• Reduction of the reporting node number</li> <li>• Censored nodes do not consume energy for reporting</li> <li>• Faulty or even malicious nodes can be censored</li> </ul>	<ul style="list-style-type: none"> <li>• The censoring process may be faulty leading to wrong decisions</li> <li>• The need for duly node selection for censoring or turning off</li> </ul>	[108, 109, 110, 150]

Continued on next page

Table 4.1 – continued from previous page

		Feature	Pros	Cons	Ref.
		B3. Voting schemes	<ul style="list-style-type: none"> <li>• Easy usage of the procedure</li> <li>• Limited number of steering messages</li> <li>• Does not demand much additional data (nodes' SNRs, locations etc.)</li> </ul>	<ul style="list-style-type: none"> <li>• Faulty or even malicious nodes may affect performance</li> </ul>	[10, 59, 87, 95, 120]
Branch C	Proper application of fusion and decision rules	C1. Selection of the key fusion rule	<ul style="list-style-type: none"> <li>• The number of reports delivered to the fusion centre depends on the selected fusion rule</li> <li>• Fusion rule can be selected depending on the required quality</li> </ul>	<ul style="list-style-type: none"> <li>• Every change of the fusion rule has to be reported to the cooperative nodes</li> <li>• The efficiency of the fusion rule has to be monitored</li> </ul>	[69, 130, 132, 136, 142, 179]
		C2. Soft or hard reporting	<ul style="list-style-type: none"> <li>• Depending on the situation, soft or hard reporting can be selected</li> <li>• Adaptation of the traffic related to data reporting</li> </ul>	<ul style="list-style-type: none"> <li>• Trade-off between the accuracy of each report and amount of data volume needed to deliver</li> </ul>	[21, 105, 156]
		C3. Decision reporting	<ul style="list-style-type: none"> <li>• Reduction of the traffic</li> </ul>	<ul style="list-style-type: none"> <li>• Reduced accuracy of information delivered to the fusion centre (compared to soft/hard reporting)</li> </ul>	[15, 74, 107, 162, 176]
Branch D	Selection of EE network organisation solutions	D1. Energy-effective routing	<ul style="list-style-type: none"> <li>• Selection of the routing scheme that minimises the consumption of energy</li> </ul>	<ul style="list-style-type: none"> <li>• Application of energy effective routing requires access to detailed information about the environment</li> </ul>	[56, 68, 78, 121, 146, 141, 171]
		D2. Cross-layer solutions	<ul style="list-style-type: none"> <li>• Possible cooperation between solutions applied in separate OSI layers, e.g., routing algorithms can consider physical-layer constraints</li> <li>• Increased degree of freedom in system design</li> </ul>	<ul style="list-style-type: none"> <li>• Increased adaptation and flexibility in system design typically results in the application of advanced (thus complicated and more energy-consuming) algorithms</li> </ul>	[94, 121]
		D3. Application of relaying nodes	<ul style="list-style-type: none"> <li>• Reduction of the transmit power (thus overall interference level observed in the system) of the reporting node due to shorter distances</li> </ul>	<ul style="list-style-type: none"> <li>• Increased energy consumption in relaying node due to processing of messages from other reporting nodes</li> <li>• Increased delay in data delivery to the fusion centre</li> </ul>	[24, 68, 101, 169, 180]

optimisation process. Optimisation of one parameter (e.g., selection of cyclostationarity-based spectrum sensing instead of energy detection in each node) increases the reliability of the decision made in one sensor at the expense of computational complexity. From the perspective of the whole network such a modification can result in relatively significant changes in energy consumption. Moreover, various factors that influence the energy consumption are mutually dependent, which makes the analysis even harder.

## 4.8 Fuzzy Logic in the Optimisation Process of the Energy-Efficient Cooperative Spectrum Sensing

### 4.8.1 Dependency Matrix

In order to identify the most promising optimisation areas, a matrix has been created that shows the key relations and dependencies between the particular CSS solutions (see Tab. 4.2). Based on the classification in Fig. 4.1 and its detailed description in Tab. 4.1, fourteen CSS features are compared which are denoted according to the branch each feature belongs to [37, 46]. Each cell in the dependency matrix defines the mutual influence of two selected features, for example, the cell in column A3 and row B2 represents the relation between message quantisation and node censoring. It has been assumed that each two features can be highly correlated (dependent) when the change of one of them significantly influences the other one. Thus, this *dependency parameter* can vary in the range from 0 to 1, where 0 means no correlation. Each cell uses colour coding, meaning that the darker the colour, the higher the correlation between the parameters of a row and a column.

Before the analysis of dependency matrix, some additional comments have to be made. First, fourteen specific CSS features have been identified, however, that selection is a matter of classification. One can easily define other sets of features allowing for drawing conclusions. Second, in the discussed example, the dependencies between the features have been assigned somehow arbitrarily, based on our observations and overall assumptions. One can identify more entries to the matrix records once the assumptions are modified. However, in order to achieve precise results, one needs to define at least a generic metric or—at best—a mathematical relation between each pair of features. This is the key challenge of the proposed approach, as such a metric could be hard or even impossible to define.

Having in mind all of these limitations (i.e., the matrix is case-dependent, it relies on user experience and knowledge, etc.), one can state that a coarse analysis of such a matrix can shed new light on the overall understanding of the CSS process and the existing relations between its particular phases. First, let us notice that by finding similarities between the rows (or columns), the most dependent features can be identified, meaning that in consequence, a dedicated optimisation function can be defined that considers these particular features. Second, as the darker entries in the matrix represent high dependency between the features, the brighter ones allow for the identification of such agents of CSS which could be optimised independently. In general, such an analysis can lead to the definition of sets of highly mutually-related features (note that these sets can overlap).

**Table 4.2:** Dependencies between the key CSS parameters

Par.	A1	A2	A3	A4	A5	B1	B2	B3	C1	C2	C3	D1	D2	D3	
A1	■	■	■	■	■	■	■	■	■	■	■	■	■	■	
A2	■	■	■	■	■	■	■	■	■	■	■	■	■	■	
A3	■	■	■	■	■	■	■	■	■	■	■	■	■	■	
A4	■	■	■	■	■	■	■	■	■	■	■	■	■	■	
A5	■	■	■	■	■	■	■	■	■	■	■	■	■	■	
B1	■	■	■	■	■	■	■	■	■	■	■	■	■	■	
B2	■	■	■	■	■	■	■	■	■	■	■	■	■	■	
B3	■	■	■	■	■	■	■	■	■	■	■	■	■	■	
C1	■	■	■	■	■	■	■	■	■	■	■	■	■	■	
C2	■	■	■	■	■	■	■	■	■	■	■	■	■	■	
C3	■	■	■	■	■	■	■	■	■	■	■	■	■	■	
D1	■	■	■	■	■	■	■	■	■	■	■	■	■	■	
D2	■	■	■	■	■	■	■	■	■	■	■	■	■	■	
D3	■	■	■	■	■	■	■	■	■	■	■	■	■	■	
A1	Reduction of the no. collected samples							B3	Voting schemes						
A2	Application of an advanced, EE front-end							C1	Selection of the key fusion rule						
A3	Message quantisation							C2	Soft or hard reporting						
A4	Optimisation of the decision threshold							C3	Decision reporting						
A5	Selection of a simpler sensing algorithm							D1	Energy-effective routing						
B1	Node selection							D2	Cross-layer solutions						
B2	Node censoring							D3	Application of relaying nodes						

In order to deal with the problem of precise definition of dependencies between any pair of features, the approach known from fuzzy logic is applied, where the exact values can be intentionally replaced with some generic, descriptive definitions. In this approach, five levels defining the degree of mutual dependency have been stated:

- Level 0 – no or very low dependency;
- Level 1 – low dependency;
- Level 2 – moderate dependency;
- Level 4 – high dependency, and
- Level 5 – very high or full dependency.

The number of levels, as well as their (fuzzy) meanings define the accuracy of the conclusions that will be drawn from it. Tab. 4.2 has been created using the five levels mentioned above.

In Tab. 4.2, one can notice that the highest correlation exists between solutions within branches B and C, it is substantial in branch D and moderate in branch A. Moreover, the solutions in the dependency matrix may generally be split into two groups: in the first group, consisting of solutions from branches B, C and D, one may observe a rather high dependency between them (these are essentially cooperation-based solutions), while in the second group, consisting of solutions from branch A (these are single-node solutions), there is a much lower dependency with the exception of A3 highly correlated with branch C ideas. Therefore, the general observation is that the introduction of one energy-efficient cooperation-based solution (e.g., the number of nodes or acceleration of the fusion rule) highly affects the others. However, the optimisation of a single node's operations does not impact significantly the energy-efficiency solutions of the other branches.

One can also notice that in the presented example, the absolute values of dependencies have been assumed. However, much effort should be put into the precise definition of mutual relation between features, i.e., the modification of a certain feature can either improve or degrade the energy efficiency of an other feature. These aspects (i.e., positive or negative influence) could also be taken into account, providing new insights into the problem.

### 4.8.2 Rose Chart

As the dependency matrix (or, in some sense, correlation matrix) provides us with some statistical insight into the energy efficiency of CSS, the key challenge would be to define a detailed energy consumption model. However, as the full model of energy consumption in a whole CSS network would be highly complicated, it is important to identify the key relations between the factors that influence the total energy consumption. It can be achieved, to some degree, by the analysis of a rose chart with key factors assigned to separate axes, where each axis of this chart represents a different feature (criterion) considered in the analysis. All of the axes start at the same zero point, and it is important to precisely define the terms and units in which the selected feature (criterion) can be defined numerically. Once the numerical values are marked on the axes, a polygon can be created through the connection of all points, and the area of this polygon to some respect reflects the overall energy consumption of the considered system. An illustrative example showing the concept has been presented in Fig. 4.4.

Here, six criteria for evaluating CSS schemes have been identified:

- Accuracy of reports delivered to fusion centre;

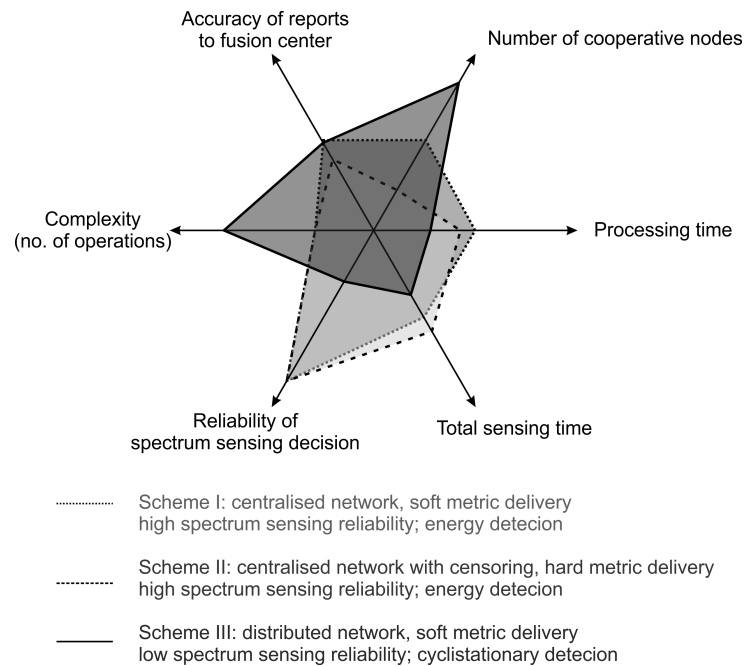


**Figure 4.4:** Rose-chart for energy consumption comparison

- Number of cooperative nodes;
- Processing time;
- Total sensing time;
- Number of operations executed in each node;
- Reliability of spectrum sensing decisions.

Similarly to the approach applied in the creation of filling in the dependency matrix, also in this case (the rose chart), particular attention has to be given to the accurate definition of the considered criteria (the rose chart axes). As it has been already stated, there always exists some mutual dependency between any pair of the proposed criteria. Having this in mind, it is proposed to select them in such a way that the mutual dependency is minimised. In order to achieve this, one can utilise the dependency matrix presented at the beginning of this section.

Once the criteria (including their number) have been defined, the most important thing would be to precisely define the quantitative metric used for the numerical assessment of a criterion. For example, the number of cooperative nodes can be straightforwardly measured in terms of integer numbers, and complexity – understood as the number of operations executed in one node, can be measured in operations per second or Floating Point Operations Per Second (FLOPS). Similarly, the processing time can be easily represented in the form of seconds. On the other hand, the numerical assessment of reliability of sensing decisions or accuracy of reports are not as straightforward. As one can consider various types of probabilities (e.g., probability of a false alarm, error probability, etc.), also other metrics could be proposed. Finally, it would be wise to translate such generic measures into concrete values of consumed energy. In other words, taking

the total sensing time as an example, although it is measured in seconds, it should rather be analysed as a function of time that gives us even a rough approximation of the energy consumed.

As the definition of accurate functions describing the energy consumption in each criterion can be complicated, it is proposed to apply the methodology known from fuzzy logic, as it has been done previously. Thus, depending on the criterion, particular levels can be defined giving coarse estimations of their impact on the energy consumption. For example, complexity or accuracy of reports can be classified as very low, low, medium, high, and very high; analogously, the number of cooperative nodes can be low, medium and high. One needs to propose the mapping function that connects pure numerical values with their descriptive counterparts.

In Fig. 4.4, a comparison of three arbitrarily selected schemes is presented, allowing to identify the key differences between them and to assess the key contributions to the total energy consumption in a CSS network in each case.

In schemes I and II, centralised networks of energy detection-based nodes are assumed. Thus, both schemes have low complexity and high reliability. However, in the second one, the nodes are censored and use hard-metric delivery, while in the first, soft metrics are used. Therefore, they have different accuracies of reports, as well as sensing and processing times. In scheme III, a distributed network is proposed (with a high number of nodes) with cyclostationary detection. Thus, it has a short sensing time at the cost of high complexity and low reliability. The three presented schemes are simple proposals, however, one may observe the great variety of parameters that influence the total energy efficiency.

### 4.8.3 Exemplary Use Cases

In this section, the proposed evaluation tools (i.e., dependency matrix and rose chart) are applied to a very specific example. Two different test scenarios (use cases) have been arbitrarily selected, deriving from them the illustrative values of the parameters and choosing appropriate methods.

The first considered use case is a mobile dense network which is monitored by densely-deployed static sensors and, additionally, by mobile users who deliver the sensing results to a centralised fusion centre. The obtained spectrum occupancy information is used for updating global databases (REMs). Each static node periodically senses the spectrum based on a cyclostationary-features algorithm while mobile users perform sequential energy detection. As the static nodes report the measured values to the fusion centre, the mobile users report their hard decisions, as well as their location. FC applies the majority rule to these reports, and: *i*) circulates the decisions to the affected users (e.g., a certain user may need to modify its transmission parameters), *ii*) updates the REM, *iii*) optimises the majority rule in order to guarantee a high detection rate and a low false alarm rate, *iv*) switches certain sensing nodes on or off in order to minimise the utilised energy, while keeping the sensing performance unchanged.

In the second scenario, machine-to-machine communication is considered, where a set of dedicated sensors is deployed over a large area and used for monitoring the occupancy of data transmission in unlicensed bands (e.g., 5 GHz). The role of the CSS system is to detect the presence of any WiFi users, particularly considering the problem of a hidden node, and to provide some valuable updates to the operator who applied the Licensed Assisted Access (LAA) spectrum sharing scheme [100, 139]. The nodes create a mesh network with the ability to define clusters, cluster heads and routing rules. However, most decisions are made by the centralised

fusion centre which receives information from the cluster heads only. FC can take the following actions: *i*) instruct the cluster heads to activate/deactivate sensing nodes, and to reconstruct the network, *ii*) deliver information about presence to databases (or other entities from the 5G network architecture), *iii*) instruct affected users (via cluster heads) about the measured activity of WiFi users. For example, when the total measured power in the observed unlicensed band is high, the 5G operator decides to switch off the LAA strategy and rely on the licensed band only. In such an approach, the decision about the measured interference should be reliable, but there are no strict requirements on the reporting time and periods.

**Table 4.3:** Dependencies between the key CSS parameters in mobile dense network use case

Par.	A1	A3	A4	B1	B2	B3	C1	C2	C3
A1	■	■	■	■	■	■	■	□	■
A3	■	■	□	□	□	■	■	■	■
A4	■	□	■	■	■	■	■	□	□
B1	■	□	■	■	■	■	■	■	■
B2	■	□	■	■	■	■	■	■	■
B3	■	■	■	■	■	■	■	■	■
C1	■	■	■	■	■	■	■	■	■
C2	□	■	□	■	■	■	■	■	■
C3	■	■	□	■	■	■	■	■	■

**Table 4.4:** Dependencies between the key CSS parameters in machine-to-machine use case

Par.	B1	B2	B3	C1	D1	D2	D3
B1	■	■	■	■	■	■	■
B2	■	■	■	■	■	■	■
B3	■	■	■	■	■	■	■
C1	■	■	■	■	■	■	■
D1	■	■	■	■	■	■	■
D2	■	■	■	■	■	■	■
D3	■	■	■	■	■	■	■

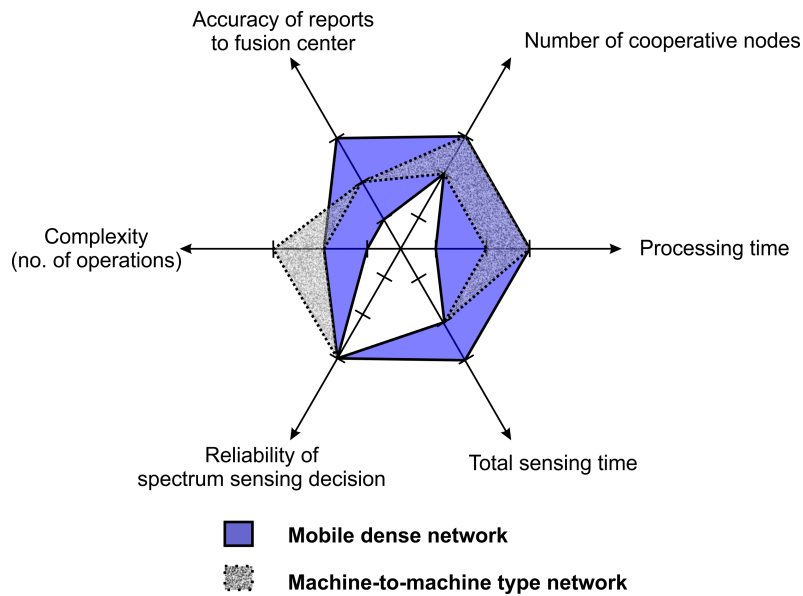


**Figure 4.5:** Rose-chart for presented use cases

In Tables 4.3 and 4.4, dependency matrices for the analysed use cases are presented. One may observe that these dependency matrices are created on the basis of Table 4.2. Each specific use case has given constraints, thus, a subset of EE methods cannot be used. Consequently, dependency matrices presented for use cases are created for a given subset of EE solutions. Now, one may define the possible directions of EE optimisation and observe the possible dependencies between features.

The picture of EE optimisation may be amended by the observation of rose charts for the two considered use cases. In Fig. 4.5, one may note that the values on the axes may be strict (e.g., for reliability) or may be determined by the range. For instance, in a machine-to-machine communication use case where the local sensing phase could not be rearranged, the value for sensing time is strict (similarly for the FC reports on accuracy and reliability). However, the three remaining axes present features that may be optimised, thus, there exist ranges of values. The application of a specific routing scheme, which is a possible direction of optimisation, may affect the complexity and processing axes in the rose chart, and is correlated with the number of cooperative nodes. The selection of a given EE solution influences other solutions (the dependency matrix highlights this) and further affects other axes of energy efficiency (observed in the rose chart).

Another considered use case of a mobile dense-network presents a higher flexibility in EE optimisation than the machine-to-machine communication use case. Just one parameter is strict (reliability), while the five remaining ones may be subject to optimisation. This goes in line with Tab. 4.3, where nine various EE methods may be adopted and may affect the values on the axes of the rose chart.

## Conclusion

- The area enclosed by the solutions on the rose chart generally *relates* to the energy consumption of the considered use case. The higher the value on the rose chart axes, the higher the energy usage.
- However, this *relation* is not linearly proportional. The exact energy usage depends on specific parameters, e.g., distances between nodes, which are not covered by the axes.
- Although energy consumption can be extrapolated from the rose chart, the energy efficiency cannot. The use case with a very limited energy consumption may *not* be energy efficient due to its low reliability or low throughput.
- There exist a high number of degrees of freedom in the CSS optimisation process. However, under specific use case constraints, the number of degrees of freedom may be significantly reduced. This may be observed in Fig. 4.5 where some values on the axes are strict and some are in a range. Therefore, instead of a polygon, one may observe a circled area which is explicitly the possible area of optimisation.

## 4.9 Energy-Efficient Cooperative Spectrum Sensing with Node Sleeping and Relaying

The aforementioned energy-efficiency-related analysis unveiled the possible directions of the optimisation in cooperative energy-efficient spectrum sensing. Following the classification presented in Section 4.2, this section presents a solution which merges in essentials the two following branches specified in the aforementioned classification: Branch B, where the number of cooperating nodes is optimised, and Branch D, highlighting the efficient network organisation [41, 42]. However, the presented dependencies analysis has shown that these parameters have high dependency. Therefore, as it is recommended, the whole system is analysed from the energy consumption and quality of detection point of view, in concert with the presented analysis.

### 4.9.1 System Model and Problem Formulation

The motivation is to maximise the energy-efficiency understood as quality of detection to total network power consumption ratio. The EE-metric employed in this section is similar to the one introduced in eq. (4.1).  $\zeta$  is the added weighing coefficient increasing the significance of the numerator of  $EE$ :

$$EE = \zeta \frac{Q_d}{P_{TOT}} \left[ \frac{1}{W} \right], \quad (4.7)$$

while  $Q_d$  and  $P_{TOT}$  correspond to the global probability of detection and the total power consumed by the network in the sensing procedure, respectively.

### Global probability of detection

The increase of energy efficiency is worthwhile if the quality of detection is not damaged. The probability of detection for sensing node  $i$  using energy detector is given as:

$$P_d^{(i)} = Q \left( \frac{\epsilon - (M + \eta^{(i)})\hat{\sigma}_n^2}{\sqrt{2(M + 2\eta^{(i)})\hat{\sigma}_n^4}} \right), \quad (4.8)$$

where  $Q(\cdot)$  is a Q function,  $\epsilon$  is the detection threshold from eq. (1.2), and  $\eta^{(i)}$  is the signal-to-noise ratio at the primary to secondary link acquired by the  $i$ -th node. In the adopted model, the CFAR requirement has been applied so every node in the network experiences the same boundary false alarm value. Thus, the detection threshold is set as constant in every node, and therefore the key parameter affecting the detection probability highlighted in eq. (4.8) is the experienced signal-to-noise ratio. In the assumed centralised-cooperation case, the FC processes local decisions and takes the global decision according to a selected fusion rule. Three major rules are considered in the fusion process: OR (1-out-of- $N$ ), AND ( $N$ -out-of- $N$ ) and majority rule ( $\lfloor N/2 \rfloor + 1$ )-out-of- $N$ .

### Power consumption

The most straightforward attitude for increasing the energy efficiency defined above is to reduce the power consumption. The total power consumption  $P_{\text{TOT}}$  in the network of  $N$  collaborating nodes, where each node reports its sensing observations directly to FC, is given as:

$$P_{\text{TOT}} = \sum_{i=1}^N \left( P_{\text{sensing}}^{(i)} + P_{\text{reporting}}^{(i)} \right), \quad (4.9)$$

where  $P_{\text{sensing}}^{(i)}$  is the power related to spectrum sensing in node  $i$ , and  $P_{\text{reporting}}^{(i)}$  is the power related to reporting of the sensing observation by node  $i$  to the FC. Note that  $P_{\text{reporting}}^{(i)}$  depends on the multipath loss  $\chi_{\text{FC}}^{(i)}$  in the link between the  $i$ -th sensing node and the FC, as well as on the distance between them  $d_{\text{FC}}^{(i)}$ :

$$P_{\text{reporting}}^{(i)} = \frac{\hat{\sigma}_n^2}{\delta} \sum_{i=1}^N \frac{(\text{erfc}^{-1}(2P_b))^2 \left( d_{\text{FC}}^{(i)} \right)^n}{\chi_{\text{FC}}^{(i)}}, \quad (4.10)$$

where  $\text{erfc}^{-1}(\cdot)$  is an inverse complementary error function,  $P_b$  is an assumed probability of binary error required for transmission with BPSK modulation,  $n$  is an exponent of the received power decrease, and  $\delta$  is the coefficient reflecting the antennas gains, used frequency and the path loss at the reference distance (measured in  $[\text{m}^{-n}]$ ). The effective SNR  $\Lambda_{\text{FC}}^{(i)}$  modelling the multipath effects is the Exponential Effective SINR Mapping (EESM) [83]:

$$\Lambda_{\text{FC}}^{(i)} = \ln \left( \frac{1}{J} \sum_{j=1}^J \exp(-\eta_j^{(i)}) \right), \quad (4.11)$$

where  $J$  is the number of the signal paths components in the link between the  $i$ -th node and the FC,  $\eta_j^{(i)}$  is a linear value of an SNR for component  $j$  and node  $i$ . The values of EESM between

different links are mutually independent as there are channels between the nodes and the FC. If  $P_{\text{sensing}}^{(i)}$  is the same for each node, formula 4.9 changes to:

$$P_{\text{TOT}} = NP_{\text{sensing}}^{(i)} + \frac{\hat{\sigma}_n^2}{\delta} (\text{erfc}^{-1}(2P_b))^2 \sum_{i=1}^N \frac{(d_{\text{FC}}^{(i)})^n}{\lambda_{\text{FC}}^{(i)}}. \quad (4.12)$$

**Power consumption for node selection.** Node selection technique has been described in Section 4.4. The energy savings are based on the idea that in case of unreliable or highly correlated sensing observations, it is more efficient to select a subset of nodes to perform the sensing. The unselected nodes turn then to the *sleeping mode* in which they are allowed neither to sense, nor to report the sensing outcomes. Thus, the total sensing-related energy consumption in the network, where  $W$  nodes is selected ( $W \in [1, N]$ ), is as follows:

$$P_{\text{TOT}}^{\text{selection}} = \sum_{i=1}^W (P_{\text{sensing}}^{(i)} + P_{\text{reporting}}^{(i)}) + P_{\text{sharing}}, \quad (4.13)$$

where  $P_{\text{sharing}}$  is the energy related to the information sharing, i.e., to the additional information exchange needed before nodes selection or relaying procedures. In the information sharing procedure, each node is first obliged to send its information to the FC, and then, the FC—on the basis of these messages—prepares node selection or/and relaying scheme and sends the broadcast message to the entire network. The power needed for message broadcasting is sufficiently low when compared with the sum of energy costs related to the transmission of separate messages by nodes, and may be neglected. Thus, the power of information sharing is defined as follows:

$$P_{\text{sharing}} = \sum_{i=1}^N P_{\text{reporting}}^{(i)}. \quad (4.14)$$

**Power consumption in relaying scenario.** In the case of relaying scenario, one or a few nodes serve as relay to forward local sensing observation to the FC. This is particularly beneficial when the relay node has a high quality channel to the FC, and could apply low transmit power, while other nodes experience bad channel qualities to the FC due to, e.g., shadowed signal, and their transmission-power cost could be high. In the relaying scenario, the total power consumed is given as:

$$P_{\text{TOT}}^{\text{relaying}} = NP_{\text{sensing}}^{(i)} + P_{\text{reporting}}^{\text{relaying}} + P_{\text{sharing}}, \quad (4.15)$$

where  $P_{\text{reporting}}^{\text{relaying}}$  is the reporting power for all nodes in the network for the relaying scenario. The assumed relaying strategy is the so-called Decode and Forward (DAF). The reporting power for node  $i$  and relaying node  $r$  is equal to:

$$P_{\text{reporting}}^{(i,r)} = (\text{erfc}^{-1}(2P_b))^2 \left( \frac{(d_r^{(i)})^n}{\Lambda_r^{(i)}} + \frac{(d_{\text{FC}}^{(i)})^n}{\Lambda_{\text{FC}}^{(i)}} \right), \quad (4.16)$$

where  $d_r^{(i)}$  and  $\Lambda_r^{(i)}$  is the distance and the effective SNR of the link between nodes  $i$  and  $r$ , respectively.

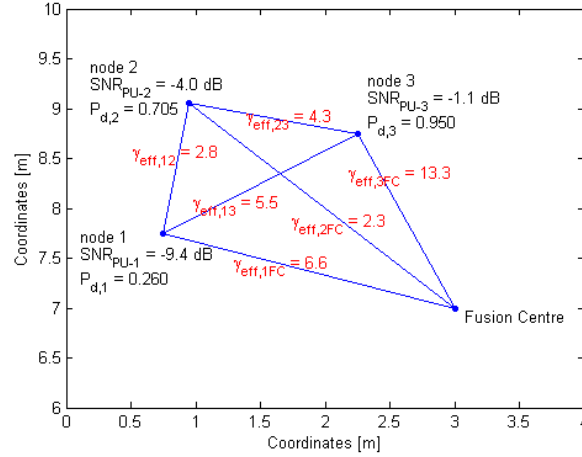


**Figure 4.6:** Exemplary topology of the network of three sensing nodes and one Fusion Centre. Note the exemplary values of the SNR between the PU and the sensing nodes, the calculated  $P_d^{(i)}$  values and effective SNRs between the nodes

#### 4.9.2 Simulation Scenario

In order to verify the impact of various parameters of the CSS network on the CSS performance, computer simulations have been conducted. The considered network area is a  $100 \times 100$  m square. The position of each sensing node is randomised by employing the two following factors: *i*) the distance to the area central point modelled with the Gaussian distribution  $N \sim (0, \sigma_c)$  and *ii*) the angle between a node-to-central-point line and the horizontal axis modelled with the uniform distribution  $(0, 2\pi)$ . The FC is located inside the network area while the PU is outside it with the distance to the central area point equal to  $d_{PU}$ . In Fig. 4.6, the considered topology is shown with three sensing nodes and one FC. The applied channel model is the six-paths ETSI GSM 05.05 with the line-of-sight path.

The attenuation of the channel between the PU and the SU is modelled by including path-loss, shadowing and fast fading components. The path-loss attenuation component is therefore calculated using the known Friis formula where the received-to-transmitted signal ratio decreases with second power of the distance. Its value is constant unless the location of the sensing node is not changing and the PU is also stationary. The coefficients of the shadowing component are time- and location-dependent. Thus, as in real radio-environment, there exists a space correlation between close SUs on the primary-to-secondary link due to similar radio environment where SUs are located and thus similar signal reflections from, e.g., obstacles. Moreover, the obstacles may be time-dependent, therefore, the shadowing coefficients, though correlated in space, may change in time. Unlike the small-scale fading whose parameters are random in the space and time domains.

In the shadowing model, the exponential correlation proposed in [67] is employed:

$$R(d) = \exp(-\omega d), \quad (4.17)$$

where  $\exp(-\omega)$  is the correlation coefficient for points separated by  $d = 1$  m, and  $\omega$  is the correlation coefficient specific for the transmission environment. However, the calculation of exponential coefficients is computationally complex, thus, in [48] one may find the low-complex creation of

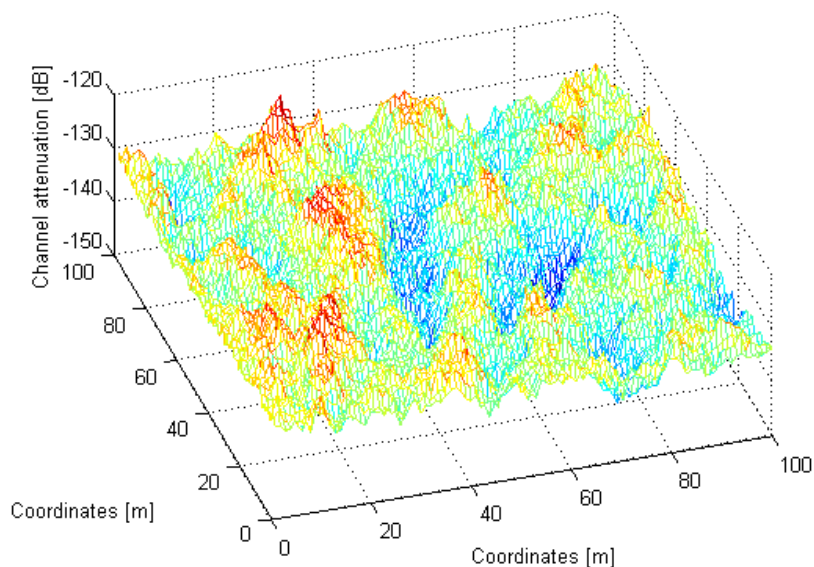


**Figure 4.7:** Exemplary channel attenuation map for the simulated area  $100 \times 100$  m. Path loss and shadowing effects are included, while fast fading is omitted as the unavailable statistics; distance to PU:  $d_{PU} = 500$  m

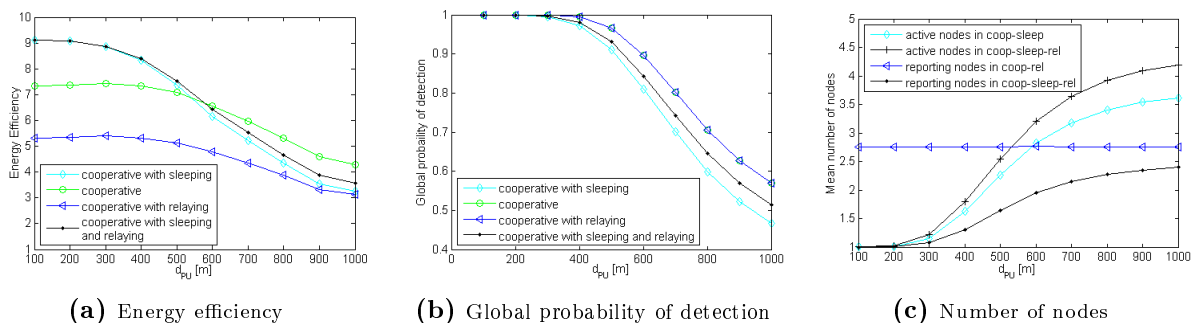


**Figure 4.8:** Simulation results vs distance to Primary User ( $d_{PU}$ ),  $N = 5$ ,  $\sigma_c = 5$  m, FC in the central area point

the shadowing map with correlated coefficients. Its low complexity is based on the observation that calculation of correlation coefficients just on the basis of a couple of neighbour values is sufficient enough and is vulnerable with low error. In Figure 4.7, one may find a map of correlated coefficients for the considered network area with the resolution of 1 m and  $\omega$  equal to  $1/20$ .

Finally, the fast (small-scale) fading coefficients in the channels between the PU and the sensing nodes are independent for every node and are modelled with Rayleigh distribution with parameter  $\sigma_{FAD}$ .

### 4.9.3 Simulation Results

The set of selected simulation parameters is as follows:  $\zeta = 10^4$ ,  $M = 50$ ,  $P_{f_{target}}^{(i)} = 0.1$ ,  $P_{sensing}^{(i)} = 10 \mu W$ ,  $J = 200$ ,  $P_b = 10^{-6}$ ,  $\sigma_c = 5$  m and  $\sigma_{FAD} = 0.5$ .

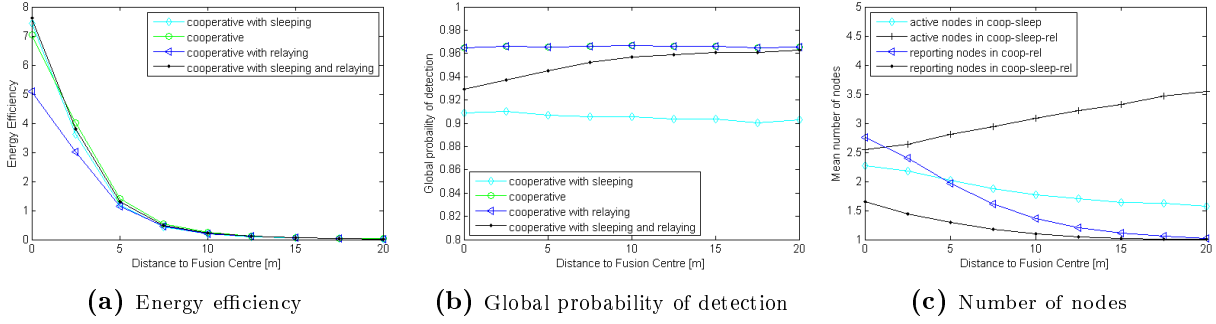


**Figure 4.9:** Simulation results vs various distance of Fusion Centre from central area point,  $N = 5$ ,  $d_{PU} = 500$  m,  $\sigma_c = 5$  m

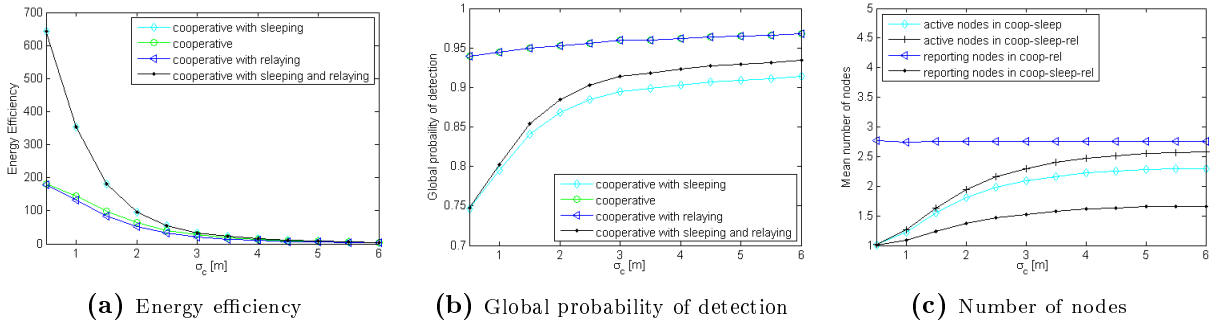


**Figure 4.10:** Simulation results vs various spread of nodes  $\sigma_c$ ,  $N = 5$ ,  $d_{PU} = 500$  m

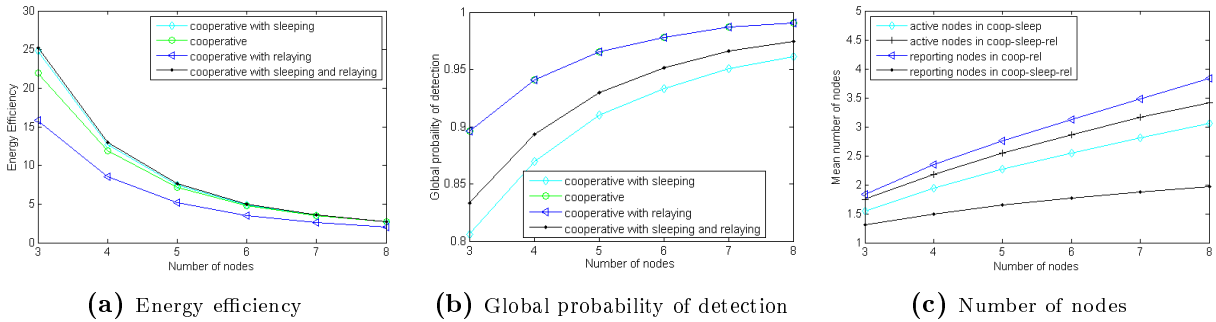


**Figure 4.11:** Simulation results vs various number of nodes  $N$ ,  $d_{PU} = 500$  m,  $\sigma_c = 5$  m

The energy efficiency has been analysed in four possible scenarios. In the first one, referred in the remainder of the section as *cooperative*, all sensing nodes transmit observations directly to the FC regardless of the experienced SNR and locations. Thus, in such a basic scenario, no information-sharing phase is needed. The second scenario is the one which employs node selection, referred as *cooperative with sleeping*. In that scenario, the number of selected nodes may vary from 1 to  $N - 1$ . Moreover, all possible network topologies have been considered. Therefore,  $2^N - 2$  possibilities have been analysed and the topology with the highest energy-efficiency has been selected. Efficient network organisation employed in the form of relays is the next scenario, referred as *cooperative with relaying*, where some constraints regarding the relays have been set: first, on the link between any sensing node and the FC no more than one relay node may serve (nodes may transmit data directly to FC or via one relay node). Second, one relay may

forward data of many nodes under the DAF employment. Thus, the number of analysed cases in the relaying scenario is equal to  $\sum_{i=1}^{N-1} \binom{N}{i} i^{N-1}$ . The last scenario is a merge of the last two aforementioned, referenced as *cooperative with sleeping and relaying*.

In Figs. 4.8, 4.9, 4.10, 4.11 one may analyse sensing performance under the various metrics unified for all figures. First, in case (a) the energy efficiency is shown; second, the global probability of detection is presented in (b), and finally, the number of active nodes (those which are not in a sleeping-mode) and reporting nodes (i.e., the nodes which are transmitting sensing observations directly to FC or are serving as a relay) can be seen in the relaying scenario (c).

In Figure 4.8, the sensing-related metrics are shown for the varying distance from the central area point to the PU ( $d_{PU}$ ). In Fig. 4.8b, one may observe that below ca. 500 m,  $Q_d$  is close to 1 so it is sufficiently high, while for  $d_{PU} > 500$  m the significant detection degradation is observed. Thus, the most significant energy efficiency is observed for below-500-m-region in scenarios denoted as *cooperative with sleeping* and *cooperative with sleeping and relaying* (Fig. 4.8a). For lower signal-to-noise ratios, where detection quality is lower (i.e., when  $d_{PU} > 500$  m), the most energy-efficient is the basic *cooperative* scheme. The highest EE for low  $d_{PU}$  is caused by selection of one node on average (see Fig. 4.8c). Moreover, the number of reporting nodes (and as a consequence a number of relays) does not depend on  $d_{PU}$ .

As in previous set, the Fusion Centre has been assumed to be at the central point of the network, the next idea is to analyse the influence of the position of the FC. In Fig. 4.9, the results in the function of the distance from the centre of the network area to the FC are shown. The minimum distance 0 means that the FC is located in the central point of the network. Note that the closer the FC to the group of nodes, the higher the EE. Moreover, the global probability of detection is stable (Fig. 4.9b) except for the case when relaying and sleeping is adopted. In Fig. 4.9b, one may observe that the number of reporting nodes is getting close to 1 when the FC is far from the group of sensing nodes (at the distance greater than 15 m). Moreover, it is interesting that the number of selected nodes in the scenario with sleeping nodes decreases, while it increases when relaying is also considered (Fig. 4.9c). Thus, the use of relays when the FC is outside the network area is advantageous in terms of power savings.

In Figure 4.10, the analysis regarding the spread of sensing nodes is conducted. The highest energy efficiency is observed for low spread of nodes (Fig. 4.10a). The EE for scenarios which include sleeping is additionally higher than in *cooperative* and in *cooperative with relaying* scenarios. However, this gain is caused by the selection of very few nodes (Fig. 4.10c), and thus is vulnerable to the decrease of global detection probability (Fig. 4.10b). The number of reporting nodes in the *cooperative with relaying* scenario does not depend on the nodes spread.

The simulation results comparing the EE for a different number of sensing nodes in the network area (Fig. 4.11a) show that the EE in all scenarios decreases, while the number of cooperating nodes increases due to the larger number of links, and therefore larger amount of energy consumed for sensing, information sharing and reporting. However, a larger number of nodes introduces diversification and increases the global probability of detection (Fig. 4.11b). Finally, the number of selected nodes and/or reporting nodes increases for all cooperative-sensing scenarios with an increase of the number of nodes (Fig. 4.11c).

## Conclusion

The presented analysis shows that the energy efficiency in the network of sensing nodes may be significantly increased while keeping the detection quality sufficiently high. The applied node selection and relaying techniques have, however, highlighted the issue that this optimisation should be designed carefully. Node selection brings substantial energy benefits when quality of the link between the PU and the SU is sufficiently high. However, a joint scheme of relaying and node selection may not be substantially more energy-efficient than the basic cooperative scenario. This is caused by the high energy cost of the information sharing phase when each node has to send its channel-quality indicator to the FC. Thus, it is not always beneficial to adopt sophisticated network organisation. Finally, the EE decrease is observed for increasing distance to the PU and to the FC, for the increasing spread of nodes and the increasing number of nodes in the network.

## 4.10 Energy-Efficient Cooperative Spectrum Sensing with a Merged Clustering Measure

As it is concluded in the previous section, if the number of nodes is increasing, then the detection quality is also enhanced. Certainly, the more cooperating nodes, the more links between them and more interchanged messages. One may constitute the following trade-off: the higher the number of cooperating nodes, the better the spectrum sensing reliability but at the same time the higher amount of data for exchange. In order to minimise the load of the system due to the huge amount of control messages to be exchanged, it would be advisable to *cluster* the nodes, identify the Cluster Head (CH) and exchange the messages only between the cluster heads. On the other hand, in the traditional attitude applied in the previous section and known as *centralised* sensing, there exists no CH and the overall network organisation is simple.

In a wider context, the key idea of grouping nodes operating in the dense network into clusters is to optimise the whole network based on the defined criteria, for example, to reduce the number of exchanged messages or to reduce the mutual interference between the nodes. Typically, these goals are achieved in a way that neighbouring nodes that fulfil the predefined selection criteria are gathered, and the chosen representative of that cluster, i.e., CH, interacts with the rest of the network on behalf of all the nodes in this cluster. Two important issues can be identified here: one is the way how the clusters are created, and the second, how to select the CH efficiently. In this thesis, in Section 3.2, one may find the correlation-based clustering scheme where a novel leader selection metric is proposed.

One may envisage various criteria for cluster creation, such as nodes density, the distance between nodes and cluster head, channel characteristic between the node and the PU or the node and the cluster head, signal-to-noise (SNR) ratio acquired by node, nodes battery life, nodes mobility etc. In this work the focus is put on two criteria: the first is based on SNRs experienced by nodes [129], and on the observation that nodes located in a similar area may experience similar radio channel conditions and then be correlated. Therefore, the correlated nodes bring similar sensing results and may make common decisions since the energy consumption may be limited [150]. The second analysed option is the cluster formation on the basis of distances between

nodes. It has been observed that the distance is mainly proportional to the energy devoted to message spread. Thus, the motivation of the work presented in this section is to find the best proportion between nodes' distances and nodes' signal-to-noise ratios in order to find the most efficient cluster formation in terms of energy efficiency, as proposed later in Section 4.10.1.

#### 4.10.1 System Model

The aim in the optimisation is to maximise the energy efficiency according to the metric introduced by the author of the thesis in eq. (4.7). The reliability of the global decision is not different in node clustering and is given by the formula in Section 1.2.3, and depends on the number of cooperating nodes.

##### Power consumption in clustering

Power consumption in the network with the applied clustering depends on the power devoted for sensing  $P_{\text{sensing}}^{(i)}$  and the power devoted for reporting the sensing information from cluster member  $i$  to the CH  $P_{\text{reporting}}^{(i,CH)}$ . The first indicator is persistent irrespective of the applied network organisation, while the second is highly dependent on the applied network organisation. Thus, the total power consumption in the network of  $N$  cooperating nodes where clustering is applied and  $C$  clusters has been formed  $C > 1$  is equal to:

$$P_{\text{TOTAL}} = \sum_{i=1}^N P_{\text{sensing}}^{(i)} + \sum_{i=1}^C P_{\text{reporting}}^{(CH,FC)} + \sum_{i=C}^N P_{\text{reporting}}^{(i,CH)} + P_{\text{sharing}}, \quad (4.18)$$

where  $P_{\text{reporting}}^{(CH(i),FC)}$  is the power devoted to forward the sensing observations from cluster members by the appropriate CH to the FC and  $P_{\text{sharing}}$  is the power devoted for message interchange between the nodes in order to form clusters and nominate cluster leaders. The sensing observation from node  $i$  to its cluster head are reported with the power:

$$P_{\text{reporting}}^{(i,CH)} = (\text{erfc}^{-1}(2P_b))^2 \frac{\left(d_{CH}^{(i)}\right)^n}{\Lambda_{CH}^{(i)}}. \quad (4.19)$$

While the power consumed by the CH in order to report the sensing observations to the FC is equal to:

$$P_{\text{reporting}}^{(CH,FC)} = (\text{erfc}^{-1}(2P_b))^2 \frac{\left(d_{FC}^{(CH)}\right)^n}{\Lambda_{FC}^{(CH)}} + \kappa, \quad (4.20)$$

where  $\kappa$  is the power devoted in Cluster Head to merge the cluster-members sensing-observations (e.g., by applying decision fusion) into one message sent to the FC under the assumption that the DAF procedure is followed. Therefore, if the sensing power is equal in each node and the  $P_{\text{sharing}}$  is the power devoted to sense one message with parameters to the fusion centre, then the total consumed power in clustering simplifies to:

$$P_{\text{TOTAL}} = NP_{\text{sensing}} + \sum_{i=1}^C P_{\text{reporting}}^{(CH,FC)} + \sum_{i=C}^N P_{\text{reporting}}^{(i,CH)} + P_{\text{sharing}}. \quad (4.21)$$

### SNR- and distance-based clustering

Efficient clustering may be conducted according to the various criteria. The analysis presented in this section has covered two. In the first instance, correlation of signal-to-noise measures experienced by the nodes is taken into account. By selection of a given number of nodes according to this criterion, the highest global detection probability is guaranteed, as stated in [129]. However, for energy efficiency the quality of detection is one side, yet relevant. The other side is the energy consumption which depends on various phenomena. In this context, the distance-based clustering is proposed which takes into account the topology of the analysed network and aims at the minimisation of the overall energy consumption. Thus, putting these two attitudes into one merged measure gives the merged clustering measure:

$$\gamma_{\text{merged}}^{(i,k)}(\lambda) = \lambda d_{\text{normalised}}^{(i,k)} + (1 - \lambda) \text{SNR}_{\text{normalised}}^{(i,k)}, \quad (4.22)$$

where  $\gamma_{\text{merged}}^{(i,k)}$  is a merged clustering measure between node  $i$  and  $k$ ,  $\lambda$  is a weighing coefficient of distance and SNR, and  $d_{\text{normalised}}^{(i,k)}$  is the normalised distance between node  $i$  and  $k$ , while  $\text{SNR}_{\text{normalised}}^{(i,k)}$  is the normalised signal-to-noise-ratio from  $i$ -th to  $k$ -th node.

The merged correlation coefficients are then calculated for each pair of nodes and put into correlation matrix  $\mathcal{A}$  (eq. 4.23):

$$\mathcal{A} = \begin{bmatrix} \gamma_{\text{merged}}^{(1,1)} & \gamma_{\text{merged}}^{(1,2)} & \cdots & \gamma_{\text{merged}}^{(1,k)} \\ \gamma_{\text{merged}}^{(2,1)} & \gamma_{\text{merged}}^{(2,2)} & \cdots & \gamma_{\text{merged}}^{(2,k)} \\ \vdots & \vdots & \ddots & \vdots \\ \gamma_{\text{merged}}^{(i,1)} & \gamma_{\text{merged}}^{(i,2)} & \cdots & \gamma_{\text{merged}}^{(i,k)} \end{bmatrix}. \quad (4.23)$$

The correlation between nodes is reciprocal, thus, the array  $\mathcal{A}$  may be transformed to upper-triangular array  $\tilde{\mathcal{A}}$ :

$$\tilde{\mathcal{A}} = \begin{bmatrix} 0 & \gamma_{\text{merged}}^{(1,2)} & \cdots & \gamma_{\text{merged}}^{(1,k)} \\ 0 & 0 & \cdots & \gamma_{\text{merged}}^{(1,k)} \\ \vdots & \vdots & \ddots & \vdots \\ 0 & 0 & \cdots & \gamma_{\text{merged}}^{(i,k)} \end{bmatrix}. \quad (4.24)$$

The clusters are then formed proceeding the clustering algorithm leveraged from Section 3.2. In short, the procedure follows the following steps. First, in correlation array  $\tilde{\mathcal{A}}$  the highest correlation coefficient is found. Thus, a pair of nodes with the highest correlation is selected and clustered. Then, the next highest correlation value is taken from the array. If both nodes have not been put in clusters so far, then they form the next cluster. If one of them is a member of a previously formed cluster, then the second node becomes a candidate. A candidate may join the cluster when it is correlated with every cluster member at the level of at least  $\beta$ . If not, then the candidate is not clustered. In an exceptional case when two candidates (nodes previously included into disjoint clusters) want to form a cluster, it is possible that their clusters are merged and form a common one. It is possible if all members of both clusters have correlation of no less than  $\beta$ . The procedure is repeated until all pairs of nodes with correlation greater than  $\beta$  from array  $\tilde{\mathcal{A}}$  are analysed.

The result of the clustering procedure completed in the network of  $N$  nodes is the formation of  $C$  clusters. Please note that the node may not become the member of any cluster unless it has fulfilled the correlation requirement. In that case, the node is referred as *alone*. This case is particularly possible while the node is separated from other network members in terms of distance or received signal-to-noise ratio.

#### 4.10.2 Simulation Results

The motivation staying behind the presented research is to assess if it is more beneficial in terms of EE to cluster nodes according to the distance or the SNR. To that end, five various scenarios have been employed, with three being the reference scenarios and two specific scenarios.

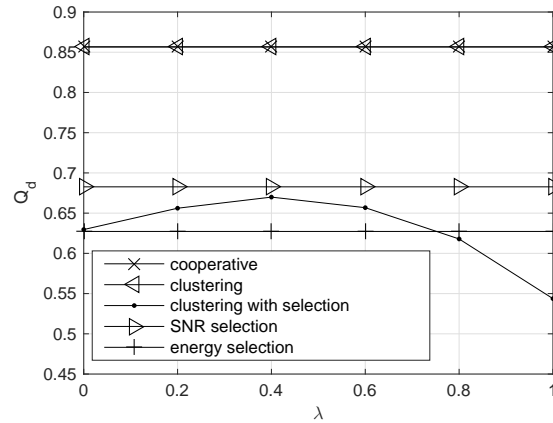
In the group of the reference scenarios, the first is the cooperative algorithm where all nodes sense the spectrum and transfer decisions directly to the FC, referred similarly to the notation found in previous section as *cooperative*. The second reference scenario is the scheme where node selection is applied according to the SNR criterion.  $N/2$  nodes with the highest experienced SNR in the link between the PU and the SU is selected and, thus, allowed to conduct spectrum sensing and report its observation. The unselected nodes turn into *sleeping* and neither can sense, nor report. The scenario is named in the remainder as *SNR selection*. Similarly, in the third case, node selection is employed, this time according to the lowest energy consumption in the reporting link from the SU to the FC. The last, *energy selection* is the selection of  $N/2$  nodes which have the lowest energy consumption at the reporting links (from SU to FC).

Apart from the references scenarios, two sophisticated scenarios have been introduced. The first one is the clustering with the novel merged clustering measure, as introduced in eq. (4.22). In this scenario, referred as *clustering*,  $N$  nodes take part in the clustering and  $C$  clusters are formed. The weighing coefficient  $\lambda$  is the variable in conducted simulations, thus, among analysed cases one may find such where just the distance between nodes is taken for cluster formation ( $\lambda = 1$ ) or only the SNR is taken for cluster formation ( $\lambda = 0$ ), or these two have been mixed ( $\lambda \in (0, 1)$ ).

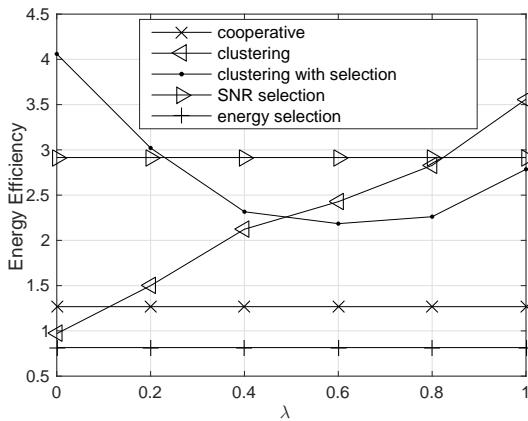
However, the sensing conducted by all network members, even if the efficient network organisation is applied in the form of clustering, is not always beneficial, as stated in the conclusion of Section 4.9. Therefore, in the fifth scenario the clustering with applied node sleeping is analysed. The clusters are formed according to the same procedure. Then, a part of nodes is selected, i.e., cluster heads and *alone* nodes. Thus, the number of selected nodes in that scenario is floating and depends on the amount of correlation in the considered network.

In Fig. 4.12, the results of the simulations are presented. One may see the five scenarios, where three are the reference scenarios whose results are constant in terms of  $\lambda$ . The reason is that, as stated in the above paragraphs, these scenarios do not employ the clustering approach with the merged measure and their performance results are conducted as reference.

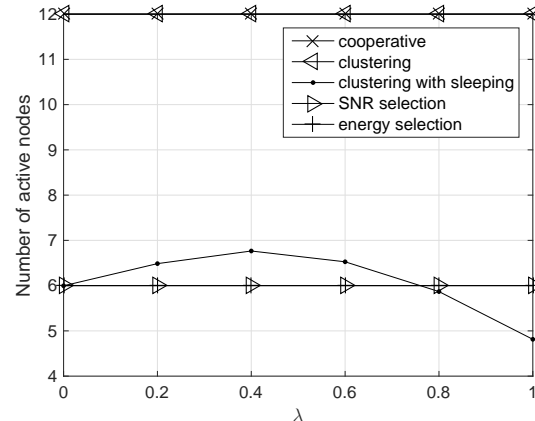
Thus, in Fig. 4.12a, the detection quality is plotted. Although the OR rule is applied, the global probability of detection depends on the number of nodes. On this account the greatest value is observed in schemes where all members of the network take part in spectrum sensing (*cooperative* and *clustering*). In three lowest cases, the subset of network members is allowed to sense, thus, the  $Q_d$  is lower. In *SNR selection* its value is the greatest (among the selection cases) even though in the *clustering and selection* case more nodes (at mean) take part in sensing (see



(a) Quality of detection



(b) Energy Efficiency



(c) Number of active nodes

**Figure 4.12:** Performance of the clustering scheme with a merged clustering measure for various weighing coefficient  $\lambda$ ,  $\sigma_c = 5$  m,  $N = 12$

Fig. 4.12c). Thus, when employing the node selection, the best quality of detection is possible if the sole SNR-criterion is employed.

Energy efficiency, plotted in Fig. 4.12b, is influenced by detection quality (plotted in Fig. 4.12a) and power consumed by the network of nodes. In three reference scenarios the highest EE is observed for *SNR selection*, while the lowest for *cooperative*. *Clustering* approach is the most efficient if the sole distance-criterion is applied in cluster formation. Although in that case the quality of detection is persistent, the EE increase is caused by the low energy consumption in reporting links while clustering according to the sole distance metric ( $\lambda = 1$ ) is applied. *Clustering with selection* brings the greatest EE among all solutions for  $\lambda = 0$ . This scenario brings the minimum value of the energy efficiency for weighing coefficient  $\lambda = 0.6$ . This is influenced by the number of selected nodes (plotted in Fig. 4.12c) which is the biggest for mediocre weighing coefficient and caused by the lowest correlation in the network for these assumptions.

### Conclusion

In the presented work the merged clustering measure has been proposed by the author of the thesis. The conducted simulations have shown that in low-SNR region, where quality of detection is relevant, it is beneficial to allow all nodes to sense the spectrum and form them into clusters according to the sole distance-criterion. However, the node selection may be added to the clustering, thus guaranteeing even higher energy efficiency, under the constraint that detection quality degradation is acceptable. Moreover, the clustering should be conducted according to the sole SNR-criterion. Among the presented reference scenarios, the reasonable performance, both in terms of detection quality and energy efficiency, is possible in the case of *SNR selection*.



## Chapter 5

---

# Conclusions

---

Based on the research and practical experiments conducted by the author of this thesis, regarding both the autonomous and cooperative spectrum sensing, the following conclusions can be drawn.

An energy detector may be enhanced by the application of the Sequential scheme. The conducted simulations and performed implementation have shown that within this technique the mean sensing time may be limited. However, the sensing reliability is insufficient. Thus, the SPCAF method has been applied, which is a cyclostationary-based approach and allows one to substantially improve detection probability at the cost of extended complexity. Therefore, hybrid scheme is proposed to join both the advantages of ED's simplicity and cyclostationary-based reliability into a hybrid approach. The aforementioned algorithms have been implemented by the author of the thesis on USRP platforms and the conducted implementations unveil various effects that may cause performance limitation. Thus, the sensing methods need to take into account hardware impairments such as DC offset, influence of temperature or various noise floor level. To address these issues the author of the thesis proposes the Sequential Pragmatic EnErgy Detection (SPEED) approach which allows one to reduce false alarm rate observed after the implementation of other schemes. Moreover, the key issue in energy detector is the proper noise estimation. Under the existing noise uncertainty limitation observed in each device, it is crucial to guarantee the accurate noise estimation. Three different methods have been tested. The general conclusion is that because the noise distribution observed in sensing device is not flat, it needs more scientific interest in order to guarantee reliable spectrum sensing.

Limited reliability in single-node detection may be improved by introducing cooperation between nodes resulting in greater spatial diversification. The prolonged implementation of the cooperative algorithm has shown that the cooperative detection results may be actually impaired. However, the proposed signal analysis directions may strictly improve the cooperative detection performance. The quality of performed sensing may be even further improved by the applied learning mechanisms that may build the *spectral awareness*, which is one of possible avenues for further investigations. There still exist many research directions such as correlation-based cooperation with included mobility. The proposed node grouping and selection algorithm that takes into account both sensing performance and mobility has been proposed by the author of the

thesis by introducing the leader selection metric. The introduced solution allows for the decrease of the number of grouping procedures. Moreover, in the correlated scenario it is possible to select one-fourth sensing devices out of their total number while keeping the sensing reliability at the same level and lowering the energy consumption.

Regarding the energy consumption limitation, the author of the thesis has put emphasis on defining the energy efficiency in CSS and has proposed classification of cooperative approaches. In the definition of energy-efficiency, the author focused on the quality of detection which should be taken into account when the energy-efficient CSS is proposed. Moreover, the author unveiled the original possibility of EE-approaches classification. The conclusion is that the approaches existing in the literature merely focus on a few aspects of EE-optimisation, usually take one or two of them into account. However, there exists a great area of opportunities when more directions taken together bring visible gains. On the other hand, there is a risk that employing a complex algorithm may not bring significant benefit over limited factors optimisation because the fact, that employing of one EE-optimisation area limits the other. Thus, the dependency matrix has been proposed in order to highlight dependencies between the optimisation areas. Moreover, the other employed tool, which is a rose-chart, has shown that it is impossible to find a universal algorithm, optimised for all use cases. The proposition is rather to neatly select the areas for optimisation on the basis of practical systems and goals. The presented energy-efficient solutions have shown that employing the energy-efficient approaches is not always straightforwardly beneficial. For example, sensing nodes selection and application of a sleep mode bring many benefits, however, the conducted research has shown that node relaying under the applied model consumes more energy than it really saves. The other point of view in sensing nodes clustering procedure is to take into account not only the acquired (sensed) signal-to-noise ratio but also the distance between the nodes which influences the energy consumption.

The author believes that the above conclusions allow to claim that the thesis of the dissertation has been proved, i.e., that there exist new methods for spectrum sensing providing both higher reliability and energy-efficiency. Some of these new methods have been proposed and evaluated in this dissertation.

---

# Bibliography

---

- [1] [www.ettus.com/product/details/UN210-KIT](http://www.ettus.com/product/details/UN210-KIT). Accessed: 30/08/2016.
- [2] Ettus Research LLC [www.ettus.com](http://www.ettus.com). Accessed: 30/08/2016.
- [3] [https://files.ettus.com/manual/page\\_uhd.html](https://files.ettus.com/manual/page_uhd.html). Accessed: 30/08/2016.
- [4] [files.ettus.com/uhd\\_docs/doxygen/html/structuhd\\_1\\_1tune\\_\\_request\\_\\_t.html](http://files.ettus.com/uhd_docs/doxygen/html/structuhd_1_1tune__request__t.html). Accessed: 30/08/2016.
- [5] [www.ettus.com/product/details/WBX](http://www.ettus.com/product/details/WBX). Accessed: 30/08/2016.
- [6] "1900.6-2011 – IEEE standard for spectrum sensing interfaces and data structures for dynamic spectrum access and other advanced radio communication systems". <http://standards.ieee.org/findstds/standard/1900.6-2011.html>. Accessed: 12/09/2016.
- [7] "1900.6-2014 – amendment 1: Procedures, protocols, and data archive enhanced interfaces". <http://standards.ieee.org/findstds/standard/1900.6a-2014.html>. Accessed: 12/09/2016.
- [8] "IEEE 1900.6 working group on spectrum sensing interfaces and data structures for dynamic spectrum access and other advanced radio communication systems". <http://grouper.ieee.org/groups/dyspan/6/index.htm>. Accessed: 12/09/2016.
- [9] IEEE 802.22 Working Group on Wireless Regional Area Networks: Enabling rural broadband wireless access using cognitive radio technology in TV whitespaces. <http://www.ieee802.org/22>. Accessed: 07/01/2016.
- [10] F. Adelantado and C. Verikoukis. A non-parametric statistical approach for malicious users detection in cognitive wireless ad-hoc networks. In *IEEE International Conference on Communications (ICC)*, pages 1–5, June 2011.
- [11] O.A. Adeniran and A. Demosthenous. An ultra-energy-efficient wide-bandwidth video pipeline ADC using optimized architectural partitioning. *IEEE Transactions on Circuits and Systems I: Regular Papers*, 53(12):2485–2497, Dec. 2006.
- [12] N. Ahmed, D. Hadaller, and S. Keshav. GUESS: Gossiping Updates for Efficient Spectrum Sensing. In *MobiShare'06*, pages 1–6, Sept. 2006.

- [13] I.F. Akyildiz, B.F. Lo, and R. Balakrishnan. Cooperative spectrum sensing in cognitive radio networks: A survey. *Physical Communications*, 4(1):40–62, Mar. 2011.
- [14] I.F. Akyildiz, W. Su, Y. Sankarasubramaniam, and E. Cayirci. A survey on sensor networks. *IEEE Communications Magazine*, 40(8):102–114, Aug. 2002.
- [15] S. Althunibat, S. Narayanan, M. Di Renzo, and F. Granelli. On the energy consumption of the decision-fusion rules in cognitive radio networks. In *IEEE 17th International Workshop on Computer Aided Modeling and Design of Communication Links and Networks (CAMAD)*, pages 125–129, Sept. 2012.
- [16] S. Althunibat, M. Di Renzo, and F. Granelli. Cooperative spectrum sensing for cognitive radio networks under limited time constraints. *Computer Communications*, 43:55–63, 2014.
- [17] P. Alvarez, N. Pratas, A. Rodrigues, N. R. Prasad, and R. Prasad. Energy detection and eigenvalue based detection: An experimental study using GNU Radio. In *14th International Symposium on Wireless Personal Multimedia Communications (WPMC)*, pages 1–5, Oct. 2011.
- [18] K. Arshad and K. Moessner. Mobility driven energy detection based spectrum sensing framework of a cognitive radio. In *Second UK-India-IDRC International Workshop on Cognitive Wireless Systems (UKIWCWS)*, pages 1–5, Dec. 2010.
- [19] E. Axell, G. Leus, E.G. Larsson, and H.V. Poor. Spectrum sensing for cognitive radio: State-of-the-art and recent advances. *IEEE Signal Processing Magazine*, 29(3):101–116, May 2012.
- [20] A. Baharlouei and B. Jabbari. A Stackelberg game spectrum sensing scheme in cooperative cognitive radio networks. In *IEEE Wireless Communications and Networking Conference (WCNC)*, pages 2215–2219, 2012.
- [21] M. Ben Ghorbel, H. Nam, and M.-S. Alouini. Cluster-based spectrum sensing for cognitive radios with imperfect channel to cluster-head. In *IEEE Wireless Communications and Networking Conference (WCNC)*, pages 709–713, Apr. 2012.
- [22] M. Ben Ghorbel, H. Nam, and M.-S. Alouini. Exact performance of cooperative spectrum sensing for cognitive radios with quantized information under imperfect reporting channels. In *IEEE 78th Vehicular Technology Conference (VTC Fall)*, pages 1–5, Sept. 2013.
- [23] V. Blaschke, H. Jaekel, T. Renk, C. Kloeck, and F.K. Jondral. Occupation measurements supporting dynamic spectrum allocation for cognitive radio design. In *2nd International Conference on Cognitive Radio Oriented Wireless Networks and Communications*, pages 50–57, Aug. 2007.
- [24] D.R. Brown and F. Fazel. A game theoretic study of energy efficient cooperative wireless networks. *Journal of Communications and Networks*, 13(3):266–276, June 2011.
- [25] E.R. Brown. RF-MEMS switches for reconfigurable integrated circuits. *IEEE Transactions on Microwave Theory and Techniques*, 46(11):1868–1880, Nov. 1998.

- [26] D. Cabric, S.M. Mishra, and R.W. Brodersen. Implementation issues in spectrum sensing for cognitive radios. In *Conference Record of the Thirty-Eighth Asilomar Conference on Signals, Systems and Computers*, volume 1, pages 772–776, Nov. 2004.
- [27] A.S. Cacciapuoti, I.F. Akyildiz, and L. Paura. Correlation-aware user selection for cooperative spectrum sensing in cognitive radio ad hoc networks. *IEEE Journal on Selected Areas in Communications*, 30(2):297–306, 2012.
- [28] S. Chaudhari, J. Lunden, V. Koivunen, and H.V. Poor. Cooperative sensing with imperfect reporting channels: Hard decisions or soft decisions? *IEEE Transactions on Signal Processing*, 60(1):18–28, Jan. 2012.
- [29] R.-R. Chen, K.H. Teo, and B. Farhang-Boroujeny. Random access protocols for collaborative spectrum sensing in multi-band cognitive radio networks. *IEEE Journal of Selected Topics in Signal Processing*, 5(1):124–136, Feb. 2011.
- [30] Y. Chen and H. Oh. A survey of measurement-based spectrum occupancy modeling for cognitive radios. *IEEE Communications Surveys Tutorials*, 18(1):848–859, Firstquarter 2016.
- [31] P. Cheraghi, Y. Ma, and R. Tafazolli. A novel blind spectrum sensing approach for cognitive radios. In *PGNET 2010 Conference*, 2010.
- [32] K. Cichoń and H. Bogucka. An energy-efficient cooperative spectrum sensing. In *IEEE International Black Sea Conference on Communications and Networking (BlackSeaCom)*, pages 24–28, May 2015.
- [33] K. Cichoń, L. De Nardis, H. Bogucka, and M. Di Benedetto. Mobility-aware, correlation-based node grouping and selection for cooperative spectrum sensing. *Journal of Telecommunications and Information Technology*, (2):90–102, 2014.
- [34] K. Cichoń and A. Kliks. The impact of hardware implementation on the performance of spectrum sensing algorithms. In *2014 11th International Symposium on Wireless Communications Systems (ISWCS)*, pages 282–286, Aug. 2014.
- [35] K. Cichoń, A. Kliks, and H. Bogucka. Performance aspects of cooperative spectrum sensing in hardware implementation. In *General Assembly and Scientific Symposium (URSI GASS), 2014 XXXIth URSI*, pages 1–4, Aug 2014.
- [36] K. Cichoń, A. Kliks, and H. Bogucka. Signal analysis in cooperative spectrum sensing hardware implementation. In *NATO IST-123/RSY-029 Symposium on Cognitive Radio & Future Networks*, pages 1–8, May 2014.
- [37] K. Cichoń, A. Kliks, and H. Bogucka. Energy-efficient cooperative spectrum sensing: A survey. *IEEE Communications Surveys Tutorials*, 18(3):1861–1886, thirdquarter 2016.
- [38] K. Cichoń. MAC algorithms in V2V transmission systems. *Przegląd Telekomunikacyjny i Wiadomości Telekomunikacyjne*, 2012(4):157–160, 2012.

- [39] K. Cichoń and H. Bogucka. Wybór węzłów mobilnych w algorytmie korelacji decyzji w radiu kognitywnym. *Przegląd Telekomunikacyjny i Wiadomości Telekomunikacyjne*, 2013(6):314–317, 2013.
- [40] K. Cichoń and H. Bogucka. Estymacja mocy szumu w praktycznej implementacji detektora energii. *Przegląd Telekomunikacyjny i Wiadomości Telekomunikacyjne*, 2014(8-9):889–894, 2014.
- [41] K. Cichoń and H. Bogucka. Oszczędność energetyczna kooperacyjnej detekcji sygnałów w radiu kognitywnym. *Przegląd Telekomunikacyjny i Wiadomości Telekomunikacyjne*, 2015(4):229–232, 2015.
- [42] K. Cichoń and H. Bogucka. Udział węzłów przekaźnikowych w oszczędności energetycznej kooperacyjnej detekcji sygnałów. *Przegląd Telekomunikacyjny i Wiadomości Telekomunikacyjne*, 2015(8-9):830–835, 2015.
- [43] K. Cichoń and A. Kliks. Sekwencyjny algorytm wykrywania transmisji użytkownika pierwotnego. *Przegląd Telekomunikacyjny i Wiadomości Telekomunikacyjne*, 2012(8-9):640–645, 2012.
- [44] K. Cichoń and A. Kliks. SEKWENS – algorytm sekwencyjnego wykrywania sygnałów. *Przegląd Telekomunikacyjny i Wiadomości Telekomunikacyjne*, 2013(8-9):1283–1289, 2013.
- [45] K. Cichoń, A. Kliks, and H. Bogucka. Praktyczna implementacja kooperacyjnego algorytmu wykrywania sygnału użytkownika licencjonowanego. *Przegląd Telekomunikacyjny i Wiadomości Telekomunikacyjne*, 2014(6):341–344, 2014.
- [46] K. Cichoń, A. Kliks, and H. Bogucka. Optymalizacja oszczędności energetycznej kooperacyjnej detekcji sygnałów w ujęciu logiki rozmytej. *Przegląd Telekomunikacyjny i Wiadomości Telekomunikacyjne*, 2016(6):385–388, 2016.
- [47] Cisco. Cisco visual networking index: Global mobile data traffic forecast update, 2015–2020. White paper, <http://www.cisco.com/c/en/us/solutions/collateral/service-provider/visual-networking-index-vni/mobile-white-paper-c11-520862.pdf>, 2016. Accessed: 30/09/2016.
- [48] H. Claussen. Efficient modelling of channel maps with correlated shadow fading in mobile radio systems. In *IEEE 16th International Symposium on Personal, Indoor and Mobile Radio Communications (PIMRC)*, volume 1, pages 512–516, Sept. 2005.
- [49] S. Cui, A.J. Goldsmith, and A. Bahai. Energy-constrained modulation optimization for coded systems. In *IEEE Global Telecommunications Conference, GLOBECOM*, volume 1, pages 372–376, Dec. 2003.
- [50] S. Cui, A.J. Goldsmith, and A. Bahai. Energy-constrained modulation optimization. *IEEE Transactions on Wireless Communications*, 4(5):2349–2360, Sept. 2005.
- [51] I. Dages, A. Polydoros, D. Denkovski, V. Rakovic, V. Atanasovski, L. Gavrilovska, K. Cichoń, A. Kliks, S. Baban, and O. Holland. An integrated platform for source detection,

- identification and localization with applications to cognitive-radio. In *Proceedings of the 2013 19th European Wireless Conference (EW)*, pages 1–6, Apr. 2013.
- [52] A. De Domenico, E.C. Strinati, and M. Di Benedetto. A survey on MAC strategies for cognitive radio networks. *IEEE Communications Surveys Tutorials*, 14(1):21–44, First 2012.
- [53] L. De Nardis, M. Di Benedetto, D. Tassetto, S. Bovelli, A. Akhtar, O. Holland, and R. Thobaben. Impact of mobility in cooperative spectrum sensing: Theory vs. simulation. In *2012 International Symposium on Wireless Communication Systems (ISWCS)*, pages 416–420, Aug. 2012.
- [54] L. De Nardis, D. Domenicali, and M. Di Benedetto. Clustered hybrid energy-aware cooperative spectrum sensing (CHESS). In *4th International Conference on Cognitive Radio Oriented Wireless Networks and Communications CROWNCOM*, pages 1–6, June 2009.
- [55] L. De Vito. A review of wideband spectrum sensing methods for cognitive radios. In *IEEE International Instrumentation and Measurement Technology Conference (I2MTC)*, pages 2257–2262, May 2012.
- [56] M. Dehghan, M. Ghaderi, and D. Goeckel. Minimum-energy cooperative routing in wireless networks with channel variations. *IEEE Transactions on Wireless Communications*, 10(11):3813–3823, Nov. 2011.
- [57] G. Ding, Q. Wu, F. Song, and J. Wang. Decentralized sensor selection for cooperative spectrum sensing based on unsupervised learning. In *IEEE International Conference on Communications (ICC)*, pages 1576–1580, June 2012.
- [58] A. Ebrahimzadeh, M. Najimi, S.M.H. Andargoli, and A. Fallahi. Sensor selection and optimal energy detection threshold for efficient cooperative spectrum sensing. *IEEE Transactions on Vehicular Technology*, 64(4):1565–1577, Apr. 2015.
- [59] S. Eryigit, S. Bayhan, and T. Tugcu. Channel switching cost aware and energy-efficient cooperative sensing scheduling for cognitive radio networks. In *IEEE International Conference on Communications (ICC)*, pages 2633–2638, June 2013.
- [60] ETSI. Environmental Engineering (EE) energy efficiency of wireless access network equipment. ETSI TS 102 706 v1.1.1, [http://www.etsi.org/deliver/etsi\\_ts/102700\\_102799/102706/01.01.01\\_60/ts\\_102706v010101p.pdf](http://www.etsi.org/deliver/etsi_ts/102700_102799/102706/01.01.01_60/ts_102706v010101p.pdf), 2009. Accessed: 13/06/2016.
- [61] FCC. In the matter of unlicensed operation in the TV broadcast bands. Second memorandum opinion and order. [http://fjallfoss.fcc.gov/edocs\\_public/attachmatch/FCC-10-174A1\\_Rcd.pdf](http://fjallfoss.fcc.gov/edocs_public/attachmatch/FCC-10-174A1_Rcd.pdf), 2010.
- [62] W.A. Gardner. Exploitation of spectral redundancy in cyclostationary signals. *IEEE Signal Processing Magazine*, 8(2):14–36, Apr. 1991.

- [63] A. Ghasemi and E.S. Sousa. Collaborative spectrum sensing for opportunistic access in fading environments. In *First IEEE International Symposium on New Frontiers in Dynamic Spectrum Access Networks*, pages 131–136, 2005.
- [64] A. Ghosh, A. Halder, and A.S. Dhar. A variable RF carrier modulation scheme for ultralow power wireless body-area network. *IEEE Systems Journal*, 6(2):305–316, June 2012.
- [65] V. Giannini, J. Craninckx, S. D’Amico, and A. Baschirotto. Flexible baseband analog circuits for software-defined radio front-ends. *IEEE Journal of Solid-State Circuits*, 42(7):1501–1512, July 2007.
- [66] V. Giannini, P. Nuzzo, C. Soens, K. Vengattaramane, J. Ryckaert, M. Goffioul, B. Debaillie, J. Borremans, J. Van Driessche, J. Craninckx, and M. Ingels. A 2-mm<sup>2</sup> 0.1-5 GHz software-defined radio receiver in 45-nm digital CMOS. *IEEE Journal of Solid-State Circuits*, 44(12):3486–3498, Dec. 2009.
- [67] M. Gudmundson. Correlation model for shadow fading in mobile radio systems. *Electronics Letters*, 27(23):2145–2146, 1991.
- [68] J. Habibi, A Ghrayeb, and A.G. Aghdam. Energy-efficient cooperative routing in wireless sensor networks: A mixed-integer optimization framework and explicit solution. *IEEE Transactions on Communications*, 61(8):3424–3437, Aug. 2013.
- [69] W. Han, J. LI, Z. Li, J. Si, and Y. Zhang. Efficient soft decision fusion rule in cooperative spectrum sensing. *IEEE Transactions on Signal Processing*, 61(8):1931–1943, Apr. 2013.
- [70] P.J.A. Harpe, C. Zhou, Y. Bi, N.P. van der Meijs, X. Wang, K. Philips, G. Dolmans, and H. de Groot. A 26  $\mu$ W 8 bit 10 MS/s asynchronous SAR ADC for low energy radios. *IEEE Journal of Solid-State Circuits*, 46(7):1585–1595, July 2011.
- [71] Z. Hasan, H. Boostanimehr, and V.K. Bhargava. Green cellular networks: A survey, some research issues and challenges. *IEEE Communications Surveys Tutorials*, 13(4):524–540, Fourth 2011.
- [72] S. Haykin. Cognitive radio: brain-empowered wireless communications. *IEEE Journal on Selected Areas in Communications*, 23(2):201–220, Feb. 2005.
- [73] S. Haykin, D.J. Thomson, and J.H. Reed. Spectrum sensing for cognitive radio. *Proceedings of the IEEE*, 97(5):849–877, May 2009.
- [74] D. Horgan and C.C. Murphy. Voting rule optimisation for double threshold energy detector-based cognitive radio networks. In *4th International Conference on Signal Processing and Communication Systems (ICSPCS)*, pages 1–8, Dec. 2010.
- [75] S. Huang, H. Chen, Y. Zhang, and H.-H. Chen. Sensing-energy tradeoff in cognitive radio networks with relays. *IEEE Systems Journal*, 7(1):68–76, Mar. 2013.
- [76] S. Huang, X. Liu, and Z. Ding. Optimal sensing-transmission structure for dynamic spectrum access. In *IEEE INFOCOM 2009*, pages 2295–2303, Apr. 2009.

- [77] G. Hueber, Y. Zou, K. Dufrene, R. Stuhlberger, and M. Valkama. Smart front-end signal processing for advanced wireless receivers. *IEEE Journal of Selected Topics in Signal Processing*, 3(3):472–487, June 2009.
- [78] A Ibrahim, Z. Han, and K.J.R. Liu. Distributed energy-efficient cooperative routing in wireless networks. *IEEE Transactions on Wireless Communications*, 7(10):3930–3941, Oct. 2008.
- [79] M.H. Islam, C.L. Koh, S. Wah Oh, X. Qing, Y.Y. Lai, C. Wang, Y.-C. Liang, B.E. Toh, F. Chin, G.L. Tan, and W. Toh. Spectrum survey in Singapore: Occupancy measurements and analyses. In *3rd International Conference on Cognitive Radio Oriented Wireless Networks and Communications*, pages 1–7, May 2008.
- [80] A. Jakubiak. *Probabilistyczne metody detekcji sygnałów na tle zakłóceń*. Oficyna Wydawnicza Politechniki Warszawskiej, 2013.
- [81] C. Jiang, Y. Chen, Y. Gao, and K.J.R. Liu. Joint spectrum sensing and access evolutionary game in cognitive radio networks. *IEEE Transactions on Wireless Communications*, 12(5):2470–2483, May 2013.
- [82] P. Kaligineedi and V.K. Bhargava. Sensor allocation and quantization schemes for multi-band cognitive radio cooperative sensing system. *IEEE Transactions on Wireless Communications*, 10(1):284–293, Jan. 2011.
- [83] F. Kaltenberger, I. Latif, and R. Knopp. On scalability, robustness and accuracy of physical layer abstraction for large-scale system-level evaluations of LTE networks. In *2013 Asilomar Conference on Signals, Systems and Computers*, pages 1644–1648, Nov. 2013.
- [84] S.H. Kang and T. Nguyen. Distance based thresholds for cluster head selection in wireless sensor networks. *IEEE Communications Letters*, 16(9):1396–1399, Sept. 2012.
- [85] B. Kasiri and J. Cai. Effects of correlated shadowing on soft decision fusion in cooperative spectrum sensing. In *INFOCOM IEEE Conference on Computer Communications Workshops*, pages 1–6, 2010.
- [86] Z. Khalaf, A. Nafkha, and J. Palicot. Blind spectrum detector for cognitive radio using compressed sensing and symmetry property of the second order cyclic autocorrelation. In *7th International ICST Conference on Cognitive Radio Oriented Wireless Networks and Communications*, pages 291–296, June 2012.
- [87] Z. Khan, J. Lehtomaki, K. Umebayashi, and J. Vartiainen. On the selection of the best detection performance sensors for cognitive radio networks. *IEEE Signal Processing Letters*, 17(4):359–362, Apr. 2010.
- [88] H. Kim and K. G. Shin. In-band spectrum sensing in IEEE 802.22 WRANs for incumbent protection. *IEEE Transactions on Mobile Computing*, 9(12):1766–1779, Dec. 2010.
- [89] I. Kim and D. Kim. Optimal allocation of sensing time between two primary channels in cognitive radio networks. *IEEE Communications Letters*, 14(4):297–299, Apr. 2010.

- [90] A. Kliks, P. Kryszkiewicz, K. Cichoń, A. Umberto, J. Perez-Romero, and F. Casadevall. DVB-T channels measurements for the deployment of outdoor REM databases. *Journal of Telecommunications and Information Technology*, (3):42–52, 2014.
- [91] A. Kliks, P. Kryszkiewicz, K. Cichoń, A. Umberto, J. Perez-Romero, and F. Casadevall. DVB-T channels power measurements in indoor/outdoor cases. In *IEICE Information and Communication Technology Forum*, pages 1–6, May 2014.
- [92] M. Kosunen, V. Turunen, K. Kokkinen, and J. Ryyanen. Survey and analysis of cyclostationary signal detector implementations on FPGA. *IEEE Journal on Emerging and Selected Topics in Circuits and Systems*, 3(4):541–551, Dec. 2013.
- [93] G. Kramer, M. Gastpar, and P. Gupta. Cooperative strategies and capacity theorems for relay networks. *IEEE Transactions on Information Theory*, 51(9):3037–3063, Sept. 2005.
- [94] L. Le and E. Hossain. Cross-layer optimization frameworks for multihop wireless networks using cooperative diversity. *IEEE Transactions on Wireless Communications*, 7(7):2592–2602, July 2008.
- [95] C.-H. Lee and W. Wolf. Energy efficient techniques for cooperative spectrum sensing in cognitive radios. In *5th IEEE Consumer Communications and Networking Conference*, pages 968–972, Jan. 2008.
- [96] J.-S. Lee and W.-L. Cheng. Fuzzy-logic-based clustering approach for wireless sensor networks using energy predication. *IEEE Sensors Journal*, 12(9):2891–2897, Sept. 2012.
- [97] S. Lee and S.-L. Kim. Optimization of time-domain spectrum sensing for cognitive radio systems. *IEEE Transactions on Vehicular Technology*, 60(4):1937–1943, May 2011.
- [98] W.-Y. Lee and I.F. Akyildiz. Optimal spectrum sensing framework for cognitive radio networks. *IEEE Transactions on Wireless Communications*, 7(10):3845–3857, Oct. 2008.
- [99] Y.-C. Liang, Y. Zeng, E.C.Y. Peh, and A.T. Hoang. Sensing-throughput tradeoff for cognitive radio networks. *IEEE Transactions on Wireless Communications*, 7(4):1326–1337, Apr. 2008.
- [100] S. Y. Lien, J. Lee, and Y. C. Liang. Random access or scheduling: Optimum LTE licensed-assisted access to unlicensed spectrum. *IEEE Communications Letters*, 20(3):590–593, Mar. 2016.
- [101] G. Lim and Jr. Cimini, L.J. Energy-efficient cooperative beamforming in clustered wireless networks. *IEEE Transactions on Wireless Communications*, 12(3):1376–1385, Mar. 2013.
- [102] X. Liu, B.G. Evans, and K. Moessner. Comparison of reliability, delay and complexity for standalone cognitive radio spectrum sensing schemes. *IET Communications*, 7(9):799–807, June 2013.
- [103] J.R. Long, W. Wu, Y. Dong, Y. Zhao, M.A.T. Sanduleanu, J.F.M. Gerrits, and G. van Veenendaal. Energy-efficient wireless front-end concepts for ultra lower power radio. In *IEEE Custom Integrated Circuits Conference*, pages 587–590, Sept. 2008.

- [104] L. Lu, X. Zhou, U. Onunkwo, and G.Y. Li. Ten years of research in spectrum sensing and sharing in cognitive radio. *EURASIP Journal on Wireless Communications and Networking*, 2012(1):1–16, 2012.
- [105] J. Ma, G. Zhao, and Y. Li. Soft combination and detection for cooperative spectrum sensing in cognitive radio networks. *IEEE Transactions on Wireless Communications*, 7(11):4502–4507, Nov. 2008.
- [106] Y. Ma, Y. Gao, X. Zhang, and L. Cuthbert. Optimization of collaborating secondary users in a cooperative sensing under noise uncertainty. In *IEEE 24th International Symposium on Personal Indoor and Mobile Radio Communications*, pages 2502–2506, Sept. 2013.
- [107] S. Maleki, S.P. Chepuri, and G. Leus. Optimal hard fusion strategies for cognitive radio networks. In *IEEE Wireless Communications and Networking Conference (WCNC)*, pages 1926–1931, Mar. 2011.
- [108] S. Maleki and G. Leus. Censored truncated sequential spectrum sensing for cognitive radio networks. *IEEE Journal on Selected Areas in Communications*, 31(3):364–378, Mar. 2013.
- [109] S. Maleki, A. Pandharipande, and G. Leus. Energy-efficient distributed spectrum sensing with convex optimization. In *3rd IEEE International Workshop on Computational Advances in Multi-Sensor Adaptive Processing (CAMSAP)*, pages 396–399, Dec. 2009.
- [110] S. Maleki, A. Pandharipande, and G. Leus. Energy-efficient distributed spectrum sensing for cognitive sensor networks. *IEEE Sensors Journal*, 11(3):565–573, Mar. 2011.
- [111] G. Miao, N. Himayat, Y.G. Li, and A. Swami. Cross-layer optimization for energy-efficient wireless communications: A survey. In *Wireless Communication and Mobile Computing Conference (IWCMC)*, volume 9, pages 529–542, 2009.
- [112] A.W. Min and K.G. Shin. Impact of mobility on spectrum sensing in cognitive radio networks. In *Proceedings of the ACM workshop on Cognitive radio networks*, pages 13–18, 2009.
- [113] S.M. Mishra, A. Sahai, and R.W. Brodersen. Cooperative sensing among cognitive radios. In *IEEE International Conference on Communications*, volume 4, pages 1658–1663, June 2006.
- [114] J. Mitola. Cognitive radio for flexible mobile multimedia communications. In *IEEE International Workshop on Mobile Multimedia Communications*, pages 3–10, 1999.
- [115] J. Mitola. *Cognitive Radio: An Integrated Agent Architecture for Software Defined Radio*, *PhD Thesis*. PhD thesis, Royal Institute of Technology (KTH), Sweden, May 2000.
- [116] J. Mitola and Jr. Maguire, G.Q. Cognitive radio: making software radios more personal. *IEEE Personal Communications*, 6(4):13–18, Aug. 1999.
- [117] M. Mustonen, M. Matinmikko, and A. Mammela. Cooperative spectrum sensing using quantized soft decision combining. In *4th International Conference on Cognitive Radio Oriented Wireless Networks and Communications*, pages 1–5, June 2009.

- [118] A. Nafkha, M. Naoues, K. Cichoń, and A. Kliks. Experimental spectrum sensing measurements using USRP Software Radio platform and GNU-Radio. In *9th International Conference on Cognitive Radio Oriented Wireless Networks and Communications (CROWN-COM)*, pages 429–434, June 2014.
- [119] A. Nafkha, M. Naoues, K. Cichoń, A. Kliks, and B. Aziz. Hybrid spectrum sensing experimental analysis using GNU Radio and USRP for cognitive radio. In *2015 International Symposium on Wireless Communication Systems (ISWCS)*, pages 506–510, Aug. 2015.
- [120] M. Najimi, A. Ebrahimzadeh, S.M.H. Andargoli, and A. Fallahi. A novel sensing nodes and decision node selection method for energy efficiency of cooperative spectrum sensing in cognitive sensor networks. *IEEE Sensors Journal*, 13(5):1610–1621, 2013.
- [121] M. Van Nguyen, S. Lee, S.-j. You, C.S. Hong, and L.B. Le. Cross-layer design for congestion, contention, and power control in CRAHNS under packet collision constraints. *IEEE Transactions on Wireless Communications*, 12(11):5557–5571, Nov. 2013.
- [122] N. Nguyen-Thanh, P. Ciblat, S. Maleki, and V.-T. Nguyen. How many bits should be reported in quantized cooperative spectrum sensing? *IEEE Wireless Communications Letters*, 4(5):465–468, Oct. 2015.
- [123] D. Nouget (ed.). Sensing techniques for cognitive radio-state of the art and trends. SCC41-P1900.6 White paper, Apr. 2009.
- [124] C. Oestges, N. Czink, B. Bandemer, P. Castiglione, F. Kaltenberger, and A.J. Paulraj. Experimental characterization and modeling of outdoor-to-indoor and indoor-to-indoor distributed channels. *IEEE Transactions on Vehicular Technology*, 59(5):2253–2265, 2010.
- [125] Ofcom. Digital dividend: cognitive access. statement on license-exempting cognitive devices using interleaved spectrum. <http://stakeholders.ofcom.org.uk/binaries/consultations/cognitive/statement/statement.pdf>, 2009.
- [126] Ofcom. Implementing TV white spaces. <http://stakeholders.ofcom.org.uk/binaries/consultations/white-space-coexistence/statement/tvws-statement.pdf>, Feb. 2015. Accessed: 17/02/2016.
- [127] K. Patil, R. Prasad, and K. Skouby. A survey of worldwide spectrum occupancy measurement campaigns for cognitive radio. In *International Conference on Devices and Communications (ICDeCom)*, pages 1–5, Feb. 2011.
- [128] N. Patwari and P. Agrawal. Effects of correlated shadowing: Connectivity, localization, and RF tomography. In *International Conference on Information Processing in Sensor Networks*, pages 82–93, 2008.
- [129] E. Peh and Y.-C. Liang. Optimization for cooperative sensing in cognitive radio networks. In *IEEE Wireless Communications and Networking Conference*, pages 27–32, Mar. 2007.

- [130] E. Peh, Y.-C. Liang, Y.L. Guan, and Y. Pei. Energy-efficient cooperative spectrum sensing in cognitive radio networks. In *IEEE Global Telecommunications Conference (GLOBECOM 2011)*, pages 1–5, Dec. 2011.
- [131] Y. Pei, Y.-C. Liang, K.C. Teh, and K.H. Li. How much time is needed for wideband spectrum sensing? *IEEE Transactions on Wireless Communications*, 8(11):5466–5471, Nov. 2009.
- [132] N. Pratas, N. Marchetti, N.R. Prasad, A. Rodrigues, and R. Prasad. Adaptive counting rule for cooperative spectrum sensing under correlated environments. *Wireless Personal Communications*, 64(1):93–106, 2012.
- [133] N. Pratas, N.R. Prasad, A. Rodrigues, and R. Prasad. Cooperative spectrum sensing: State of the art review. In *2nd International Conference on Wireless Communication, Vehicular Technology, Information Theory and Aerospace Electronic Systems Technology (Wireless VITAE)*, pages 1–6, Feb. 2011.
- [134] W. Prawatmuang and D.K.C. So. Quantized cooperative spectrum sensing for cognitive radio. In *IEEE 24th International Symposium on Personal Indoor and Mobile Radio Communications (PIMRC)*, pages 585–589, Sept. 2013.
- [135] L. Pucker. Review of contemporary spectrum sensing technologies. Report for IEEE-SA P1900.6 Standards Group, 2010.
- [136] Z. Quan, S. Cui, and A.H. Sayed. Optimal linear cooperation for spectrum sensing in cognitive radio networks. *IEEE Journal of Selected Topics in Signal Processing*, 2(1):28–40, Feb. 2008.
- [137] Z. Quan, W.-K. Ma, S. Cui, and A.H. Sayed. Optimal linear fusion for distributed detection via semidefinite programming. *IEEE Transactions on Signal Processing*, 58(4):2431–2436, Apr. 2010.
- [138] GNU Radio. The free and open-source toolkit for software radio. <http://gnuradio.org/>. Accessed: 23/08/2016.
- [139] R. Ratasuk, N. Mangalvedhe, and A. Ghosh. LTE in unlicensed spectrum using licensed-assisted access. In *Globecom Workshops*, pages 746–751, Dec. 2014.
- [140] B. Razavi. Design of millimeter-wave CMOS radios: A tutorial. *IEEE Transactions on Circuits and Systems I: Regular Papers*, 56(1):4–16, Jan. 2009.
- [141] P. Ren, Y. Wang, and Q. Du. CAD-MAC: A channel-aggregation diversity based MAC protocol for spectrum and energy efficient cognitive ad hoc networks. *IEEE Journal on Selected Areas in Communications*, 32(2):237–250, Feb. 2014.
- [142] F.C. Ribeiro, M.L.R. de Campos, and S. Werner. Distributed cooperative spectrum sensing with adaptive combining. In *IEEE International Conference on Acoustics, Speech and Signal Processing (ICASSP)*, pages 3557–3560, Mar. 2012.

- [143] P. Rousseeuw. Least median of squares regression. *Journal of the American Statistical Association*, 79(388):871–880, December 1984.
- [144] P. Rousseeuw. *Robust Regression and Outlier Detection*. John Wiley&Sons, 1987.
- [145] H. Rowaihy, S. Eswaran, M. Johnson, D. Verma, A. Bar-noy, T. Brown, and T. La Porta. A survey of sensor selection schemes in wireless sensor networks. In *In SPIE Defense and Security Symposium Conference on Unattended Ground, Sea, and Air Sensor Technologies and Applications IX*, 2007.
- [146] W. Saad, Z. Han, T. Basar, M. Debbah, and A. Hjørungnes. Coalition formation games for collaborative spectrum sensing. *IEEE Transactions on Vehicular Technology*, 60(1):276–297, Jan. 2011.
- [147] W. Saad, Z. Han, R. Zheng, A. Hjørungnes, T. Basar, and H.V. Poor. Coalitional games in partition form for joint spectrum sensing and access in cognitive radio networks. *IEEE Journal of Selected Topics in Signal Processing*, 6(2):195–209, Apr. 2012.
- [148] F.H. Sanders. Broadband spectrum surveys in Denver, CO, San Diego, CA, and Los Angeles, CA: methodology, analysis, and comparative results. In *IEEE International Symposium on Electromagnetic Compatibility*, volume 2, pages 988–993, Aug. 1998.
- [149] S.R. Saunders. *Antennas and propagation for wireless communication systems*. John Wiley&Sons, 1999.
- [150] Y. Selen, H. Tullberg, and J. Kronander. Sensor selection for cooperative spectrum sensing. In *3rd IEEE Symposium on New Frontiers in Dynamic Spectrum Access Networks*, pages 1–11, Oct. 2008.
- [151] H. Shokri-Ghadikolaei, Y. Abdi, and M. Nasiri-Kenari. Learning-based spectrum sensing time optimization in cognitive radio systems. In *2012 Sixth International Symposium on Telecommunications (IST)*, pages 249–254, Nov. 2012.
- [152] C. Stevenson, G. Chouinard, Z. Lei, W. Hu, S.J. Shellhammer, and W. Caldwell. IEEE 802.22: The first cognitive radio wireless regional area network standard. *IEEE Communications Magazine*, 47(1):130–138, Jan. 2009.
- [153] S. Stigler. Gauss and the invention of least squares. *The Annals of Statistics*, 9(3):465–474, 1981.
- [154] L. Suarez, L. Nuaymi, and J.-M. Bonnin. An overview and classification of research approaches in green wireless networks. *EURASIP Journal on Wireless Communications and Networking*, 2012(1):1–18, 2012.
- [155] C. Sun and C. Yang. Energy efficiency analysis of one-way and two-way relay systems. *EURASIP Journal on Wireless Communications and Networking*, 2012(1):1–18, 2012.
- [156] C. Sun, W. Zhang, and K. Ben. Cluster-based cooperative spectrum sensing in cognitive radio systems. In *IEEE International Conference on Communications*, pages 2511–2515, June 2007.

- [157] Y. Sun, H. Hu, F. Liu, H. Yi, and X. Wang. Selection of sensing nodes in cognitive radio system based on correlation of sensing information. In *4th International Conference on Wireless Communications, Networking and Mobile Computing*, pages 1–6, Oct. 2008.
- [158] R. Tandra and A. Sahai. Fundamental limits on detection in low SNR under noise uncertainty. In *2005 International Conference on Wireless Networks, Communications and Mobile Computing*, volume 1, pages 464–469, June 2005.
- [159] R. Tandra and A. Sahai. SNR walls for signal detection. *IEEE Journal of Selected Topics in Signal Processing*, 2(1):4–17, Feb 2008.
- [160] Z. Tian and G.B. Giannakis. A wavelet approach to wideband spectrum sensing for cognitive radios. In *1st International Conference on Cognitive Radio Oriented Wireless Networks and Communications*, pages 1–5, June 2006.
- [161] D. Triantafyllopoulou, K. Moessner, A. Kliks, H. Bogucka, A. Zalonis, I. Dages, N. Dimitriou, and A. Polydoros. A context-aware decision making framework for cognitive and coexisting networking environments. In *Proceedings of the 19th European Wireless Conference (EW)*, pages 1–6, Apr. 2013.
- [162] J. Unnikrishnan and V.V. Veeravalli. Cooperative sensing for primary detection in cognitive radio. *IEEE Journal of Selected Topics in Signal Processing*, 2(1):18–27, Feb. 2008.
- [163] R. Uргаonkar and M.J. Neely. Optimal routing with mutual information accumulation in wireless networks. *IEEE Journal on Selected Areas in Communications*, 30(9):1730–1737, Oct. 2012.
- [164] R. Viswanathan and V. Aalo. On counting rules in distributed detection. *IEEE Transactions on Acoustics, Speech and Signal Processing*, 37(5):772–775, May 1989.
- [165] P. Wang, L. Xiao, S. Zhou, and J. Wang. Optimization of detection time for channel efficiency in cognitive radio systems. In *IEEE Wireless Communications and Networking Conference*, pages 111–115, Mar. 2007.
- [166] Y. Wang, C. Feng, Z. Zeng, and C. Guo. A robust and energy efficient cooperative spectrum sensing scheme in cognitive radio networks. In *11th International Conference on Advanced Communication Technology*, volume 01, pages 640–645, Feb. 2009.
- [167] J. Wei and X. Zhang. Energy-efficient distributed spectrum sensing for wireless cognitive radio networks. In *INFOCOM IEEE Conference on Computer Communications Workshops*, pages 1–6, Mar. 2010.
- [168] W. Xia, S. Wang, W. Liu, and W. Chen. Cluster-based energy efficient cooperative spectrum sensing in cognitive radios. In *5th International Conference on Wireless Communications, Networking and Mobile Computing*, pages 1–4, Sept. 2009.
- [169] K. Xie, J. Cao, X. Wang, and J. Wen. Optimal resource allocation for reliable and energy efficient cooperative communications. *IEEE Transactions on Wireless Communications*, 12(10):4994–5007, Oct. 2013.

- [170] Y. Xu, A. Anpalagan, Q. Wu, L. Shen, Z. Gao, and J. Wang. Decision-theoretic distributed channel selection for opportunistic spectrum access: Strategies, challenges and solutions. *IEEE Communications Surveys Tutorials*, 15(4):1689–1713, Fourth 2013.
- [171] Y. Xu, C. Wu, C. He, and L. Jiang. A cluster-based energy efficient MAC protocol for multi-hop cognitive radio sensor networks. In *IEEE Global Communications Conference (GLOBECOM)*, pages 537–542, Dec. 2012.
- [172] T.-H. Yu, O. Sekkat, S. Rodriguez-Parera, D. Markovic, and D. Cabric. A wideband spectrum-sensing processor with adaptive detection threshold and sensing time. *IEEE Transactions on Circuits and Systems I: Regular Papers*, 58(11):2765–2775, Nov. 2011.
- [173] T. Yucek and H. Arslan. A survey of spectrum sensing algorithms for cognitive radio applications. *IEEE Communications Surveys Tutorials*, 11(1):116–130, First 2009.
- [174] Y. Zeng and Y. C. Liang. Maximum-minimum eigenvalue detection for cognitive radio. In *IEEE 18th International Symposium on Personal, Indoor and Mobile Radio Communications (PIMRC)*, pages 1–5, Sept 2007.
- [175] J.q. Zhai, H.-S. Zhang, Y. Li, and Y.-w. Zhang. Energy efficient RF front-ends architecture design for wireless sensor networks. In *Second International Conference on Networks Security Wireless Communications and Trusted Computing (NSWCTC)*, volume 1, pages 236–239, Apr. 2010.
- [176] W. Zhang, R.K. Mallik, and K.B. Letaief. Cooperative spectrum sensing optimization in cognitive radio networks. In *IEEE International Conference on Communications*, pages 3411–3415, May 2008.
- [177] W. Zhang, R.K. Mallik, and K.B. Letaief. Optimization of cooperative spectrum sensing with energy detection in cognitive radio networks. *IEEE Transactions on Wireless Communications*, 8(12):5761–5766, 2009.
- [178] W. Zhang, Y. Yang, and C.K. Yeo. Cluster-based cooperative spectrum sensing assignment strategy for heterogeneous cognitive radio network. *IEEE Transactions on Vehicular Technology*, 64(6):2637–2647, June 2015.
- [179] N. Zhao, F.R. Yu, H. Sun, and A Nallanathan. An energy-efficient cooperative spectrum sensing scheme for cognitive radio networks. In *IEEE Global Communications Conference (GLOBECOM)*, pages 3600–3604, Dec. 2012.
- [180] Z. Zhou, S. Zhou, J.-H. Cui, and S. Cui. Energy-efficient cooperative communication based on power control and selective single-relay in wireless sensor networks. *IEEE Transactions on Wireless Communications*, 7(8):3066–3078, Aug. 2008.